ECMWF Newsletter

Number 154 – Winter 2017/18

European Centre for Medium-Range Weather Forecasts
Europäisches Zentrum für mittelfristige Wettervorhersage
Centre européen pour les prévisions météorologiques à moyen terme

New probability-of-precipitation-type products

ECMWF's new seasonal forecasting system

Why warm conveyor belts matter

Ocean coupling and tropical cyclones

EC-Earth climate prediction research

www.ecmwf.int/en/about/news-centre/media-resources

CONTENTS

Florence Rabier
Director-General

Inspiration for 2018

ECMWF had a busy and inspiring start to 2018. For the first time we were an exhibitor at the Annual Meeting of the American Meteorological Society in Austin, Texas. This was a great opportunity to catch up with colleagues and partners from around the world and to share findings and exchange views on some of the events that had marked 2017, such as the devastating hurricanes which hit the Caribbean islands and the US. There were also intense discussions on the technical challenges meteorology is facing, from adopting the Python programming language for data analytics and machine learning to using cloud computing to run models and perform big-data computations.

An important development at the beginning of the year was the publication of complete climate data for 2017 produced by the Copernicus Climate Change Service we operate on behalf of the EU. As predicted, 2017 turned out to be one of the three warmest years on record, and the warmest year not influenced by a warming El Niño. This latest finding adds to the weight of evidence of global warming in the 21st century, which now includes 16 of the 17 warmest years on record.

These results came at the end of a year that had its fair share of extreme weather and environmental conditions. In Europe this included catastrophic wildfires in Portugal in June, a heat wave in large parts of southern Europe in August and devastating windstorms that hit Poland, the Czech Republic and Germany in August and October. We know that climate change affects the frequency and severity of extreme weather events. However, a lot more research and data are now required to be able to assess with more certainty the full breadth of the impact the changing climate has on our weather.

At ECMWF 2018 will be very much about supercomputing. The year will see the start in earnest of the procurement for our new supercomputer and of the migration of our data centre to Bologna. The building work is scheduled to start, as is the recruitment for the technical roles which will be located in Bologna. At the heart of the new building will be the new supercomputer. We are looking forward to a good response to the invitation to tender to be issued later this year.

We will run our usual range of workshops and seminars this year, covering topics such as data assimilation, sea-surface temperatures, radiation, physics–dynamics coupling and high-performance computing. We will also aim to live-stream as many of our events as possible so that those of you who cannot physically travel to us can still take part virtually.

Let me conclude by wishing you on behalf of all of us at ECMWF a great 2018, with many opportunities to discuss the fascinating science and technology of weather forecasting and how it will evolve in the future.

New products for precipitation type probabilities

**ESTÍBALIZ GASCÓN,
TIM HEWSON, CIHAN SAHIN**

ECMWF has included two new products in ecCharts, based on ensemble forecasts of instantaneous precipitation type: a map showing the most probable precipitation type and a meteogram showing probabilities of different precipitation types for a user-selected site. These new products, created in the framework of the EU-funded ANYWHERE project and inspired by a similar bar chart product from the Hungarian national meteorological service (OMSZ), exploit the probabilistic information provided by ensemble forecasts. This is especially useful in more challenging situations, where there is a risk of snow or freezing rain. In designing these new products, we have incorporated the instantaneous precipitation rate variable in a new way, to define for each type a cut-off between precipitating and dry. This helps to eliminate the misleading impression that miniscule precipitation rates can give in a forecast.

Meteogram product

The new meteogram-style product depicts the temporal evolution of probabilities (in percentages) for a specific location in bar chart format. Probabilities are calculated from the instantaneous precipitation type variable, which has seven different categories: dry, rain, sleet, wet snow, snow, ice pellets, and freezing rain. The categories are represented by different colours. Different hues provide details on the probability of different instantaneous precipitation rates for different precipitation types, which can be key for determining the severity of, for example, potential freezing rain or snowfall events. Three different rate categories are used: <0.2, 0.2 to 1 and >1 mm/hour. On the meteogram, the bars are stacked in such a way that the nominally most hazardous type (freezing rain in the high intensity category) is shown at the bottom, and the least hazardous (low intensity rain) at the top. Blank areas at the very top denote dry. The temporal resolution is 3-hourly for T+0h to T+144h and

24-hour forecast
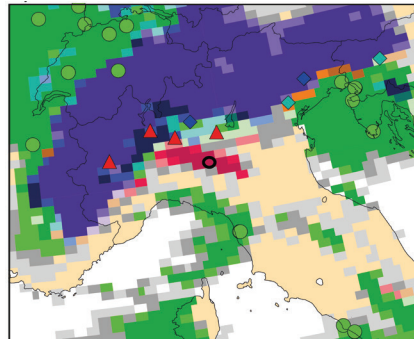
48-hour forecast
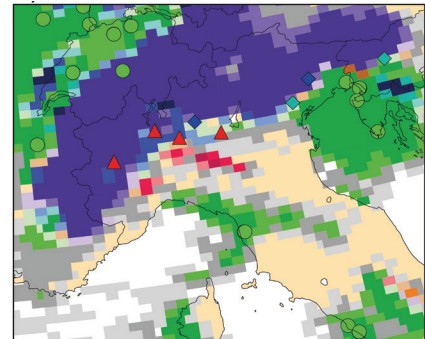
72-hour forecast

96-hour forecast

Rain (%)	Sleet (%)	Wet snow (%)	Snow (%)	Ice pellets (%)	Freezing rain (%)	Precipitation (%)
>70	>70	>70	>70	>70	>70	30–50
50–70	50–70	50–70	50–70	50–70	50–70	10–30
<50	<50	<50	<50	<50	<50	

Observations ● Rain ◆ Sleet ◆ Snow ◆ Ice pellets ▲ Freezing rain
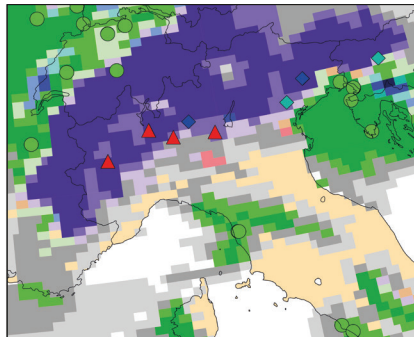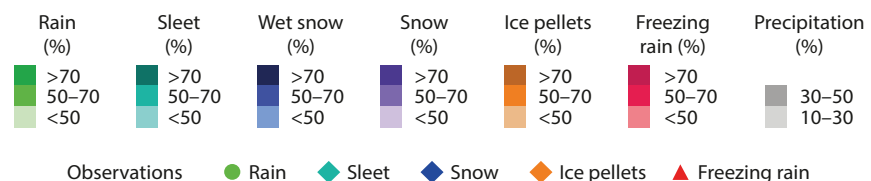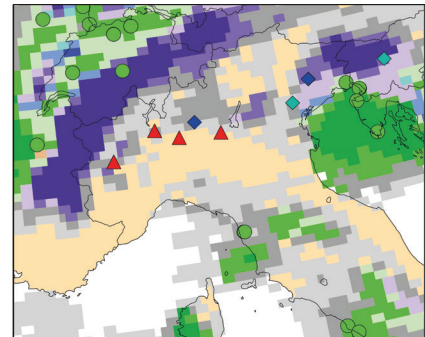
Map product for a freezing rain event in northern Italy. The forecasts are valid at 00 UTC on 13 January 2017, with starting times of 00 UTC on 12 (top left), 11 (top right), 10 (bottom left) and 9 January (bottom right). SYNOP weather observations for the valid time are shown as symbols. The black circle in the top left map corresponds to a location near Parma, which was severely affected by freezing rain.

6-hourly for T+144h to 168h, matching the standard ecCharts meteogram style.

Map product

The map product shows which of the six precipitation types, represented by different colours, is most probable whenever it is more likely than not to be precipitating – i.e. the probability of any type is >50%. The hue is used to denote what the probability of the type denoted by the colour is, in three ranges: <50, 50–70 and >70%. In order to expand on this, particularly for longer lead times when high probabilities are less common, we also use grey shading to denote two further categories: probability of any type of precipitation = 10–30 or 30–50%. Another design aspect is that,

whenever the lightest shade of a given colour (except grey) appears on a map, the user immediately knows that more than one precipitation type has been predicted for that time, which can serve as an alarm bell for uncertainty.

Bias correction and verification

Over a training period comprising four winter months, we computed the frequencies, amongst weather reports from European SYNOP weather station observations, of different precipitation types, and also type frequencies seen in the corresponding model forecasts for these sites. By adjusting the threshold of minimum permissible instantaneous precipitation rate in the latter, one can achieve a frequency bias of 1 (i.e. unbiased) for each type. The thresholds
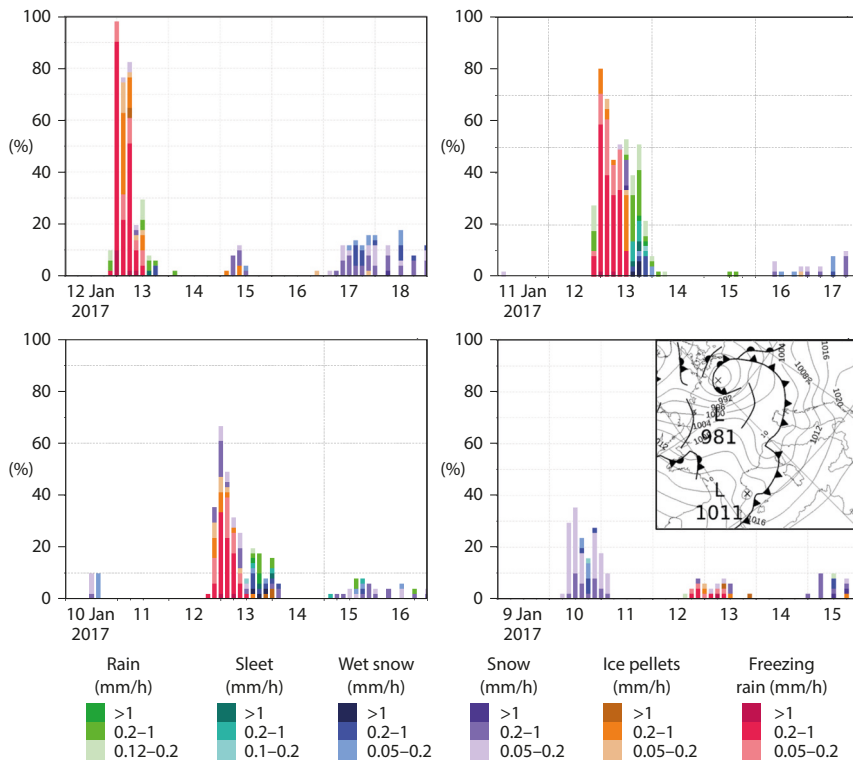
Meteogram product for a location near Parma, Italy. The forecast starting times are 00 UTC on 12 (top left) 11 (top right) 10 (bottom left) and 9 January 2017 (bottom right). The model height at this location is 74 m. The synoptic chart inset is valid at 06 UTC on 13 January 2017. (Chart inset: UK Met Office)

thus computed for model cycle 43r3, which are now used for generating both products described here, were 0.12, 0.1 and 0.05 mm/h, respectively for rain, sleet and all other types. We expect that these values may change as the model physics is upgraded in future cycles, and indeed perform routine monitoring to check this. After applying these filters, verification of both products showed that they are highly skilful in forecasting rain and snow, but only moderately skilful for sleet and freezing rain (little useful skill beyond day 2 overall),

whilst predictive ability for ice pellets is negligible. Another revealing result was that the thresholds required to deliver unbiased forecasts turned out to be fairly consistent across the lead time range, encouragingly suggesting that there is little model drift.

Examples: how to use the products

From the night of 12 January 2017 to the morning of 13 January 2017, the areas of Lombardy and Emilia-Romagna (Italy) suffered a rare freezing rain event, related to the passage of a cold front over cold near-surface air trapped south

of the Alps. This caused dozens of traffic accidents including the overturning of a bus near Bologna. In the 24-hour forecast map valid at 00 UTC on 13 January, an area with probabilities of freezing rain greater than 70% is observed in northern Italy, matching quite well with observations from the nearest SYNOP stations. The freezing rain area was smaller in earlier forecasts but there was a signal of a risk even at 48-hour and 72-hour lead times.

One of the most affected places was the town of Parma, corresponding to the black circle in the top left map of northern Italy. The meteogram indicates high probabilities of freezing rain during the first half of 13 January, in forecasts initialised one to three days in advance. Most ensemble members also show moderate rates, between 0.2 and 1 mm/hour (medium red). The small signal of probabilities under 10% observed in a forecast initialised four days in advance may not be not enough for decision-making, but it would alert forecasters to the need to pay close attention in the following days.

Other familiar atmospheric structures can often be seen on the map product in winter. These include the formation of a freezing rain band between rain and snow areas related to a depression (marked '1' in the forecast chart for the North Atlantic–Europe region), the transition from rain to sleet to wet snow and then snow in a region of warm advection (2), and a geographically focused distribution of rain probabilities for an Atlantic front for which the timing is uncertain (3).

In practice we recommend that users generally start with the map product to identify possible events, then investigate in more detail the actual probabilities and rates using the meteogram product, noting also how model site altitude (in the meteogram title) matches the true site altitude, and interpreting accordingly. Users may also wish to compare the charts with the high-resolution forecast (HRES) precipitation type product that was already available in ecCharts. All such products can help with decision-making for local or regional warnings.

For further information, please consult an article on the new products by Estíbaliz Gascón et al. in *Weather and Forecasting* (doi:10.1175/ WAF-D-17-0114.1).
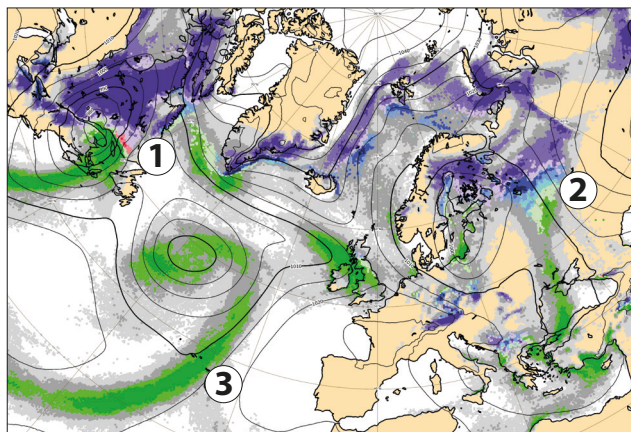
Map product example showing some typical wintertime precipitation-type structures. The starting time of the forecast is 00 UTC on 17 November 2017, the valid time is 72 hours later.

Two storm forecasts with very different skill

**LINUS MAGNUSSON,
IVAN TSONEVSKY, TIM HEWSON**

During autumn 2017, extreme weather events in Europe included the ongoing drought on the Iberian Peninsula, flash floods in Greece, and the landfall of ex-tropical cyclone Ophelia in Ireland. In this article we focus on two devastating windstorms for which the skill level in ECMWF forecasts was very different.

11 August 2017

On 11 August 2017 severe winds hit northern Poland, causing the deaths of five people, significant damage to

trees and power disruptions affecting 340,000 households. This severe storm was caused by a mesoscale convective system. Wind gusts of over 40 m/s were reported in the region. However, even the shortest-range high-resolution forecasts (HRES) failed to predict anything near these values, nor did the Extreme Forecast Index (EFI) or Shift of Tails (SOT) for wind gusts show any significant signal, at any time range. This illustrates that directly capturing fine-scale extremes in convective cases is still out of reach for global models. The finer-scale COSMO-EPS from the

German national meteorological service DWD (data archived at ECMWF as part of TIGGE-LAM) did predict extreme wind gusts in the region. However, ECMWF has developed a number of products that make the best use of information contained in the medium-range forecast to identify potential fine-scale weather hazards consistent with the large-scale flow. Examples of this are the EFI for convective indices, and also point rainfall (sub-grid) precipitation probabilities. Indeed in this case the risk of severe convective hazards in the affected region was captured in ECMWF medium-range

11 August 2017   **29 October 2017**
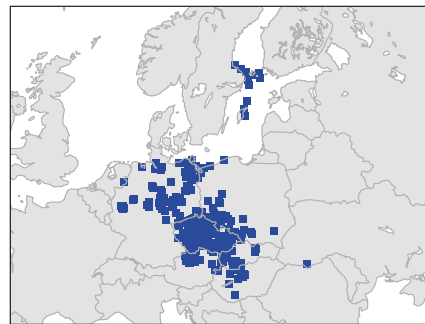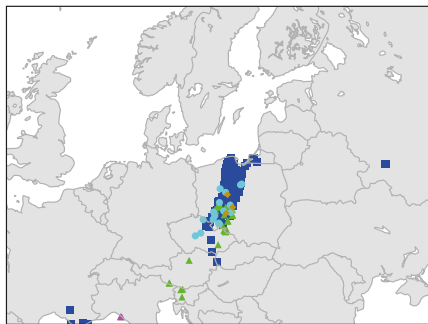
▲ Tornado   ▲ Hail   ■ Severe wind   ◆ Lightning   ● Heavy rain

One-day forecast, EFI/SOT, wind gusts   One-day forecast, EFI/SOT, wind gusts
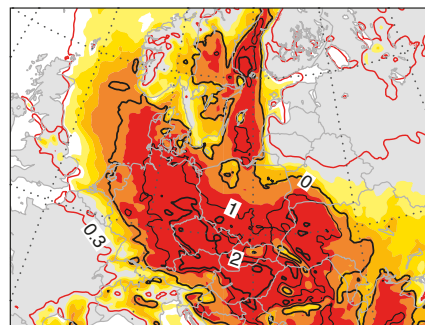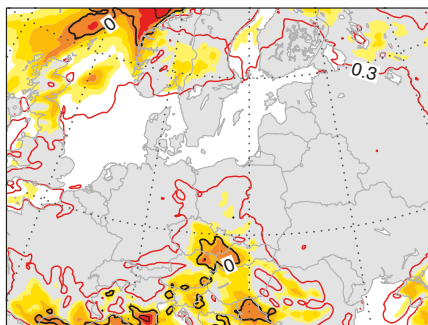
Six-day forecast, EFI/SOT, CAPE–shear   Six-day forecast, EFI/SOT, wind gusts

0.5   0.6   0.7   0.8   0.9   1
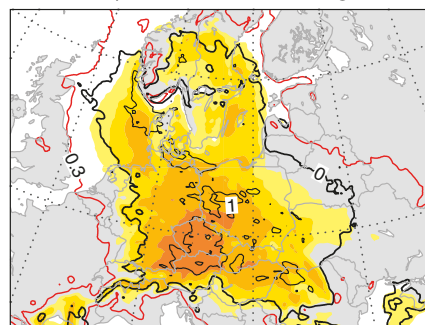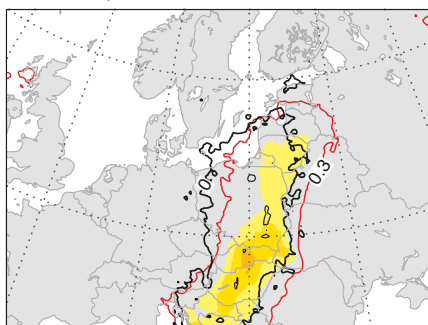
Observations and forecasts for the two windstorms. Reports of severe weather from the European Severe Weather Database (ESWD) for 11 August (top-left) and 29 October (top-right); one-day forecasts of EFI (shading) and SOT (contours) for 24-hour maximum 10-metre wind gusts for the two respective cases (middle); and 6-day forecasts of EFI and SOT for CAPE–shear in the August case (bottom-left) and for 10-metre wind gusts in the October case (bottom-right).

forecasts by the EFI and SOT product for a composite parameter that combines CAPE and wind shear, albeit somewhat too far east in the 6-day forecast.

28–29 October 2017

On the night of 28 October a deepening cyclone, named Herwart by the Free University of Berlin, moved southeastwards across southern Sweden and the southern Baltic Sea. Within the large circulation of this cyclone, very strong winds developed, most notably over Germany, the Czech Republic and Poland. There were at least four fatalities, damage to trees and buildings and disruption to infrastructure. According to reports in

the European Severe Weather Database (ESWD), the Czech Republic was probably worst affected. The short-range EFI for wind gusts agrees well with those reports. Even at a lead time of six days, the ECMWF EFI and SOT clearly highlighted a greatly elevated risk of a severe wind event over a large area. Indeed, the strongest signal in the EFI was centred on the Czech Republic. Throughout the lead-up to this event, ECMWF ensemble forecasts (ENS) provided a consistent signal for a dangerous windstorm, which grew stronger with time.

Conclusion

These two cases illustrate very different

skill for the same variable (wind gusts). In the first case no skilful forecast regarding the extreme wind was provided directly by ECMWF forecasts, while in the other case the forecast showed skill almost a week in advance. As discussed, the meteorological conditions behind the two events were very different. Such differences should be borne in mind when interpreting verification results for wind gusts as both cases contribute to the statistical sample. Indeed verification over a full year shows significantly lower skill during summer, when the contribution of deep moist convection to cases of severe wind gusts is higher in the sample.

MozFest – a must-go event to get inspired!

CLAUDIA VITOLO, FATIMA PILLOSU

ECMWF had a stand on open data at this year's MozFest, an annual event organised by the non-profit Mozilla Foundation around themes such as digital empowerment, open data innovation and digital literacy. The Mozilla Foundation develops and supports Firefox, the internet browser, but also actively "promotes openness, innovation and participation on the Internet, [...] which must always remain a global public resource that is open and accessible to all". MozFest is a highly interactive event where enthusiasts gather to celebrate and promote this idea.

This year MozFest opened with a science fair where companies and organisations demonstrated products, software and services for the public good. This type of event attracts a diverse audience, ranging from software developers to artists, journalists, students and others, and covering a wide age range. We decided to play an active role in the event and presented some creative ways of using open data from ECMWF, including the two EU-funded Copernicus services implemented by the Centre. These are a few examples:

- a machine-learning application to predict bus delays given the weather

The ECMWF contingent at MozFest 2017. From left to right: Claudia Vitolo, Fatima Pillosu and Florian Rathgeber (now at Google) with the winners of the ECMWF OpenDataHack 2017, Laurent Geffert and Gordon Rates. *(Photo: Florian Rathgeber)*

- gamification of natural disaster management
- predicting malaria outbreaks using temperature and precipitation
- spotting wildfires using satellite images
- tracking hurricanes.

Given the diverse audience, we designed the session around a few simple concepts that could resonate with people of all ages and backgrounds. We decided to use examples based on events in the news (hurricanes, malaria, wildfires) or everyday annoyances (bus delays), and to demonstrate how the weather can influence them. We were extremely impressed by the participants' curiosity and the depth and variety of their

contributions to the discussion. It was no surprise that young kids were interested in hurricanes. More surprising was the number of teachers interested in open data; biomedical students interested in the consequences of climate change on embryogenesis; natural resources scientists interested in efficient data queries; and physicists interested in how we plan to embrace the era of quantum computing.

We had come well prepared to speak about the science developed at ECMWF including Copernicus. However, the audience's curiosity took us well beyond our comfort zone. As scientists we found this experience greatly inspiring and can only encourage others to attend this event next year.

Forecast performance 2017

DAVID RICHARDSON, THOMAS HAIDEN, MARTIN JANOUSEK

ECMWF maintains a comprehensive range of verification statistics to evaluate the accuracy of its forecasts. Each year, a summary of verification results is presented to ECMWF's Technical Advisory Committee (TAC). Their views about the performance of the operational forecasting system in 2017 are given in the box.

The overall performance of the operational forecasts is summarised using a set of headline scores endorsed by the TAC, which highlight different aspects of forecast skill. Upper-air performance is monitored through the anomaly correlation of 500 hPa geopotential height of the high-resolution deterministic forecast (HRES) and the continuous ranked probability score (CRPS) for temperature at 850 hPa for the ensemble forecast (ENS), both over the northern hemisphere extratropics. The most recent upgrades to the Integrated Forecasting System (IFS) on 22 November 2016 (Cycle 43r1) and 11 July 2017 (Cycle 43r3) have enabled ECMWF to remain the leading centre in terms of overall medium-range forecast skill, for both deterministic and ensemble forecasts. The 12-month running mean value of the ENS skill now consistently exceeds nine days, which is an increase of more than a day over the last decade, as shown in the first figure. Note that ERA5

now provides a useful benchmark and reference for the identification of interannual variations in predictability, replacing ERA-Interim in this regard.

Headline scores for the surface weather focus on precipitation for both HRES and ENS. The ENS skill for precipitation is shown in the second figure – skill is maintained consistently out to 7 days. The resolution upgrade from 32 to 18 km for the ENS in 2016 contributed to a noticeable increase in skill. HRES skill also continues to increase for precipitation, as does the skill for the Extreme Forecast Index (EFI) for precipitation.

Surface skill has increased for 2 m temperature, humidity and 10-m wind speed. However, there are still issues with seasonally and diurnally varying regional biases in 2 m temperature which need to be resolved. Forecasts of tropical cyclones have improved in terms of position errors both for the HRES and ENS, with both showing lowest values so far, while speed errors slightly increased compared to the previous year. Mean absolute intensity errors decreased compared to the previous year, but there are still significant intensity biases, especially for the ENS. Wave forecast skill has further increased both with respect to wave height and peak period, and ECMWF generally maintains a lead compared to other global wave forecasting systems.

The El Niño of 2015–16 ended in early summer 2016, and subsequent

conditions have remained relatively close to neutral. With no strong El Niño Southern Oscillation (ENSO) forcing, a general drop in seasonal predictive skill would be expected for 2016–17. Nevertheless, there were some large-scale temperature anomalies that the forecast captured to some extent. The pattern of 2 m temperature in the northern-hemisphere winter (December–January–February 2016–17) was characterized by strong warm anomalies in the Arctic, and over North America and Eurasia. These warm anomalies, which are a combination of the effect of global warming and interannual variability, were captured reasonably well by the seasonal forecast in North America, but not in Eurasia. Parts of Europe experienced a hot summer season in 2017. The forecast for June–August predicted positive anomalies over Southern Europe and the Mediterranean, as well as parts of Siberia (again, part of this pattern is due to global warming). The verifying analysis confirmed the basic pattern, although the magnitude of the observed cold anomaly stretching from Scandinavia eastward was less well captured.

Each summer ECMWF invites Member and Co-operating States to submit updated reports on the application and verification of ECMWF's forecast products. In this year's reports, verification corresponds mainly to periods since the introduction of the higher-resolution HRES and ENS (IFS Cycle 41r2 in March 2016), and several countries noted recent improvements in the verification results for HRES. A number of countries also noted improved scores for winter temperature since last year, consistent with the expected improvements from IFS Cycle 41r2 (resolution increase) and 43r1 (e.g. modified surface coupling for 2 m temperature).

These reports tend to focus on HRES, and there is less verification reported for ENS. However, Denmark reported that verification of the ENS is used as a reference (benchmark) for the development of their COMEPS limited-area ensemble system. They note especially that for 10 m wind COMEPS outperforms the ENS because of its much higher horizontal resolution (2.5 km HARMONIE-AROME grid). Switzerland compares probabilistic scores for the ENS and
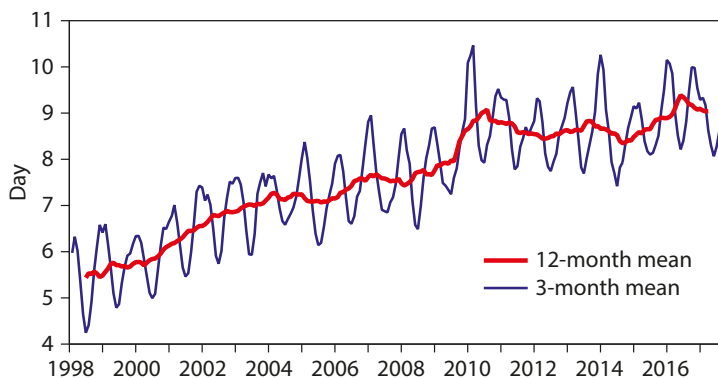
Skill of the ENS as measured by ECMWF's primary headline score. Evolution with time of 850 hPa temperature ensemble forecast performance, verified against analysis. Each point on the curves is the forecast range at which the 3-month mean (blue lines) or 12-month mean centred on that month (red line) of the continuous ranked probability skill score (CRPSS) falls below 25% for the northern hemisphere extratropics.

the COSMO-E ensemble. Some of the IFS performance issues raised by the users are known, and most of these are also listed on the ECMWF 'Known IFS Forecasting Issues' web page, which is regularly updated.

The complete set of annual results is available in two ECMWF Technical Memorandums, No. 817 on the 'Evaluation of ECMWF forecasts, including 2016–2017 model upgrades', and No. 818 on the 'Use and Verification of ECMWF products in Member and Co-operating States (2017)'. Both are downloadable from http://www.ecmwf.int/en/research/publications. These documents present recent verification statistics and evaluations of ECMWF forecasts (including weather, waves and severe weather events), whilst No. 817 also includes information about changes to the data assimilation/forecasting and post-processing systems. The performance of the monthly and seasonal forecasting systems is also assessed.

Other sources of information:

- Verification pages on the ECMWF web server are regularly updated. They are accessible at

http://www.ecmwf.int/en/forecasts/charts

- Interactive plots showing intercomparisons of global model forecast skill can be found on the WMO Lead Centre for Deterministic Forecast Verification (WMO-LCDNV) web page at

http://apps.ecmwf.int/wmolcdnv/

- All IFS forecasting system cycle changes since 1985 are described at

http://www.ecmwf.int/en/forecasts/documentation-and-support/changes-ecmwf-model

Probabilistic skill of the precipitation forecast. Results for the northern hemisphere extratropics show that the skill of the ENS in predicting 24-hour precipitation totals continues to increase. The computation of skill is based on the continuous ranked probability skill score (CRPSS). The chart shows 12-month running average values of the forecast range at which the CRPSS drops below 0.1.

Assessment of ECMWF's Technical Advisory Committee, 12–13 October 2017

With regard to its overall view of the performance level of ECMWF's operational forecasting system, the Committee:

a. acknowledged the very good level of information provided by ECMWF in its evaluation of performance, including some of the information that the TAC Subgroup on verification measures is proposing to add to the current set;

b. appreciated the very good summary of feedback received from Member and Co-operating States and supported the new deadline for providing this feedback, which gives ECMWF more time for extracting the most important information;

c. was pleased to see continued improvement of important headline scores, for example ECMWF maintaining and sometimes increasing its lead with respect to other global NWP providers;

d. noted that the use of ERA5 as a benchmark provides very useful assistance in interpreting the impact of model improvements vs interannual variability;

e. noted the improvement of precipitation forecasts with special interest; HRES, ENS and the EFI verification scores have reached their best ever levels this year and several Member and Co-operating States have also reported positive feedback on this improved quality;

f. noted some remaining problems such as too much light precipitation and insufficient inland advection of precipitation. ECMWF has reported preliminary results showing improvements to these aspects, which will be included in the coming model cycle;

g. welcomed the prospect of improvements in the handling of lying snow in future model cycles;

h. noted that the improvement for surface parameters, relative to ERA5, is smaller than for upper level parameters. Random errors have been further reduced although biases persist;

i. noted that higher model resolution has been reported by several Member States as significantly improving the quality of wind forecasts. However, little improvement for extreme wind events was found in the EFI headline score over the last few years;

j. noted that temperature forecasts still have some biases, notably in the representation of the diurnal cycle; appreciated the creation of a dedicated project to investigate this and is looking forward to their findings;

k. appreciated the inclusion, or future inclusion, of new user-oriented parameters such as visibility and lightning density. Member and Co-operating States have started using and evaluating some of these, and improvements for some of the identified biases were included in the most recent model cycle;

l. noted that for ocean waves, ECMWF's lead in verification scores compared to others has been reduced but that improvements are expected with 45r2;

m. welcomed the smallest ever tropical cyclone track errors for HRES and ENS. Improvements are expected in forecasting tropical cyclone intensity in future model cycles, including improvements in tropical cyclone analysis;

n. noted that the monthly forecast has shown improvement over time for week 2 and no clear trend for weeks 3 and 4;

o. welcomed promising results from SEAS5 and noted successful modelling of summer 2017 by the seasonal forecasting system;

p. welcomed the earlier delivery of ENS forecasts that has been achieved without compromising quality. This has been appreciated by users, especially forecasters.

ECMWF introduces two additional headline scores

**THOMAS HAIDEN,
DAVID RICHARDSON,
MARTIN JANOUSEK,
ZIED BEN BOUALLEGUE,
LAURA FERRANTI,
FREDERIC VITART**

The ECMWF Technical Advisory Committee (TAC) Subgroup on Verification Measures has recommended the introduction of two new headline scores for the monitoring of forecast skill in the medium and extended range. The new scores are user oriented and make a contribution to the overall evaluation of progress towards ECMWF's strategic goals.

Both new scores measure ensemble forecast skill, one in the medium range, one in the extended range. Both are based on the verification of 2 m temperature against SYNOP weather station observations. In other respects they are quite different. The additional headline measure for the medium range is the percentage of large errors, defined by the continuous ranked probability score (CRPS) exceeding 5 K at day 5 in the extratropics. It is sensitive to developments in boundary-layer physics as well as overall forecast system improvements, such as model resolution increases. Over the last ten years, the occurrence of large errors defined in this way has decreased from 6–7% to about 5% in the annual

average. A large fraction of these errors occur in stable boundary-layer situations, where 2 m temperature is particularly sensitive to errors in low cloudiness, wind speed or snow cover.

The additional headline measure for the extended range is the discrete ranked probability skill score (RPSS$_D$) for terciles of the weekly mean 2 m temperature in the northern extratropics in week 3 of the forecast (days 15–21). Unlike the medium-range score, which is based on real-time forecasts, this score is based on the evaluation of re-forecasts covering the preceding 18 to 20 years in order to increase sample size and improve the signal-to-noise ratio. The re-forecasts, run with the same model version as the real-time forecast, are used in the generation of the operational extended-range forecast products: forecasts are presented as anomalies relative to the re-forecast climate to account for model bias. The headline score is insensitive to bias because model quantiles are used for the forecast and analysis quantiles for the verification. The focus on week 3 means that the score targets a forecast range which still has relatively low skill, although this has improved substantially over the last ten years. The downward trend from 2012–2015 visible in the plot is due to interannual atmospheric variability, which is driven by large-scale phenomena such as the El Niño Southern Oscillation (ENSO) or the Madden–Julian

Oscillation (MJO). It occurs in spite of the relatively long (18-year to 20-year) re-forecast period on which each skill score value is based.

Another TAC Subgoup recommendation is to provide information on the partitioning of ENS improvements over time into resolution and reliability components. The former represents the information content (or discriminating ability) of the forecast, the latter shows how well the forecast is calibrated. Also, in addition to 2 m temperature, the skill of the forecast for 10 m wind speed and precipitation in week 3 will be monitored. The Subgroup agreed that the four Euro–Atlantic weather regimes are relevant for users. It encouraged ECMWF to continue its work on regimes and regime transitions, some of which could be carried out within the sub-seasonal to seasonal (S2S) project. Furthermore, it recommended that the MJO and North Atlantic regime real-time indices be included as supplementary scores. This would make it possible to monitor the skill of ECMWF's Integrated Forecasting System (IFS) with respect to one of the main sources of extended-range predictability and its effects on European weather.

ECMWF would like to take this opportunity to thank the representatives of the Member States and verification experts for their work within the TAC Subgroup.
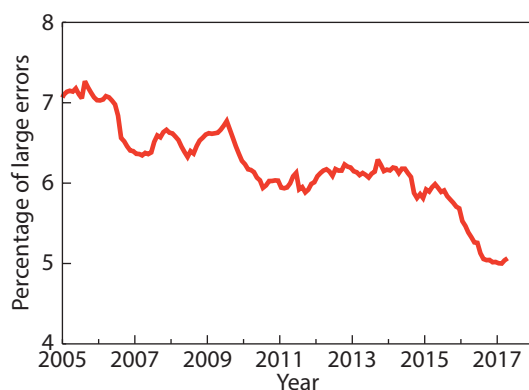
New headline score in the medium range. The plot shows the 12-month running mean percentage of continuous ranked probability score (CRPS) values for 2 m temperature exceeding 5 K at day 5 in the extratropics (poleward of 30° latitude), verified against SYNOP observations.
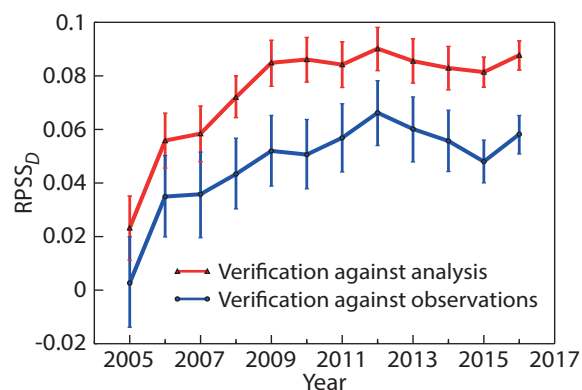
New headline score in the extended range. The plot shows the discrete ranked probability skill score (RPSS$_D$) for terciles of the weekly mean 2 m temperature in the northern extratropics in week 3 of the forecast (days 15–21). The score is based on the evaluation of re-forecasts against SYNOP observations. A perfect forecast would score the value 1, and values above 0 indicate positive skill relative to climatology. Confidence intervals (95%) were estimated using the bootstrap method. Verification against analysis (ERA-Interim) is shown in red for comparison.

The Stratosphere Task Force one year on

ROBIN J. HOGAN,
INNA POLICHTCHOUK
(ECMWF and University of Reading)

ECMWF's strategic goal of improving tropospheric predictions on timescales from one day to one year requires us to carefully study all potential sources of predictive skill. The stratosphere is one such source, particularly on monthly and seasonal timescales. However, ECMWF's Integrated Forecasting System (IFS) has large biases in stratospheric temperature and wind as well as numerous more subtle problems related to the stratosphere. These issues also affect atmospheric reanalysis, for which a good representation of the middle atmosphere is important in its own right. The Stratosphere Task Force was set up in November 2016 to bring together scientists from the Research, Forecast and Copernicus Departments of ECMWF to work together to evaluate and improve IFS performance in the middle atmosphere, including analyses, reanalyses and forecasts. This concerted effort has been boosted by the participation of stratosphere experts Professor Ted Shepherd and Dr Inna Polichtchouk from the University of Reading.

Achievements

Nine meetings were held in the first 12 months, each with around 20 attendees, and the discussions inspired collaborative work to tackle individual problems. Additionally, Ted and Inna each gave a longer seminar during the year. The main achievements of the Task Force so far include:

- In the free-running (i.e. long runs without assimilating observations) IFS Cycle 41r1 there was a warm bias of up to 10 K in the upper stratosphere and up to 20 K in the mesosphere. Several changes have led to this being reduced in the current operational cycle (43r3). The figure shows our recent findings that much of the remaining bias can be eliminated by introducing diurnally varying ozone and reducing solar ultraviolet by 7–8% to match observations of the sun. These changes are being considered for a

IFS Cycle 41r1
\+ ozone climatology from Copernicus Atmosphere Monitoring Service
\+ averaged solar zenith angle
\+ better longwave in new radiation scheme (Cycle 43r3)
\+ diurnally varying ozone
\+ observed solar spectrum with reduced ultraviolet
\+ no sponge
Microwave Limb Sounder (MLS) 2004–2008
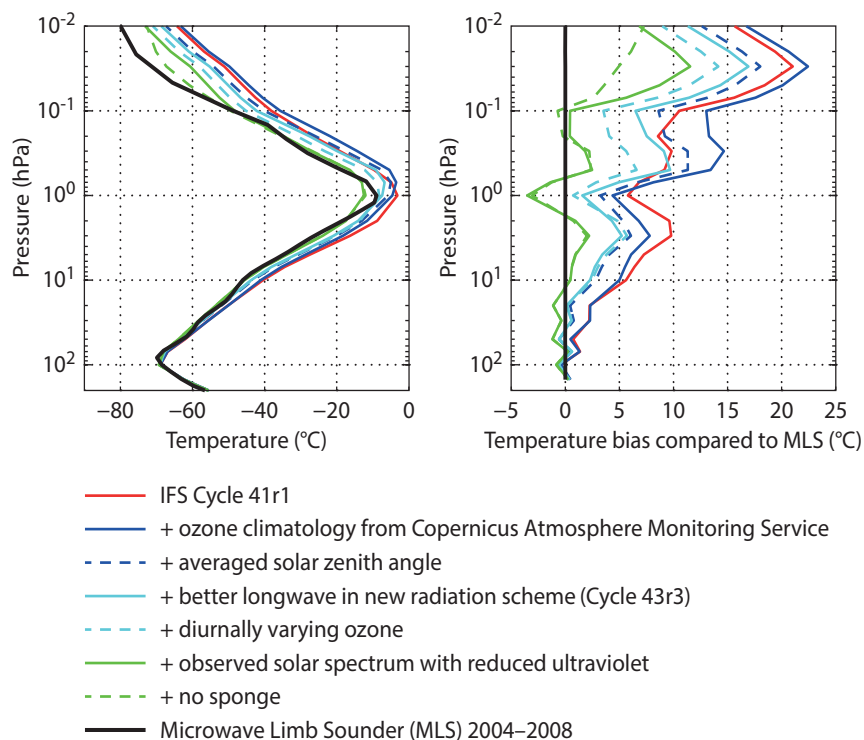
Improving the temperature bias. Annual-mean temperature (left) and temperature bias (right) from four 1-year uncoupled TL255 137-level climate simulations using different configurations of the radiation scheme, and observations by the Microwave Limb Sounder (MLS). See *ECMWF Technical Memorandum* No. 816 for details.

future cycle. Note that part of the mesosphere bias is a side effect of the 'sponge' used to prevent waves from reflecting from the model top.

- Like most other global models, the free-running IFS has a 5 K cold bias in the polar lower stratosphere. This has been found to be due to a large moist bias in this region due to excessive transport from the troposphere. Experiments in which the humidity seen by radiation is artificially reduced not only eradicate the cold bias but also improve monthly forecast skill (see *ECMWF Technical Memorandum* No. 816). Work to provide a physically based solution to the excessive humidity transport is ongoing.

- From March 2016, the operational analysis was affected by an erroneous mesosphere jet of up to 180 m/s. This problem has been solved by a modification of the climatological part of the

background error covariance model in the data assimilation system. It is nevertheless present in the version of the IFS being used to produce the ERA5 reanalysis.

- A careful analysis has been performed on the impact of model parametrizations, particularly non-orographic gravity wave drag, on the Brewer-Dobson circulation, the Quasi-Biennial Oscillation and seasonal temperature biases in the stratosphere (see *ECMWF Technical Memorandum* No. 809). This has provided valuable information for future adjustments to these parametrizations.

Ongoing challenges

A wide range of other important issues have been identified and discussed and will be the focus of activities by the Task Force in the coming year. For example, despite simulating the evolution of Sudden Stratospheric Warmings very well, the stratosphere–troposphere coupling in

the IFS is too weak. What is needed to improve the coupling, and therefore predictive skill? Mean stratospheric temperature has been found to have a noticeable dependence on resolution: increasing horizontal resolution from TL255 to TCo1279 results in a 1–2 K cooling at 70 hPa unless it is also accompanied by a modest increase in vertical resolution (e.g. 137 to 162 levels). Do we need more vertical levels operationally, or can the resolution dependence be removed with better numerics? We also wish

to make prognostic ozone interactive in the radiation scheme, and work is ongoing to address some of the shortcomings of the available linear ozone schemes to make this possible. Finally, whilst ERA5 brings significant improvements over the older ERA-Interim reanalysis in most respects, it has been found that ERA5 has larger stratospheric temperature biases than ERA-Interim from the 1990s to 2006. This is believed to be due to larger model biases in the newer IFS cycle used for ERA5, compounded by less

weight being given to radiosonde data in the newer cycle. The model biases were well corrected by data assimilation only when sufficient GPS radio occultation measurements came online. This highlights the need to improve both the model and the data assimilation in the stratosphere.

We have found the Task Force approach very effective for tackling IFS issues that cut across ECMWF sections and departments, and we envisage that it could be used productively for other topics.

Antarctic downslope winds affect ice sheet snowfall

JACOPO GRAZIOLI (EPFL/MeteoSwiss), **ALEXIS BERNE** (EPFL – Switzerland), **RICHARD FORBES** (ECMWF), **JEAN-BAPTISTE MADELEINE** (LMD – France), **HUBERT GALLÉE, CHRISTOPHE GENTHON, GERHAD KRINNER** (all Université Grenoble Alpes – France)

A collaboration between European scientists has shed new light on the effect of strong winds flowing from the high Antarctic plateau on the Antarctic ice sheet surface mass balance, by bringing together new observations of snowfall at an Antarctic research station with a

year of analysis data from ECMWF's Integrated Forecasting System (IFS).

Snowfall over Antarctica

The continent of Antarctica is often considered to be a desert as so little precipitation falls in the interior. However, precipitation around the coastal regions is much higher, with significant snowfalls from incursions of frontal systems associated with the Southern Ocean storm track. This snowfall increases the mass of the Antarctic ice sheets and is an integral part of the ice sheet surface mass balance. It is therefore important to quantify the amount of snowfall at the surface across the continent. In situ observations in Antarctica are sparse

and satellite data cannot directly observe the precipitation at the surface. A dedicated campaign was therefore needed to help to understand the relevant precipitation processes.

New observations

A year-long observational field campaign was initiated in November 2015 to monitor precipitation at the Dumont d'Urville (DDU) research station in Adélie Land on the coast of East Antarctica. This provided an unprecedented time series of weather radar measurements of the vertical profile of precipitation. The data recorded the radar reflectivity of the precipitation through the year and how it changed in the vertical due to

Total snowfall reaching ground
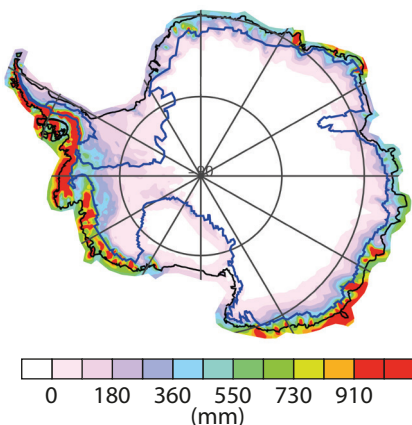
Total sublimated snowfall
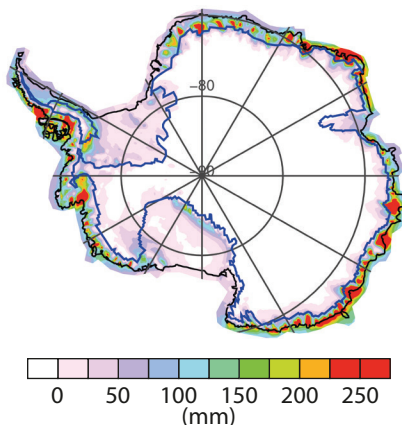
Ratio of sublimated snowfall
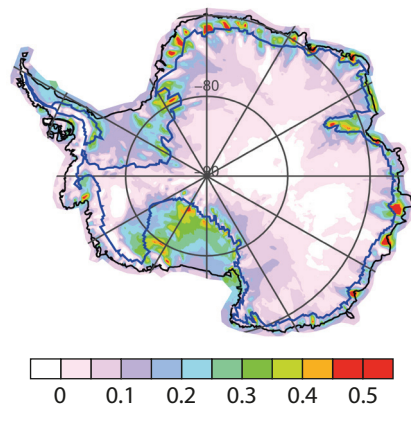
Snowfall sublimation over Antarctica. The left-hand map shows the total annual amount of snowfall (water equivalent depth) reaching the ground, with significant snowfall around the coastal regions. The middle map shows the total annual amount of snowfall that sublimates before it reaches the ground, highlighting the effect of the dry low-level air from localised but persistent katabatic flows, particularly along the East Antarctica coast. The right-hand map shows the ratio of annual snowfall sublimation to the maximum snowfall in the vertical column, with locally up to 50% of the snowfall sublimating before it reaches the surface. The blue line indicates the 1,000 m altitude of the orography. Data are from 24-hour forecasts produced by ECMWF's Integrated Forecasting System from November 2015 to November 2016. (Figure from Grazioli et al., doi:10.1073/pnas.1707633114).

the microphysical processes of snow particle growth and sublimation (solid to vapour). This led to the discovery that the process of sublimation of snow falling through the lowest layers of the atmosphere has an important effect on the accumulation of Antarctic precipitation at the surface. This process had previously been neglected in the Antarctic ice sheet mass balance.

Katabatic winds

The DDU research station is at a location that is frequently affected by strong downslope winds flowing from the high Antarctic plateau, called katabatic winds. These winds are channelled by the topography and are particularly persistent in specific regions around the coast. The katabatic winds are dry and the air warms adiabatically as it descends, leading to low relative humidity in a layer above

the surface. Very close to the surface, air is moistened by sublimation of surface snow, but aloft the low relative humidity layer leads to significant sublimation of falling snow particles as observed by the radar at the DDU station.

Modelling the sublimation of snowfall

The profiles of falling snow at the station location were compared with results from three numerical models including the IFS. All three confirmed the important role of snow sublimation caused by katabatic winds. The IFS operational global analysis and 24-hour forecasts for the whole year were then used to quantify the impact of sublimation on falling snow over the entire Antarctic continent. The IFS results show that the total Antarctic continent cumulative precipitation near the ground was 17% lower than its

maximum level higher in altitude, due to snowfall sublimation. The largest reductions were around the coast in the regions of persistent katabatic winds, particularly in East Antarctica, where the data suggest precipitation is as much as 35% lower than it would be without sublimation.

The new radar observations and modelling results from this scientific collaboration have, for the first time, identified and quantified the impact of snowfall sublimation in Antarctic katabatic winds. This will help to inform our understanding of the Antarctic ice sheet mass balance, which is essential for predicting how sea levels will evolve.

Further information can be found in an article published by Grazioli et al. in the *Proceedings of the National Academy of Sciences* (doi:10.1073/pnas.1707633114).

Rapidly developing cyclones in ECMWF reanalyses

ZITA KRISZTINA BALÁZS (Eötvös Loránd University)**, ISTVÁN IHÁSZ** (Hungarian Meteorological Service)

The last few years have seen major developments in climate reanalysis at ECMWF. The production of ECMWF's fifth-generation global climate reanalysis ERA5 is under way, and the production of CERA-20C, a coupled reanalysis which covers the entire 20th century, is complete. In 2016 and 2017, in the framework of a master's thesis, rapidly developing cyclones in the North Atlantic–European region were studied at the Hungarian Meteorological Service (OMSZ), based on different reanalysis datasets. As part of this work, we investigated whether there are systematic differences in the monthly or seasonal number of such cyclones identified by the coarse-resolution but state-of-the-art CERA-20C on the one hand and the older satellite-era ERA-Interim reanalysis on the other. We also looked for long-term trends in the number of rapidly developing cyclones in CERA-20C. We found that fewer rapidly developing cyclones are identified by CERA-20C than by ERA-Interim. We also found that the number of such cyclones per 30-year period changes little in CERA-20C after 1920.

	Winter	Spring	Summer	Autumn	Total
ERA-Interim	1117	259	32	454	1865
CERA-20C	877	177	37	328	1419

Number of rapidly developing cyclones 1981–2010. The table shows the number of rapidly developing cyclones identified by ERA-Interim and CERA-20C in the North Atlantic–European region in the period 1981 to 2010.

Rapidly developing cyclones

The dynamic conditions which give rise to rapidly developing extratropical cyclones have been intensively studied over the last few decades. The defining characteristic of these cyclones is their very fast development, with a rapid change in mean sea level pressure at the core. Typically such cyclones move fast and have a relatively small diameter (about 1,500 km). When they are generated in the North Atlantic, in a later stage of their life they may cause severe storms in Europe, especially from October to April. In summer such cyclones are quite rare. The criterion used in our study for the identification of rapidly developing cyclones in the CERA-20C and ERA-Interim reanalyses is a change in mean sea level pressure of at least 24 hPa in 24 hours at the core of the cyclone.

CERA-20C and ERA-Interim compared

There are several significant differences between the ERA-Interim and CERA-20C reanalyses. ERA-Interim is a global atmospheric reanalysis from 1979. The data assimilation system used to produce ERA-Interim is based on a 2006 version of ECMWF's Integrated Forecasting System (IFS Cycle 31r2). The system uses the 4D-Var technique with a 12-hour analysis window. The horizontal resolution of the dataset is approximately 80 km with 60 vertical levels going up to 0.1 hPa. CERA-20C reconstructs the weather and climate of the Earth system including the atmosphere, ocean, land, waves and sea ice for the period 1901–2010. Unlike ERA-Interim, CERA-20C does not use satellite data. To account for errors in the observational record as well as model error, CERA-20C

provides a 10-member ensemble of reanalyses. CERA-20C was produced with IFS Cycle 41r2 (implemented in 2016) and has a horizontal resolution of about 125 km with 91 vertical levels going up to 0.1 hPa.

One of our findings is that there are considerable differences between the numbers of rapidly developing cyclones identified by the two reanalyses in the North Atlantic–European region. Between 1981 and 2010 CERA-20C identifies 24% fewer such cyclones than ERA-Interim. Broken down by season, in winter, spring and autumn CERA-20C identifies 20–30% fewer, while in summer it identifies 15% more. It should be noted that the latter percentage is based on very small absolute numbers (see the table for details). The identification of such cyclones thus appears to be sensitive to the type of reanalysis. At the same time, the distribution of rapidly developing cyclones across the seasons (spring, summer, autumn, winter) is very similar in ERA-Interim (13, 2, 25, 60%) and CERA-20C (12, 3, 24, 61%). There are no significant differences in these patterns for any selected subdomains.

In selected cases, such as cyclone Kyrill (January 2007), some relatively large differences between the two reanalyses in mean sea level pressure (4–6 hPa) can be seen in some areas, especially above the ocean and in the Arctic region. These differences do not show any systematic patterns around the core of the cyclone, and they can change quite quickly during a cyclone's lifetime. In continental Europe differences in mean sea level pressure are always smaller than 2 hPa. A frequency map of rapidly developing cyclones shows that many of them form in the area of southeast Greenland.

Long-term trends

To study long-term trends, we defined overlapping thirty-year intervals, shifted by ten years from one interval to the next and starting from 1921. In the first two decades of the 20th century, significantly fewer rapidly developing cyclones are identified in CERA-20C than in later decades. This is probably a result of less dense observation networks. For this reason we did not include the first two decades of the century in our investigation. For any particular season or month, some relatively small fluctuations in the number and intensity of rapidly developing cyclones can be seen, but there is no significant overall trend (increasing or decreasing) in the number of such cyclones over the North Atlantic–European area or any subdomains.

Outlook

Reanalysis datasets provide useful information for studying rapidly changing weather systems, such as rapidly developing cyclones in the North Atlantic–European region. We have started to study data from the latest ECMWF reanalysis, ERA5, which provides a 10-member ensemble at a horizontal resolution of 31 km. As we have found that there may be considerable differences in the representation of rapidly changing weather systems between two reanalyses, especially above the ocean and in the Arctic region, a high-resolution ensemble reanalysis is likely to provide valuable information about the uncertainty associated with cases where such differences are found.

For more information on reanalysis, visit: https://www.ecmwf.int/en/research/climate-reanalysis

5   15   25   35   45   55   65   75   85   95   105   115
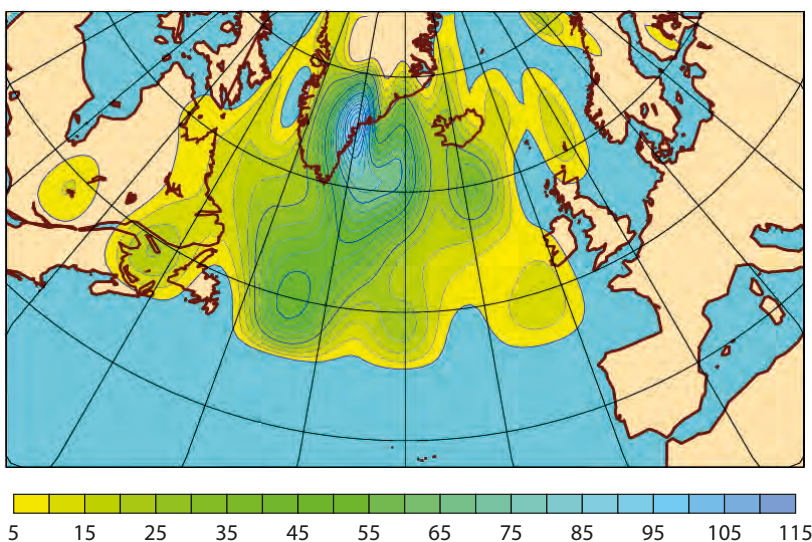
Geographic distribution of rapidly developing cyclones 1981–2010. The map shows the number of rapidly developing cyclones broken down by 5°x5° grid box in the North Atlantic–European region based on CERA-20C for the period 1981 to 2010.
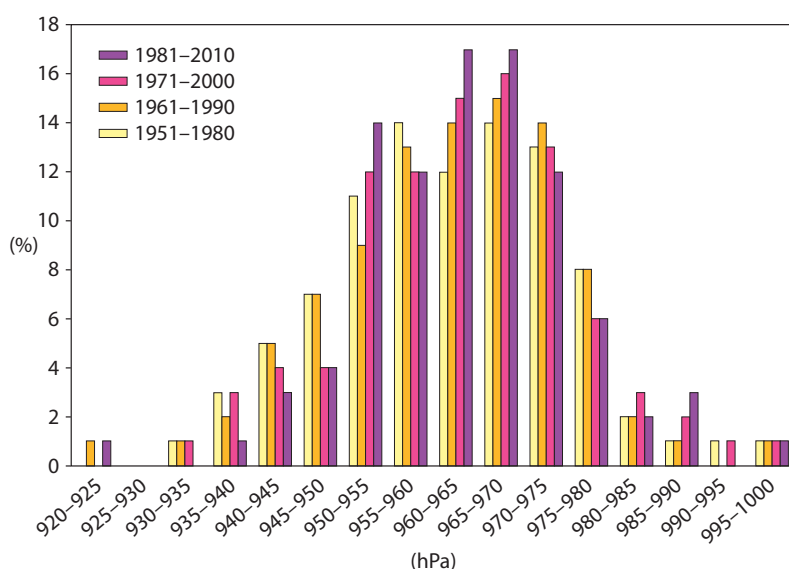
Breakdown according to minimum mean sea level pressure. The chart shows the percentage of rapidly developing cyclones in the North Atlantic–European region from October to March identified by CERA-20C that fall into different minimum mean sea level pressure bins, for four 30-year periods: 1951–1980, 1961–1990, 1971–2000 and 1981–2010.

ECMWF Computing Representatives tell their story

A quarter of ECMWF's supercomputing resources are made available to the Centre's Member States. Of these, up to ten per cent are reserved for Special Projects. Member and Co-operating States also have access to ECMWF's archive. Computing Representatives play a crucial role in authorising users in their countries – currently more than 3,000 in total – to access those resources. They meet once a year at ECMWF for updates on the latest developments at the Centre and to exchange experiences. Here three of them describe the benefits and challenges the role brings.

HANS DE VRIES

I am a weather and climate modelling scientist at the Dutch national meteorological service, KNMI, and have been an ECMWF Computing Representative since 1997. I believe that makes me the longest-serving one. It all started when my boss asked me whether I could take the role over. I agreed and I've never looked back!

Users based in the Netherlands make extensive use of ECMWF's archives and use the high-performance computing facility (HPCF) to run the limited-area model HARMONIE, the KNMI regional atmospheric climate model RACMO, and the EC-Earth Earth system model. Many HARMONIE experiments and EC-Earth analyses would not have been possible without ECMWF's HPCF.

I act as a central contact point who knows about access to the HPCF and has a fairly broad understanding of the possibilities. One of the challenges is to deal with the HPCF budget: it always seems too small at the beginning of the year but invariably turns out to be adequate in the end.

The Computing Representative meetings at ECMWF are very useful. They provide an opportunity to learn about the Centre's plans and to talk to ECMWF staff, including members of the User Support team, and other Computing Representatives. Finding out what other countries are doing is always inspiring. My highlight from last year's meeting was learning about ECMWF's plans for a new data centre.

RAÚL CORREDOR

I am the Head of Administration and Maintenance of Linux Systems at the Spanish national meteorological service, AEMET. I took over the role of ECMWF Computing Representative from a colleague nearly ten years ago.

It was a good move as it has given me an opportunity to participate in and learn from one of the world's best centres in meteorology and computing science. The role has given me a much broader view of the state of the art in computing and helps me with my decision-making at AEMET. An important aspect is to give first-level support to users based in Spain, which is generally very gratefully received.

We run a lot of weather and climate modelling experiments at ECMWF. Currently our main application running at the Centre is the ensemble forecasting system Gamma-SREPS, which is being tested before it is migrated to AEMET's HPCF. ECMWF's facilities were of critical importance to us between 2010 and 2015, when we tested and ran an operational suite of HARMONIE on them until the installation of our new HPC system was complete.

The annual Computing Representative meetings are perfect for collaboration and the exchange of knowledge. Since 2008 I have only missed one meeting. After each meeting I compile a report for users in my country and my organisation so that they know about ECMWF's plans and where to find more information.

TOM DALY
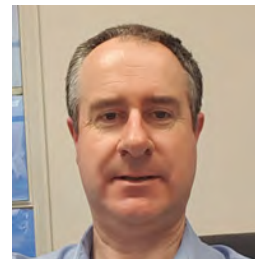
I work as an IT manager in the Technology Division of Ireland's national meteorological service, Met Éireann. Being the Irish Computing Representative is a small but important part of my job. Working at one of the smaller European meteorological services, it is great to be interacting with a world-leading organisation such as ECMWF and knowing that Ireland has a stake in it by virtue of being a member.

Met Éireann users run many applications on ECMWF's HPCF, particularly post-processing tasks. We are currently also operating our limited-area models at ECMWF. The MERÁ (Met Éireann ReAnalysis) climate reanalysis project, which was completed last year, was produced on the Centre's HPCF too. The project was very successful and recently won an Irish Civil Service Excellence and Innovation Award.

Sometimes it can be difficult to devote as much time to the role as I would like. Keeping track of user accounts can also be a challenge. When I took over the role initially there were many dormant Irish user accounts and, with ECMWF's help, I had to do some 'spring cleaning'.

The Computing Representative meetings at ECMWF enable me to meet my European counterparts and to hear what technology each meteorological service is currently using. It is also very beneficial to meet our User Support contact, Paul Dando, as well as other ECMWF colleagues face to face. Last but not least, I enjoy the social side of the meetings!

May meeting

Once a year ECMWF hosts a meeting of Computing Representatives. The next such meeting will take place from 16 to 18 May 2018.

For more information on ECMWF Computing Representatives, visit: https://www.ecmwf.int/en/about/who-we-are/representatives.

For more information on Special Projects, visit: https://www.ecmwf.int/en/research/special-projects.

ECMWF engages with Python community

STEPHAN SIEMEN, BAUDOUIN RAOULT, IAIN RUSSELL

With the development of the Python-based toolbox for the Copernicus Climate Data Store (CDS) and the new Python interface to Metview, ECMWF is stepping up its efforts to provide processing and visualisation options in the Python programming language. Building a Python framework is challenging. ECMWF is therefore looking to benefit as much as possible from activities in the wider Python community.

To engage with the community, ECMWF hosted a 'Workshop on developing Python frameworks for Earth system sciences' on 28 and 29 November 2017. The aim was to bring together key actors from the Python community who develop packages for Earth system sciences. The workshop was a great success as many participants had not met before and could for the first time exchange experiences. The event was split evenly between presentations and working groups. The presentations showed the different functionalities provided by the packages and offered insights into the challenges involved in their development and distribution. Packages represented at the workshop included MetPy, IRIS, MET, Pytroll, MetWork, EPyGrAM, CliMAF, ESMValTool and the Community Intercomparison Suite. For ECMWF, it was a chance to show first results of the work on the CDS toolbox and Metview's new Python interface. Presentations about the xarray package and Cray's plans regarding Python and containers helped to frame these developments in the context of the wider community.

Workshop outcomes

Three working groups were set up to discuss the various challenges and how we as a community can work together better. Each group tackled a different aspect:

- Deploying and packaging Python frameworks
- Handling Big Data in Python
- (Code) Interoperability and common data structures

The discussions focused on the challenge of enabling better interoperability between the various frameworks represented at the workshop. Some of the main points made were that:

- There needs to be a good mapping of metadata between data formats, especially between GRIB and NetCDF. This is because interoperability between packages relies on the handling of data, and metadata plays a crucial role in giving meaning to the data. It was noted that various attempts have been made to solve these problems.
- It is essential to make as much use as possible of core Python packages, such as NumPy, Pandas, xarray and Dask. This will automatically reduce incompatibilities between packages.
- ECMWF needs to support efforts to engage with the Python community and explain its community's needs, for example by participating in a Python-for-Earth-system-sciences session at the annual European Conference on Python in Science.

Everyone was encouraged to contribute to the core packages to improve them instead of implementing new solutions. Participants stressed that it is also important to pick the right tool for the job, ideally one with good community support. The various attempts to implement units for Python packages are an example. By supporting one implementation (with NumPy/xarray), interoperability will be easier. Similarly, interoperability can be achieved if all packages use Dask as their main choice for distributed computation. Here the community could work together to achieve an automatic chunking of data when data are read from NetCDF or GRIB.

There was a strong message on community-led developments and distribution. All packages presented were Open Source, but it was pointed out that putting projects up on GitHub also allows Open Development, which is the first step towards building a community. The UK Met Office has worked on providing conda-forge, a community-driven repository of Python packages for the conda package manager. Using services like this enables developers to automate most of their software release work. Some participants reported that these repositories were not only popular with single users installing Python packages but also very suitable for operational environments.
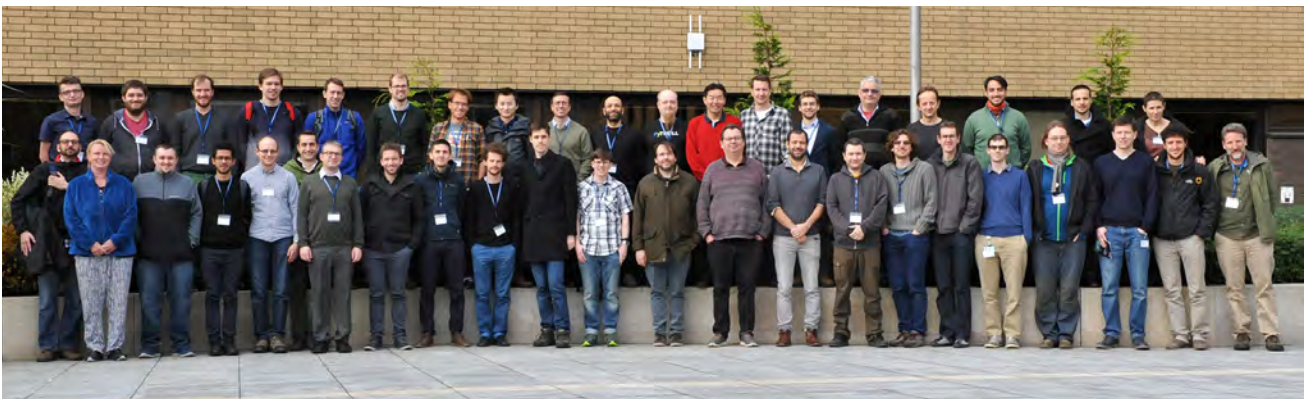
Group photo. The Python frameworks workshop was attended by 55 developers.

ECMWF's new long-range forecasting system SEAS5

TIM STOCKDALE, STEPHANIE JOHNSON,
LAURA FERRANTI, MAGDALENA BALMASEDA,
SIMONA BRICEAG

On 5 November 2017, the latest generation of ECMWF's seasonal forecasting system, SEAS5, became operational. As the name suggests, this is the fifth system we have run at ECMWF to produce real-time seasonal forecasts. Seasonal forecasts provide predictions of how the average atmospheric, ocean and land surface conditions over particular areas and periods of time are likely to be different from the long-term average. They are useful to a number of sectors, such as agriculture, water management, energy and health, and they can help to prepare for potential periods of extreme conditions.

In SEAS5 a number of upgrades have been implemented, in particular in the ocean model, atmospheric resolution, and land surface initialisation. The new configuration also represents a move towards a seamless approach to forecasting across timescales. SEAS5 forecasts show substantial improvements in the tropics, in particular for sea-surface temperature in the equatorial Pacific.

Unlike the configurations of ECMWF's Integrated Forecasting System (IFS) used to produce medium-range high-resolution and ensemble forecasts (HRES and ENS), which are typically upgraded at least once a year, SEAS is upgraded only occasionally, at intervals of four to six years. This slow refresh cycle is partly due to the resources needed to complete the large re-forecast sets required for calibration, and partly to offer users a more stable service. It is possible that this approach might change at some point in the future. We discuss the future evolution of seasonal forecasting at the end of this article.

From System 4 to SEAS5

SEAS5 replaces 'System 4', referred to here as S4. SEAS5 uses IFS Cycle 43r1 and represents six years of IFS development in terms of physics, numerics, new Earth system components and initialisation methods. Many of these improvements were focused on our medium-range forecasts and have been described elsewhere. We focus here on the aspects most important for SEAS5 and on improvements that have been made specifically for the long-range forecasts.

ORCA025, sea-ice model and ORAS5

As for S4, SEAS5 uses the community ocean model NEMO (Nucleus for European Modelling of the Ocean), but with an upgraded model version, ocean physics and resolution. The resolution has been increased from 1 degree and 42 layers in S4 to 0.25 degrees and 75 layers in SEAS5 (ocean model configuration ORCA025z75). The vertical resolution is particularly high in the uppermost part of the ocean, with an increase in the number of levels in the first 50 metres from 5 to 18. The increase in horizontal resolution improves

the representation of sharp fronts and ocean transports. The vertical resolution increase means that the diurnal cycle of sea-surface temperatures (SST) is much better captured, with a 1-metre top level in the new configuration compared to the previous 10-metre top level. The high-resolution ocean model is used both by SEAS5 and the ENS medium-range forecasts.

An important innovation in SEAS5 is the inclusion of prognostic sea-ice. The sea-ice model is LIM2, part of the NEMO modelling framework. In S4, the sea ice was prescribed by sampling the recent history of sea-ice occurrences. The prognostic sea-ice model allows sea-ice cover to respond to changes in the atmosphere and ocean states. The intention is to capture interannual variability and trends in the sea-ice cover. Therefore SEAS5 provides seasonal outlooks of sea-ice cover, which is a product of interest for users.

SEAS5 ocean and sea-ice initial conditions are provided by the new ocean analysis and reanalysis ensemble (ORAS5). ORAS5 uses the same ocean model and sea-ice as the coupled forecasts in SEAS5 and is driven by ocean observations from floats, buoys, satellites and ships. It consists of five ensemble members covering the period 1975 to the present. The ensemble provides information on the uncertainty associated with the (re)analysis. Compared to its predecessor ORAS4, which was used for S4, ORAS5 has higher resolution and updated data assimilation and observational datasets. It provides sea-ice initial conditions by assimilating sea-ice concentration. The underlying SST analysis before 2008 comes from the HadISST2 dataset, the same as that used in the ERA5 climate reanalysis, which is currently in production at ECMWF. From 2008 onwards, the SST and sea ice are given by the OSTIA product, which is used in ECMWF's operational analysis for numerical weather prediction (NWP).

An improved perturbation scheme is used to generate the ensemble of ocean reanalyses. The scheme consists of two distinct elements: perturbations to the assimilated observations, both profiles and surface observations, and perturbations to the surface forcing fields.

Atmospheric resolution upgrade

Horizontal resolution in the atmospheric component of SEAS5 is also significantly higher, increasing from TL255 in S4 to TCo319 in SEAS5. The corresponding grid-point resolution has increased from 80 km to 36 km. Although the spectral resolution increase is less dramatic than the change in grid-point resolution, the ability of the cubic grid to better represent the smallest spectral scales and the energy within them more than makes up for this. The wave model resolution has increased from 1 degree to 0.5 degrees to maintain a match to the atmosphere. The vertical resolution remains at L91. With these resolution changes, the IFS resolution in SEAS5 now exactly matches that used in the extended part of ENS, which covers the 15–45 day time range.
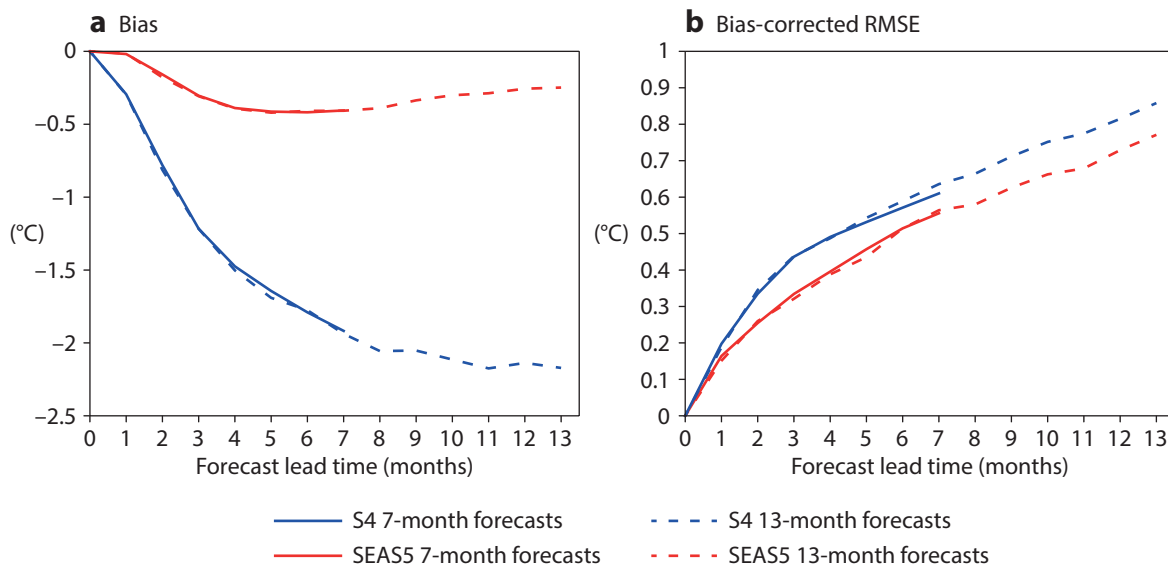
Figure 1 Verification charts for SST anomaly forecasts in the NINO3.4 region showing (a) bias and (b) bias-corrected RMSE for S4 and SEAS5. The long-range forecast (out to 7 months, produced monthly) is shown by the solid line, and the annual-range forecast (out to 13 months, only produced quarterly) is shown by the dashed line. All re-forecast start dates in 1981–2016 are included, a total of 432 dates for the 7-month forecasts and 144 dates for the 13-month forecasts.

Land surface initialisation

A key requirement for seasonal forecasting is that the initialisation of the re-forecasts is consistent with that of the real-time forecasts, otherwise the calibration of the forecasts becomes invalid. This is a particular challenge for the land surface, where real-time analyses and reanalyses have very different resolutions of the heterogeneous land surface. Values from the ERA-Interim climate reanalysis cannot be used anyway because they come from an incompatible land surface model.

In S4 the problem was partially addressed by a custom offline recalculation of the land surface for the ERA-Interim period, which subsequently became known as 'ERA-Interim Land'. This provided initial conditions compatible with the land surface model used in S4, but the mismatch in horizontal resolution between real-time and reanalysis remained severe, and there were also problems with the precipitation forcing used. For SEAS5 a new offline recalculation of the land surface initial conditions was made, at the required TCo319 resolution and with a revised precipitation forcing. Comparison of test forecasts made using this dataset with others using the operational analysis for a recent overlap period showed a generally very good degree of consistency, while also demonstrating the superiority of the operational analysis in terms of the impact on 2 m temperature forecast anomalies. Thus this configuration was used in SEAS5, despite the fact that the consistency between past and present is still not perfect. Similar land surface initial conditions are also now used for the ENS re-forecasts. In future, we expect to be able to create consistent land surface reanalyses on demand, further improving the consistency and reliability of the land surface and snow cover initial state.

Working towards a seamless approach

SEAS5 is a move towards a seamless approach to forecasting across timescales at ECMWF. Our initial goal is, to the extent possible, to minimise the number of IFS configurations used and ensure that the model is run consistently across timescales. SEAS5 is thus configured almost identically to Cycle 43r1 of the extended-range ENS. There are a few small differences which were included because of their perceived relevance or importance for longer-range forecasting. In SEAS5 the tropospheric sulphate aerosol forcing has a decadal time variation, using the same values as in ERA5. Sulphate aerosol has greatly reduced over Europe in the last 30 years, while it has increased over regions such as China, and using a present-day climatology for all of the re-forecasts would slightly affect their accuracy, and thus the calibration of the real-time forecasts. In future it should be possible to find a unified treatment of time-varying sulphate aerosols for all our forecast configurations. SEAS5 also uses the same treatment of time-varying volcanic aerosol as was used in S4 – damped persistence of a highly simplified specification of an initial state. In principle, this method allows us to respond in real time to any large volcanic eruption: we simply add an estimate of the optical depth of the aerosol from a large volcano after it has happened. Although forecasts from before the eruption will be invalid, we have some capability to adjust the real-time system to predict the expected impact once the eruption has occurred. However, our ability to handle a future large eruption is still fairly rudimentary, and we would expect substantial errors to occur, particularly in the response of the northern hemisphere winter circulation.

A final difference from ENS is that the tropical non-orographic gravity wave drag was retuned to ensure a

a S4
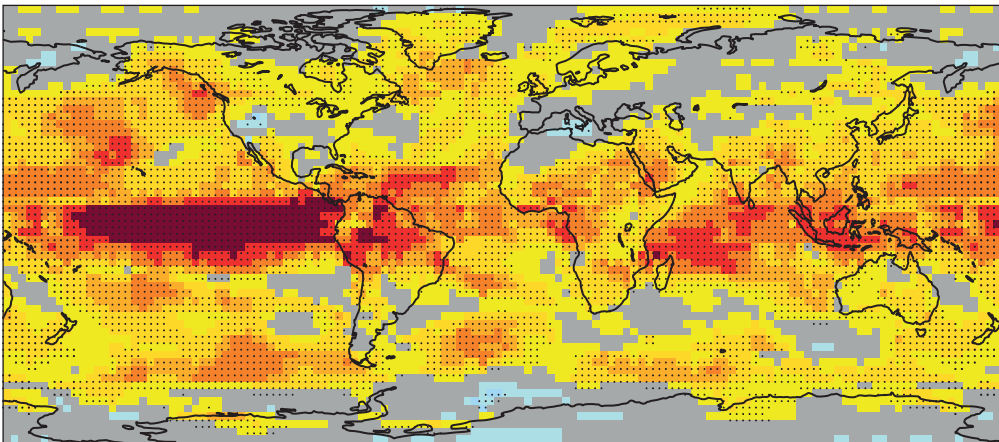
b SEAS5
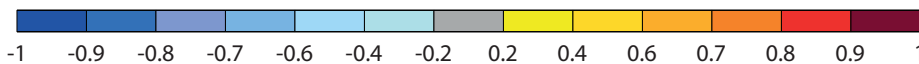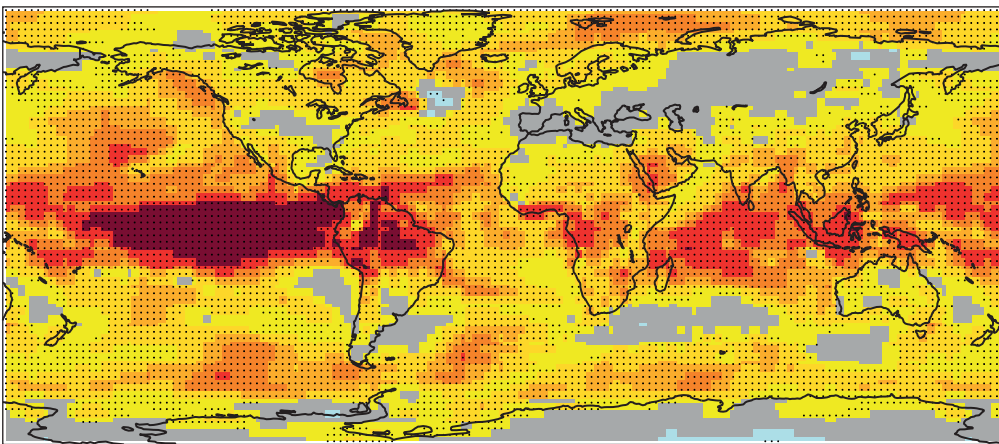
Figure 2 Anomaly correlation for ensemble mean December–January–February 2 m temperature predictions from 1 November for (a) S4 and (b) SEAS5. Measured skill in SEAS5 is higher partly due to the increased ensemble size, but beyond this there are real and statistically significant improvements in the tropics and in the Arctic. An anomaly correlation of 1 corresponds to a perfect deterministic forecast, while 0 means no skill.

| -1 | -0.9 | -0.8 | -0.7 | -0.6 | -0.4 | -0.2 | 0.2 | 0.4 | 0.6 | 0.7 | 0.8 | 0.9 | 1 |

reasonable phase evolution of the stratospheric quasi-biennial oscillation (QBO). This retuning, which is resolution dependent, has now been applied to the ENS. This is an example of how we expect our seamless approach to work: even if the same configuration choices (e.g. horizontal and vertical resolution, or the balance of resources between different parts of the Earth system model) may not be quite optimal for different forecast timescales, by reducing the number of effective configurations we can become more efficient in identifying and fixing problems, to the benefit of forecast quality at all timescales.

Operational implementation

Important changes have been made to how seasonal forecasts are run operationally, so as to enhance the service given to users. The release date has been brought forward from 12 UTC on the 8th day of each month to 12 UTC on the 5th day of each month. The re-forecast period has been increased to cover 1981–2016, a 36-year period, compared to 1981–2010 for S4. When it comes to assessing past performance, the longer the period available the better. The re-forecast ensemble size has also been increased from

15 to 25, which reduces sampling uncertainty in assessing performance, especially in the mid-latitudes.

Users accessing the plots on our website will see a restructuring of the plots, with the verification plots now grouped in separate families. Full verification based on the 1981–2016 re-forecasts is available. There are also some minor enhancements to the range of forecast plots available, most notably the addition of SST anomaly plumes for the NINO1+2 region, which is important for Peru and Ecuador.

A final important change is that, although the verification is made using the full 1981–2016 re-forecast period, the charts of fields such as 2 m temperature and precipitation are presented as anomalies relative to the more recent 1993–2016 period. This is to ensure that the anomalies remain relevant in the context of climate change. Temperatures (and some other fields such as geopotential height) have changed sufficiently over the last 36 years for seasonal mean values to be almost always warm compared to the early years of the re-forecast period. The result is that all too often the temperature forecasts are that it will always

be warm everywhere, relative to an increasingly distant past. This may be a correct probabilistic statement about next season's expected weather, but it is of limited use to a typical user who wants to know what to expect relative to a more recent past. We do not want to use too short a reference period, which would bring its own problems regarding stability and sampling issues, but the 24-year period 1993–2016 seems broadly appropriate. It is also consistent with how the EU-funded Copernicus Climate Change Service (C3S) being implemented by ECMWF will present its new multi-model forecasts (see next section). For users who want to calibrate and reference the SEAS5 forecasts in ways specific to their own application, the full 36 years of re-forecast data remains available.

SEAS5 and C3S

The combination of a major resolution increase and large increases in the number of re-forecast integrations has come at a very substantial computational cost. A significant part of the cost of SEAS5 production is met by C3S because SEAS5 is one of the core contributions to the new C3S multi-model seasonal forecasting service. The fact that C3S was willing to fund the computational costs of the re-forecasts, together with some human resources, enabled us to implement a substantially higher resolution system than we had otherwise planned for.

While ECMWF retains ownership and control of the full-resolution real-time forecasts, both the re-forecast dataset and a comprehensive 1 degree resolution dataset from the real-time forecasts will be publicly distributed by C3S. In its operational phase, the C3S release date will be the 10th day of each month, and any user anywhere in the world will be able to access both multi-model and individual SEAS5 plots on the C3S website, and download C3S multi-model and SEAS5 data for use in whatever product the user wants. The participation of SEAS5 in the open-access C3S multi-model system should bring major benefits, such as the increased use of our forecasts and enhanced feedback to us from the global community. C3S and other Copernicus services have the resources and community engagement to enhance and develop seasonal forecast products and applications way

beyond what was possible as an ECMWF core activity.

SEAS5 performance

SEAS5 has brought consistent improvements in seasonal forecasts in the tropics while the picture in the extratropics is more mixed.

Tropical performance

SEAS5 tropical SST biases have substantially improved over S4, particularly in the equatorial Pacific. As shown in Figure 1, the bias in the NINO3.4 region has improved by nearly 2°C in the annual-range forecast, and the root-mean-square error (RMSE) has improved by approximately 0.1°C at forecast leads longer than two months. Accumulated improvements in physics since S4 have improved various aspects of the tropical mean climate, and the combination of the improved ocean model and improved atmospheric physics results in improved 2 m temperature prediction skill in the tropical Pacific, visible in Figure 2. Skill is slightly degraded in the tropical Atlantic, though.

Extratropical performance

In the extratropics, increased ocean horizontal resolution and improvements in ocean vertical mixing have improved some SST biases, for example in the North Pacific, while degrading others. In the North-West Atlantic, a region of decreased skill has appeared (visible as a small patch of blue in Figure 2). As shown in Figure 3, this is due to SEAS5 failing to capture the decadal variability of this region. In contrast, S4 was able to simulate the long-term oscillation. Initial investigations suggest this is due to the change from ORAS4 to ORAS5 initial conditions; investigations are ongoing.

Improving the skill of seasonal forecasts over Europe is always challenging because average predictability is low, and scores are subject to considerable sampling uncertainty. Nonetheless, recent seasonal forecast systems have tended to show a fairly consistent picture of the pattern of grid-point skill over the European region, including marked seasonal variation. Figure 4 shows grid-point anomaly correlation skill for 2 m temperature
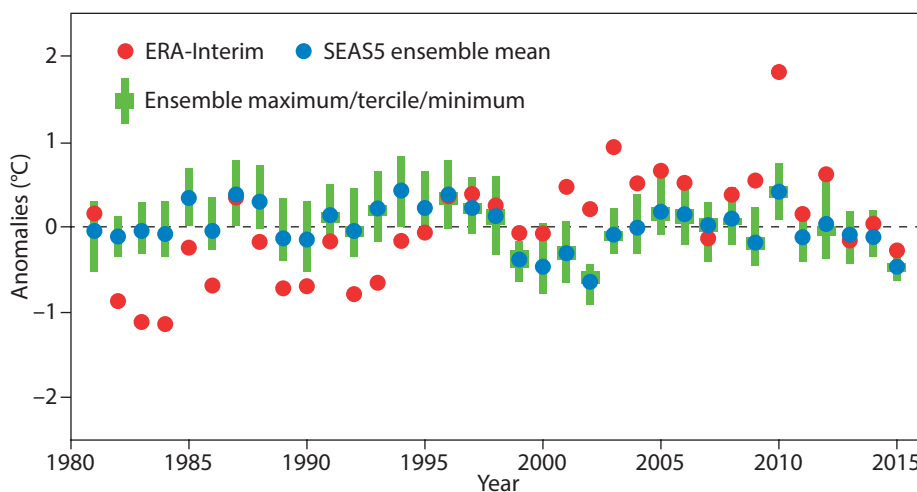
Figure 3 Time series of December–January–February SST anomalies in a small box in the North-West Atlantic from 1981 to 2015. Red dots are from the ERA-Interim reanalysis, while blue dots and green bars are SEAS5 forecasts from 1 November. The SEAS5 forecasts do not capture the shift from negative anomalies to positive anomalies in the late 1990s, compromising the skill in this region.

forecasts for Europe for different seasons. Skill comes from capturing both interannual variations and long-term trends. This deterministic measure of skill can be complemented by probabilistic measures such as reliability, shown for summer and winter in Figure 5. This score is created by aggregating forecast performance over all grid points in Europe, so we lose spatial detail to gain a better probabilistic assessment. Such compromises are inevitable given the relatively small number of cases (36 years) that we verify. The reliability plot suggests that, although average skill is often low over Europe, particularly in winter, reliability is generally quite high. Note, though, that reliability aggregated across a region does not guarantee reliability at individual points. For full information, including all start dates, target seasons and multiple measures of skill, users should look at the extensive long-range verification charts provided online at: *www.ecmwf.int/en/forecasts/charts/catalogue/*

Sea ice and stratosphere

The new prognostic sea ice gives SEAS5 the ability to predict sea-ice cover in the coming season. Although the forecasts are not completely unbiased, they result in more accurate sea-ice concentrations than S4, as shown in Figure 6. In the stratosphere, zonal wind and temperature biases have increased with respect to S4. Part of this is due to an unusual situation where higher horizontal resolution degrades the model in this area, for reasons that are still not fully understood. Stratosphere biases are currently being worked on at ECMWF.

Future strategy

SEAS5 was developed to be very close to the IFS configuration used for the monthly extension of the ENS. We plan to continue the path of scientific convergence, so that any improvements needed by SEAS are implemented on a continuous basis in the IFS, ready to be picked up when the next seasonal system is configured. The ENS and SEAS will be consistent in the sense that any desired changes important for the long range will already have been implemented in ENS. Each new IFS cycle will be tested for its long-range forecast performance, both in re-forecasts

a Spring   **b** Summer

c Autumn   **d** Winter

-1 -0.9 -0.8 -0.7 -0.6 -0.4 -0.2 0.2 0.4 0.6 0.7 0.8 0.9 1

Figure 4 SEAS5 anomaly correlation skill for 2 m temperature in the European region, based on 1981–2016 re-forecasts, for (a) March–April–May, (b) June–July–August, (c) September–October-November, and (d) December–January–February, predicted from 1 February, May, August and November, respectively.

a Europe, summer

b Europe, winter

Figure 5 Reliability of forecasts of the probability that 2 m temperature anomalies will be in the upper tercile category for points in Europe (land and sea) for (a) 1 May forecasts for June–July–August and (b) 1 November forecasts for December–January–February. Both seasons have good overall reliability, as indicated by points lying close to the diagonal, but the June–July–August forecasts are sharper, i.e. more forecasts are far from the climatological value of 0.33. The distribution of forecast probabilities is indicated on the plot by the size of the circles, with bigger circles corresponding to more cases.
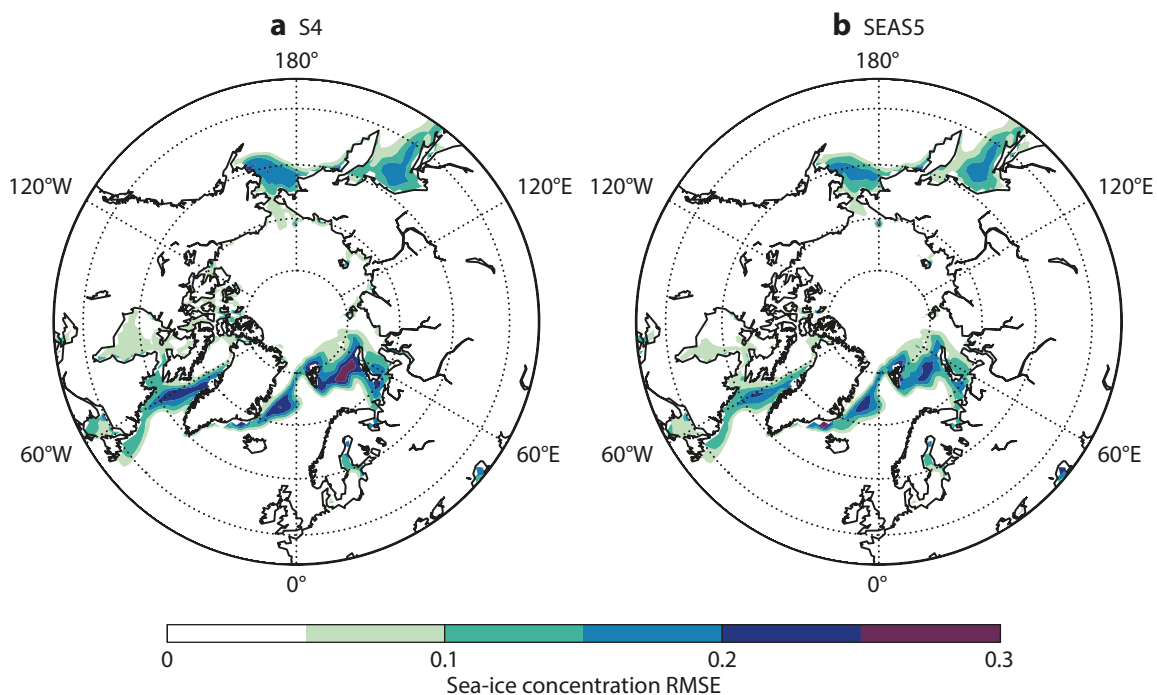
Figure 6 RMSE in predictions of December–January–February sea-ice concentration, for forecasts from 1 November, for the period 1981–2016 from (a) S4 and (b) SEAS5, showing the reduction in error due to the interactive sea-ice model.

and a real-time configuration, so that once it is decided to update SEAS, this can be done easily.

This behind-the-scenes approach to making our forecast configurations more seamless leaves open the question as to whether more substantial changes might be made in how SEAS is run. Firstly, might SEAS be updated with every IFS cycle? This has some obvious drawbacks: a substantial increase in the cost of the re-forecasts; re-forecasts are only available a short time before the corresponding real-time forecast; a much more frequently changing system for users to work with. It also comes with a dilemma: if we insist that each new cycle at least maintains the long-range forecast performance, then the cost and difficulty of creating new IFS model cycles may substantially increase. If, on the other hand, we accept that the long-range forecast performance may fluctuate from cycle to cycle, then this could have a negative impact on seasonal forecast users.

However, if frequent updates of the long-range forecasts were considered beneficial overall, for example because the IFS long-range performance was sufficiently stable for us to be confident that cycle updates would only ever have a small impact, then it might be feasible to better integrate the ENS and long-range ensembles. That is, it should be possible to design a single ensemble system where a range of resolutions and forecast lengths produce a truly seamless forecast system on timescales from days to seasons. Such a system would have some attractions beyond the purely aesthetic: cost savings might ensue from a well-designed ensemble (perhaps enough to compensate for the extra cost of more frequent long-range re-forecasts); long-range

forecast products could be issued more frequently; and forecast products would be consistent across the different time ranges.

The future evolution of ENS and SEAS will in the end be determined by user requirements and priorities. Our scientific goal is to build a forecast model that fully exploits all sources of long-range predictability, and the necessary data assimilation systems to initialise the relevant parts of the Earth system. SEAS5 is but one step on the journey; there is still much ahead to look forward to.

For more information on SEAS5 and access to the SEAS5 User Guide, visit: *www.ecmwf.int/en/forecasts/documentation-and-support/long-range*

FURTHER READING

Tietsche, **S.**, **M.A. Balmaseda**, **H. Zuo** & **K. Mogensen**, 2015: Arctic sea ice in the global eddy-permitting ocean reanalysis ORAP5. *Climate Dynamics*, **49**, 775–789, doi:10.1007/s00382-015-2673-3.

Zuo, **H.**, **M.A. Balmaseda** & **K. Mogensen**, 2015: The new eddy-permitting ORAP5 ocean reanalysis: description, evaluation and uncertainties in climate signals. *Climate Dynamics*, **49**, 791–811, doi:10.1007/s00382-015-2675-1.

Zuo, **H.**, **M.A. Balmaseda**, **E. de Boisseson**, **S. Hirahara**, **M. Chrust** & **P. De Rosnay**, 2017: A generic ensemble generation scheme for data assimilation and ocean analysis. *ECMWF Technical Memorandum* **No. 795**.

Why warm conveyor belts matter in NWP

MARK RODWELL, RICHARD FORBES,
HEINI WERNLI (ETH Zurich)

A warm conveyor belt (WCB) is a coherent warm and moist airstream, which originates in the boundary layer of an extratropical cyclone's warm sector. Air within the WCB ascends in a day or two to the upper troposphere while moving poleward. WCBs are the primary cloud- and precipitation-generating flow in extratropical cyclones, and they can be associated with extreme precipitation. In this article, based on work carried out jointly with ECMWF Fellow Heini Wernli and his team at ETH Zurich and discussed at a recent bilateral meeting, we illustrate two more ways in which WCBs are important in numerical weather prediction (NWP): The microphysical processes they involve can have a strong impact on the larger-scale dynamics and they are a major source and magnifier of forecast uncertainty.

Correctly modelling WCBs is of great relevance to ECMWF's Strategy to 2025, which calls for improved forecasts of extreme weather and regime transitions and increased reliability and sharpness of ECMWF ensemble forecasts. Here we suggest two ways to improve the representation of WCBs in weather models: better cloud microphysics and improvements in the initialisation of humidity.

An ascending airstream

In the northern hemisphere, WCBs are more frequent in winter than in summer, with two preferential ascending regions in the western North Atlantic and North Pacific. In
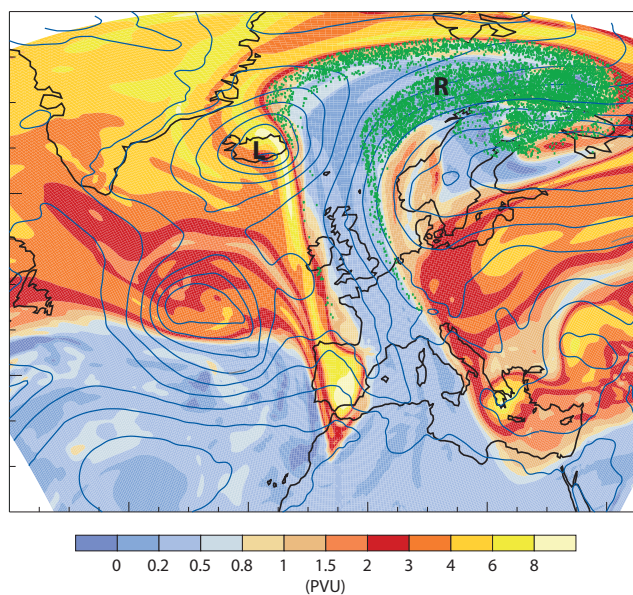
Potential vorticity　A

To a good approximation on synoptic scales, potential vorticity (PV) is the product of the vertical component of the absolute vorticity and the stratification, where absolute vorticity is a measure of the spin of the air and stratification is the vertical gradient in potential temperature (the temperature that air would have if it were brought to a reference pressure of 1,000 hPa). PV is conserved by an air parcel in the absence of friction and diabatic heating.

In the context of WCBs, ascent and poleward mass transport leads to the formation and amplification of upper-level negative PV anomalies, which can cause downstream wave-breaking and the subsequent initiation of periods of calm, 'blocked' conditions.

Figure 1, a WCB is associated primarily with a low-pressure system near Iceland (L). It is seen to transport low values of potential vorticity (PV, blue shading) from the subtropical lower troposphere to the extratropical upper troposphere (Box A). 'WCB trajectories' can be calculated by searching for air parcels that rise more than 600 hPa in 2 days and which, at some time, are coincident with a low pressure system. Green dots show where such ascending air-parcel trajectories intersect with the upper-tropospheric 310 K isentropic surface (the surface of constant potential temperature) and thus contribute to the formation of a large-amplitude upper-level ridge (R). Most of the low-PV air masses forming the ridge ascended cross-isentropically as part of the WCB and experienced intense diabatic heating during the previous one to two days.

Figure 2 shows another WCB event over the eastern North Atlantic. Ascending air parcels are shown at various heights along the WCB trajectories (blue, yellow and red circles). The pressure level of cloud tops, indicated by grey shading, and the occurrence of deep convection (green dots) highlight the intense heating taking place. The grey contours show mean sea-level pressure with a low pressure system to the west of the WCB, and the red contour shows 2 PVU potential vorticity at 320 K. Again a ridge can be seen building at the end of the WCB trajectories.

Amplification of uncertainties

Poor forecasts for Europe are often associated with the initiation of such ridge events, which can lead to blocking conditions (*Ferranti et al.*, 2015). One such case is shown in Figure 3a for ECMWF high-resolution forecasts (HRES), ensemble forecasts (ENS) and the control forecast (a forecast at ensemble resolution with unperturbed initial conditions and model physics, CTR). Time series of root-mean-square errors (RMSE) for forecasts of European 500 hPa geopotential height at day 6 show a spike in errors for forecasts initiated between about 6 and 7 March 2016. The fact that some ENS members did not suffer large errors suggests that this is a situation of low predictability rather than a situation which

Figure 1 Potential vorticity (PV) on the 310 K isentropic surface (shading), mean sea-level pressure (contour interval 5 hPa) and the locations where 2-day WCB trajectories intersect the 310 K surface (green dots) at 0600 UTC on 31 January 2009. Figure from *Joos & Wernli* (2012).
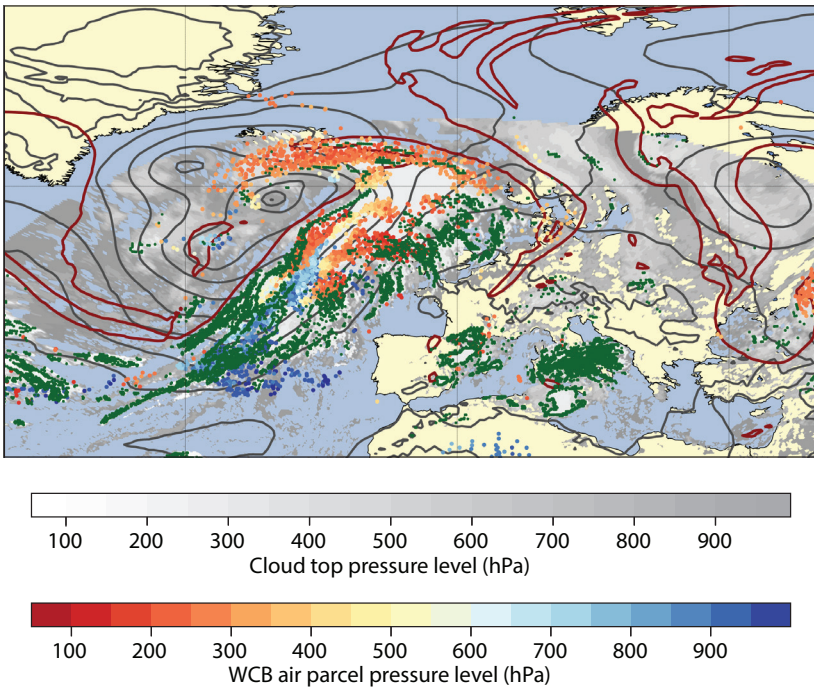
Figure 2 Cloud structure and WCB of cyclone Vladiana at 15 UTC on 23 September 2016. Blue, yellow and red dots indicate the pressure levels of WCB air parcels for this time. The grey shading shows the pressure at cloud-top level and the green dots indicate deep convective clouds based on Meteosat Second Generation satellite data. The grey contours show mean sea-level pressure (with contour interval 5 hPa) and the red contour shows 2 PVU at 320 K. Plot courtesy of Annika Oertel.

the model is unable to represent adequately. Figure 3b shows the differences at day 2 between the five best and the five worst performing members at day 6, a form of 'ensemble sensitivity' experiment. It highlights that the differences at day 6 originate from differences in a trough–ridge feature over the central North Atlantic at day 2. Figure 3c shows the presence of WCB trajectories at this time and location, suggesting that WCBs (including any embedded convection) act to enhance uncertainty in the subsequent forecast flow evolution.

Based on very short (12-hour) forecasts within the Ensemble of Data Assimilations (EDA), Figure 4a shows an example of the uncertainty growth rate in PV at 315 K. This is high in the WCB event over the North Atlantic and in the mesoscale convective system (MCS) event over North America, particularly to the north of some of the moist processes depicted by the ensemble-mean precipitation, where the 315 K isentropic surface is closer to the strong PV gradients at the tropopause. In both cases, convective aspects appear to be emphasized. Their combined effect on the forecast was high uncertainty about the formation
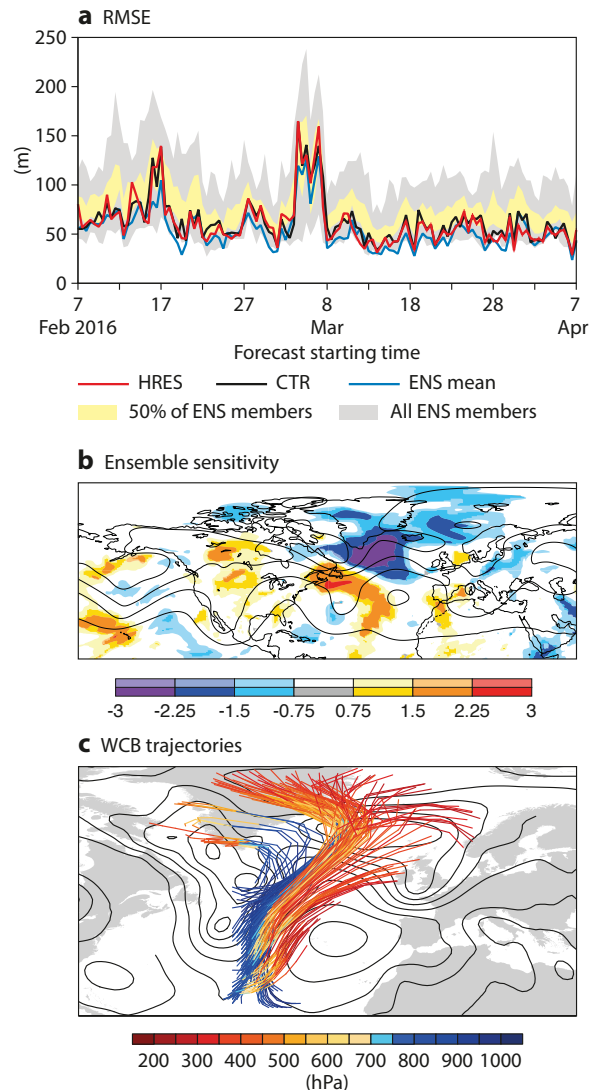
Figure 3 The plots show (a) the evolution of root-mean-square error (RMSE) of 500 hPa geopotential height for ECMWF forecasts over Europe (12.5°W–42.5°E, 35°N–75°N) at day 6, (b) the normalised difference at day 2 of the 5 forecasts with largest RMSE over Europe at day 6 and the 5 members with the smallest RMSE over Europe at day 6, for forecasts starting at 00 UTC on 7 March 2016 (statistically significant differences at the 95% confidence level are shown in bold colours, contours show the ensemble mean of geopotential height at 200 hPa at day 2), and (c) two-day forward WCB air parcel trajectories based on ECMWF analysis data, starting at 00 UTC on 9 March 2016 in the region 70°W–20°W, 20°N–60°N and fulfilling the criterion of ascending more than 550 hPa within 2 days (contours show mean sea-level pressure at 00 UTC on 9 March 2016). Panels (a) and (b) are from *Magnusson* (2017), panel (c) courtesy of Christian Grams, Linus Magnusson and Erica Madonna.

a Uncertainty growth rate

b Change in background variance

-21   -15   -9   -3   3   9   15   33
(0.01/hour)
→ 30 m/s

-30   -10   -6   -2   2   6   10   18
(m²/s²)
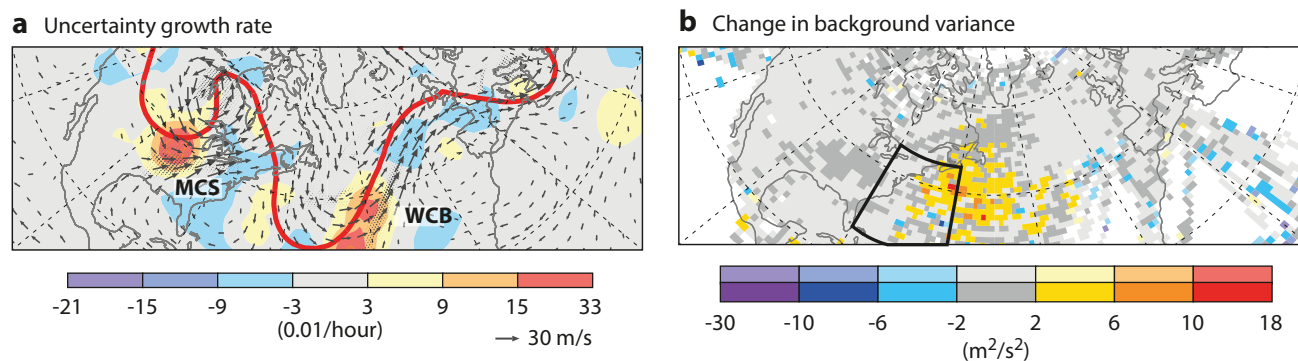
Figure 4 The plots show (a) the one-day mean, centred on 06 UTC on 7 March 2017, of the synoptic-scale uncertainty growth rate (shading) for PV on the 315 K isentropic surface (derived from the background forecasts of the ECMWF Ensemble of Data Assimilations, EDA, and with the transport of uncertainty by the ensemble-mean horizontal winds removed to highlight local sources), the 2 PVU contour on the 315 K surface (red, indicating where this surface intersects the tropopause) and horizontal winds on the 850 hPa surface (vectors) based on the unperturbed control member of the EDA, and the ensemble-mean 24 h accumulated precipitation (dots, with the largest indicating about 50 mm precipitation), and (b) the change in EDA background variance in zonal winds at 200 hPa, co-located with aircraft observations and based on a composite of the 50 strongest WCB events with inflow in the box indicated one day before, and a corresponding composite of 87 non-WCB situations.

of a block over Europe by day 6. More systematically, for a composite of many WCB events off the east coast of North America, we can see in Figure 4b that, after one day, such events lead to an increase (approximately a doubling) of uncertainty in upper-tropospheric winds compared to no-WCB events. Results are only plotted for locations where aircraft observations are available; this co-location with observations is important if we are to be able to assess whether this doubling of uncertainty is warranted.

Sensitivities to clouds and convection

Latent heating clearly contributes to the ascent within WCB events, but how sensitive are the upper-level PV and downstream impacts to the details of cloud microphysics and convection? Figure 5 shows the upper-level PV structure and the blocking evolution for a WCB event which occurred during the NAWDEX (North Atlantic Waveguide and Downstream Impact Experiment) field campaign in September and October 2016. The left-hand panels show a single control forecast and the right-hand panels show a single forecast where latent heating was artificially turned off in the WCB region within the layer 900–500 hPa. For the control forecast we see that strong ascent leads to upper-level divergent outflow on the western flank of an amplifying ridge. In the event this ridge then broke anticyclonically and led to the onset of blocking conditions. When latent heating is turned off (right-hand panels), the ascent and outflow are reduced, the ridge does not amplify and, in the absence of wave-breaking, the block is not initiated. This example illustrates how the physics within WCBs can play a crucial role in the initiation of blocking anticyclones, and for the upper-level wave dynamics in general.

To consider the consequences of more realistic forecast model deficiencies, Figure 6 shows heating rates due to individual microphysical processes integrated along WCB trajectories for the North Atlantic cyclone investigated by *Joos & Wernli* (2012) and shown in Figure 1. The heating rates were simulated with ECMWF's Integrated Forecasting

System (IFS – left) and the regional COSMO (Consortium for Small-scale MOdelling) model (right). There are striking differences between the respective contributions to the total heating from condensation and depositional growth of ice and snow, implying large uncertainties in the details of the cloud microphysics. Note also that convective heating is likely to mean that real air parcels will deviate from the derived trajectories. Such differences are likely to lead to different trajectory slopes, and thus to differences in the magnitude and latitude of the upper-tropospheric PV anomaly and the subsequent downstream development. For example, *Gray et al.* (2014) highlighted too weak forcing by WCBs as a possible reason for upper tropospheric ridge errors in the IFS.

The impact on the circulation of uncertainties in cloud microphysics is demonstrated in Figure 7, which shows a snapshot of a rapidly deepening cyclone over the North Pacific, simulated with the IFS. Figure 7a shows lower-tropospheric PV associated with the cyclone on 11 April 2017. As the precipitating air wrapped around and into the cyclone centre, snow sublimation (Figure 7b) and snow melting (Figure 7c) at low levels led to relatively more cooling below than above the 24h back-trajectories of air parcels within this layer, and thus to increased stratification and PV at the level of the parcels. However, further east in the band of descending air beneath the cold frontal region, sublimation (Figure 7b) tends to occur above the parcel trajectories, as the snow falls into the cold dry air from the frontal cloud, and this acts to decrease stratification and PV at the level of the parcels. The melting aspect seems to have less impact on the stratification and PV along the cold front at this level. These results (and more idealised studies such as by *Crezee et al.*, 2017) demonstrate that the details of microphysics can have a significant impact on the material change in PV, and thus potentially on the larger-scale circulation (*Hoskins et al.*, 1985).

a Control, day 3

b Sensitivity experiment, day 3

c Control, day 6

d Sensitivity experiment, day 6

0   0.5   1   1.5   2   2.5   3   3.5   4   5   6   8
(PVU)
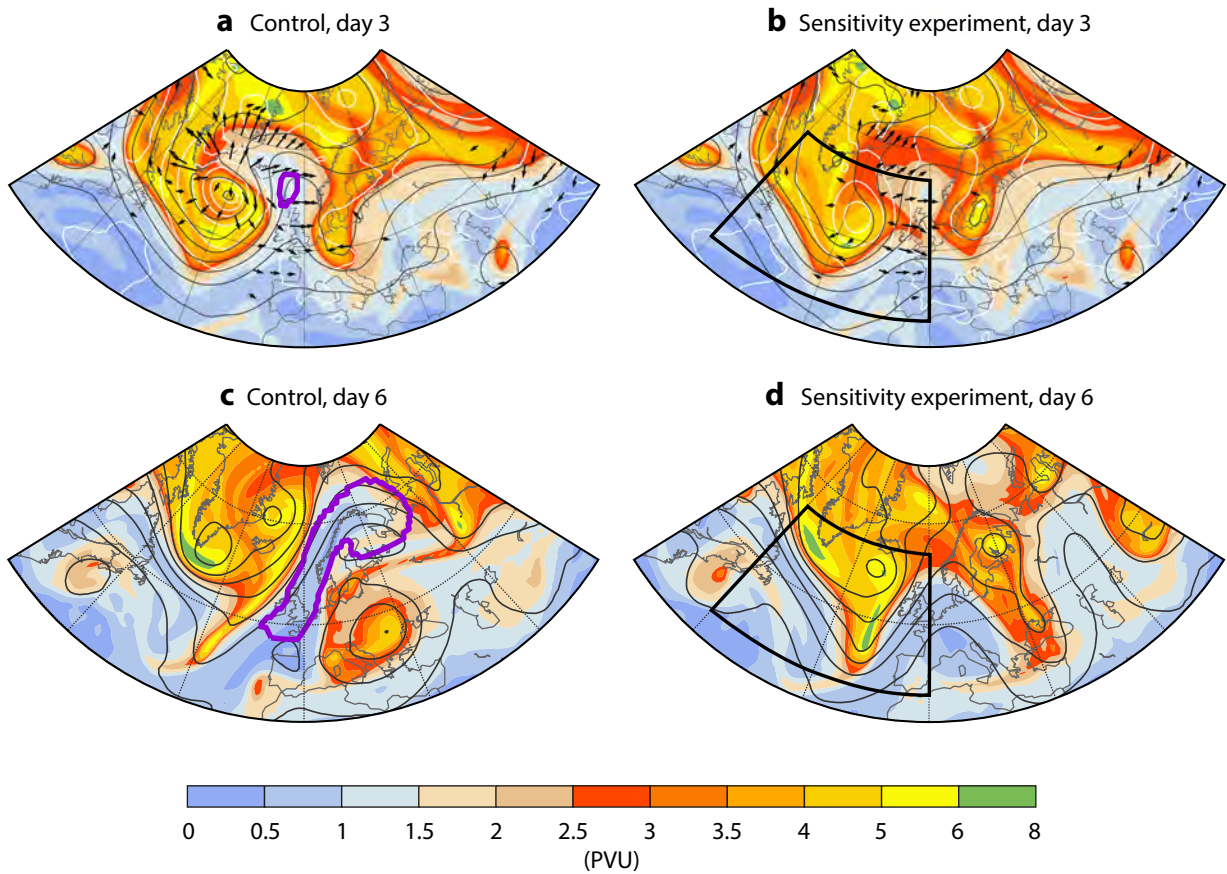
Figure 5 Vertically averaged PV between 500 and 150 hPa (shading), 500 hPa geopotential height (black contours), diagnosed block (purple contour), and vertically-averaged divergent wind between 500–150 hPa (arrows, upper panels only) for (a) the IFS control simulation after 3 days, (b) a sensitivity experiment with latent heating turned off in the box indicated within the layer 900–500 hPa, after 3 days, (c) the control simulation after 6 days, and (d) the sensitivity experiment after 6 days. Plots from work with Daniel Steinfeld, Maxi Boettcher and Stephan Pfahl.

a IFS

b COSMO

— Total   — Condensation   — Dep. growth   — Convection   — Evaporation rain   — Melting of snow
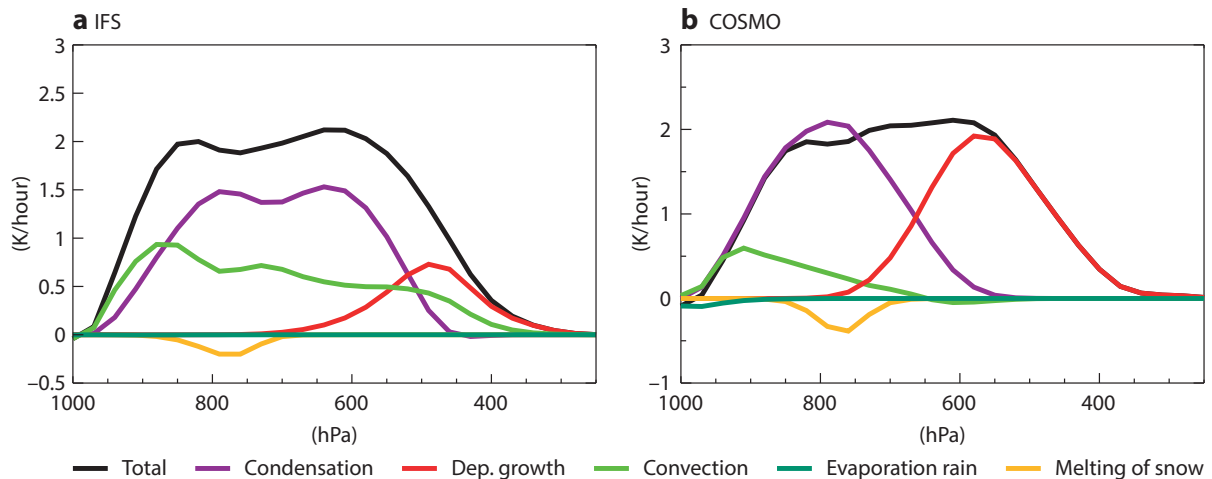
Figure 6 Average diabatic heating rates as a function of pressure, following the WCB trajectories initiated at 06 UTC 29 January 2009 as shown in Figure 1, for each of the dominant physical processes, based on (a) IFS Cycle 41r1 microphysics (adapted from *Joos & Forbes*, 2016) and (b) the regional COSMO model used in *Joos & Wernli* (2012).
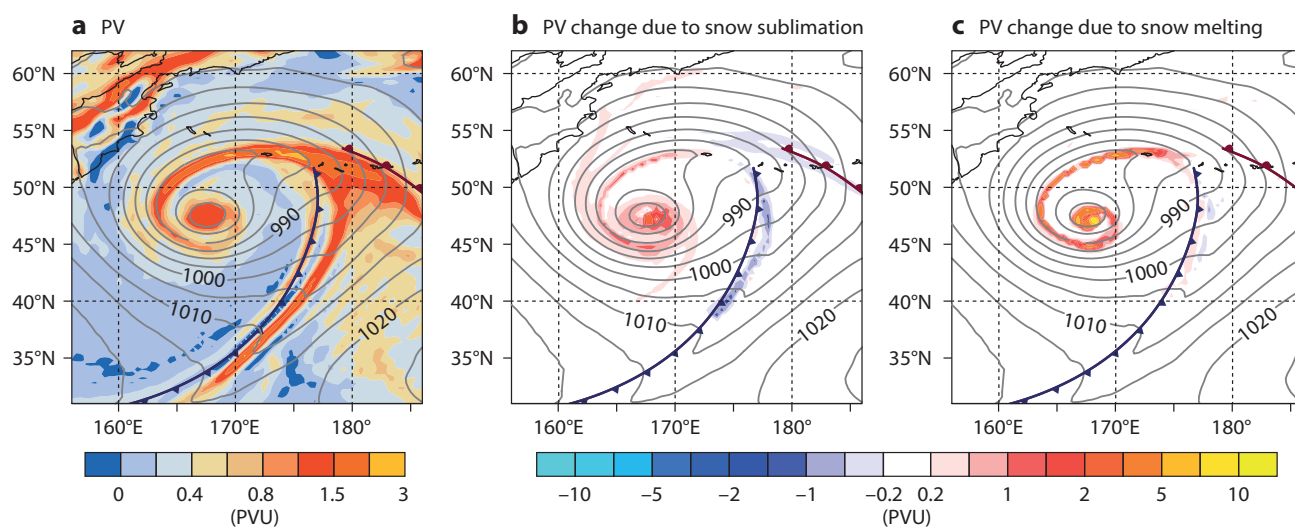
Figure 7 The shading in these plots shows (a) the PV distribution in the lower troposphere (the 950 to 850 hPa layer) for a cyclone in its mature stage (about 2 days after genesis), (b) the change in PV associated with the sublimation of snow over the previous 24 hours, and (c) the change in PV associated with the melting of snow over the previous 24 hours. PV changes are integrated along back-trajectories of air parcels ending up within the lower tropospheric layer. Contours show mean sea-level pressure and the warm and cold fronts are drawn using the usual symbols. The forecast was produced using IFS Cycle 43r1 at a resolution of TCo639. Plots from work with Roman Attinger, Maxi Boettcher and Hanna Joos.

Using observations to identify model deficiencies

Given the importance of WCBs in forecasting and in view of the forecast sensitivities to model formulation, there is a clear potential for forecast model improvement. Observations are key to any such improvement. In numerical weather prediction, millions of observations (conventional in-situ and satellite remote-sensing) are assimilated each day and there is scope to use these to guide the development process. Nevertheless, in cloudy situations such as WCBs, there is a lack of relevant observations and there are difficulties with assimilating existing observations. Hence there is also a need to make use of non-assimilated observations and to undertake dedicated field campaigns.

Radar and lidar data from the 'A-train' satellite constellation provide useful information on cloud composition and can be used to diagnose deficiencies in forecast models. In Figure 8 the modelled cloud phase of WCB air parcels is overlaid on CloudSat radar reflectivity observations at 00 UTC on 3 January 2014. Although there is no simple relationship between reflectivity and cloud phase, the high reflectivity values below 6–8 km indicate that the WCB air parcels form part of very strongly precipitating clouds, with snow above and rain or melting snow below the melting layer. In the upper part of the clouds, the lower reflectivity values indicate ice clouds rather than falling snow. This ability to match A-train observations such as CloudSat radar and CALIPSO lidar with WCB events, and the use of observation operators (which map model fields to observations) should help in the diagnosis of modelling deficiencies. Research to assimilate such radar/lidar data is under way and will be useful for forecast initialisation when the coverage of such observations increases through the EarthCARE satellite programme.

Figure 8b shows data from a return flight across the WCB of cyclone Vladiana made on 23 September 2016 during the NAWDEX field campaign. Ice particle concentrations measured by an instrument on the BAe146 FAAM aircraft are plotted in a narrow observation band on top of the corresponding predicted profiles from a short forecast. Note that high concentrations are observed around 1310 UTC when the aircraft first passed through the WCB region. Lower values are then observed on the other side of the WCB at around 1320 UTC before the aircraft returned back through the WCB at around 1330 UTC. These rises and falls in observed concentrations agree qualitatively with those predicted by the short forecast, but there is scope for improvements based on this co-location of observational and short forecast data.

Another intensive observational period during the NAWDEX campaign focused on the strong water vapour transports that are important for downstream high-impact precipitation events. Figure 9 shows water vapour profiles observed by lidar on board the HALO aircraft. The strong low-level humidity along the eastern return leg (within a strong south-westerly flow) is indicative of an 'atmospheric river' (*Lavers et al.*, 2011) and led to heavy precipitation over Scandinavia when strong WCB ascent occurred from this moist filament. Dropsonde data from this and other NAWDEX flights were assimilated in real time into the ECMWF operational analysis, and comparisons with the background forecast and model process tendencies should provide insight into model deficiencies.

Improving the forecast initialisation

It is important to correctly initialise moisture in situations with strong moisture transports in our forecasts (see also *Schäfler & Harnisch*, 2015), but this is difficult to achieve in practice. For example, Figure 10 shows a variance budget
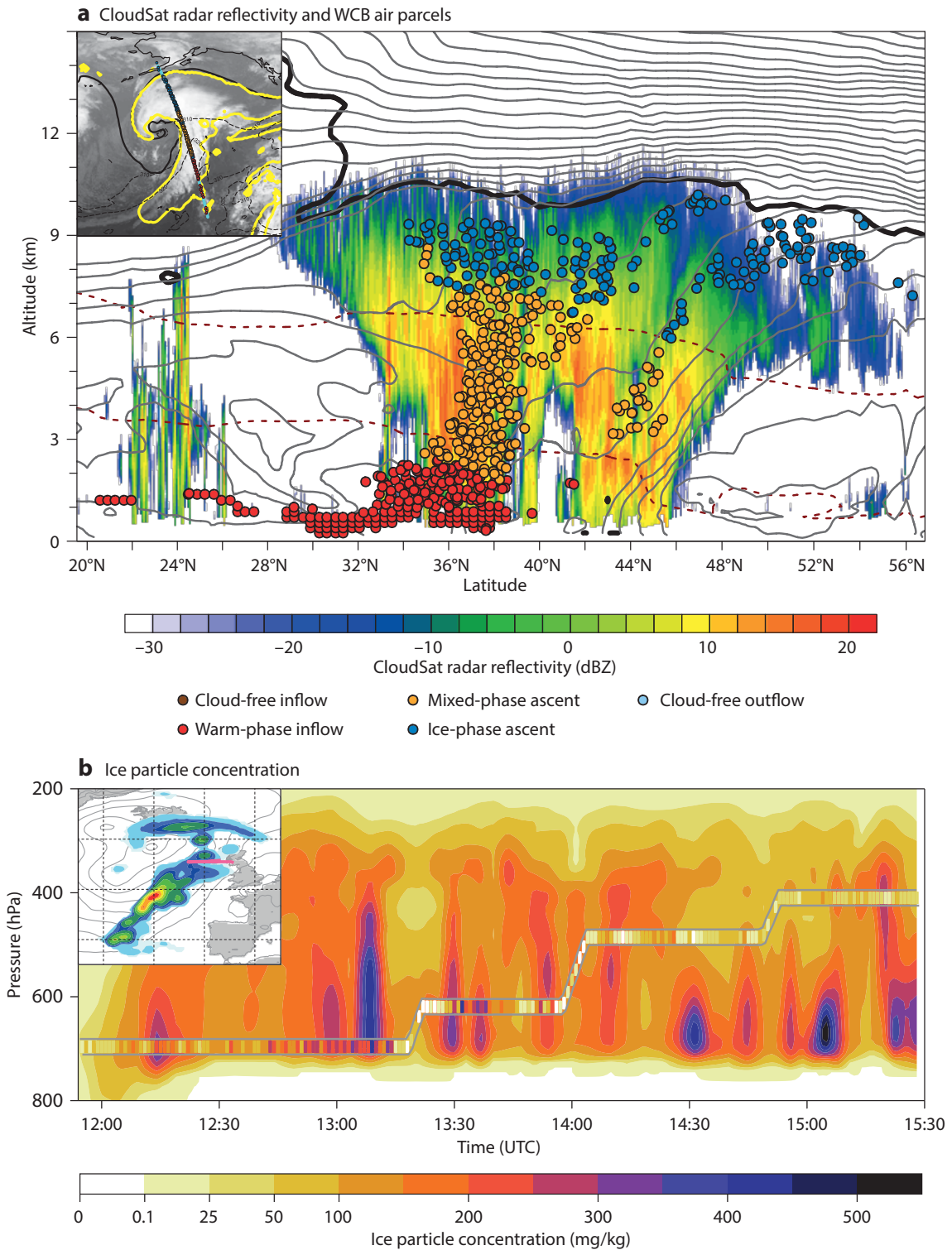
Figure 8 The plots show (a) CloudSat radar reflectivity (shading) at 00 UTC on 3 January 2014, for a cross section of the atmosphere along the line shown in the inset, together with ECMWF operational analyses of interpolated equivalent potential temperature (black contours every 5 K), temperature (red dashed contours at 0° and -23°C), the 2 PVU contour (thick black line), and the positions of the intersected WCB trajectories, i.e., the WCB air parcels located within less than 20 km of the satellite track (dots, coloured according to their cloud phase), and

(b) in-situ ice particle concentration as a function of time and height on 23 September 2016 from Nevzorov probe observations on board the BAe146 FAAM aircraft during the NAWDEX field campaign as it flew across a WCB associated with cyclone Vladiana (inset). These are overlaid onto the profile of corresponding ice particle concentrations (the sum of cloud ice and snow) based on the ECMWF operational forecast starting at 12 UTC. The in-situ measurements are averaged over 60 s and the forecast data has 1 h temporal resolution and 0.5° spatial resolution. Panel (a) is from *Binder* (2017) and panel (b) is based on work with Elisa Spreitzer, Maxi Boettcher and Hanna Joos, in collaboration with Geraint Vaughan and Chris Dearden (aircraft data).
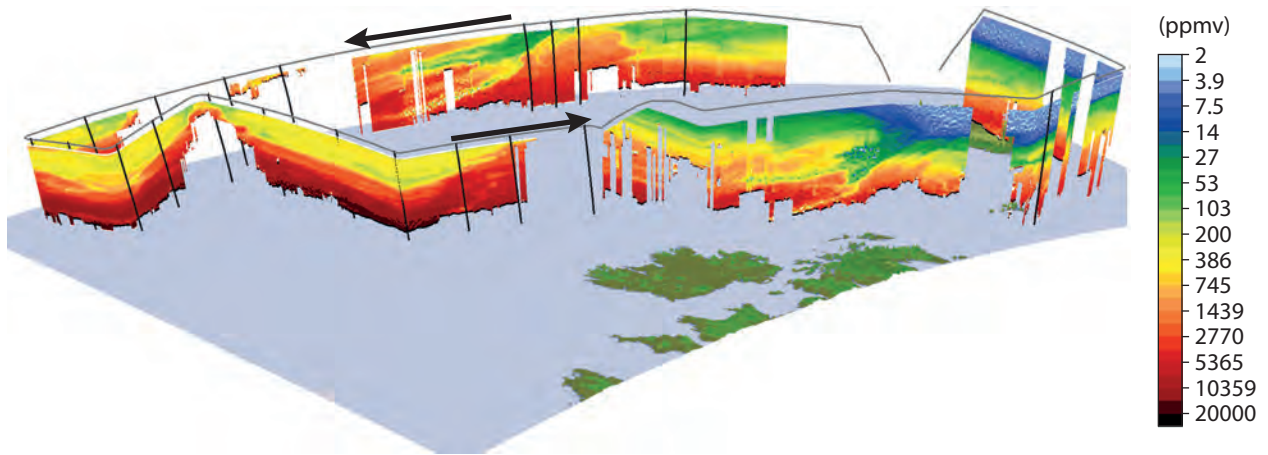
Figure 9 Water vapour profiles as derived from Differential Absorption Lidar (DIAL) observations made from the HALO aircraft on 27 September 2016 as part of the NAWDEX field campaign over the North Atlantic. Figure courtesy of Andreas Schäfler.

a Depar^2

b Bias^2

c EnsVar

d ObsUnc^2

e Residual

f Observation density
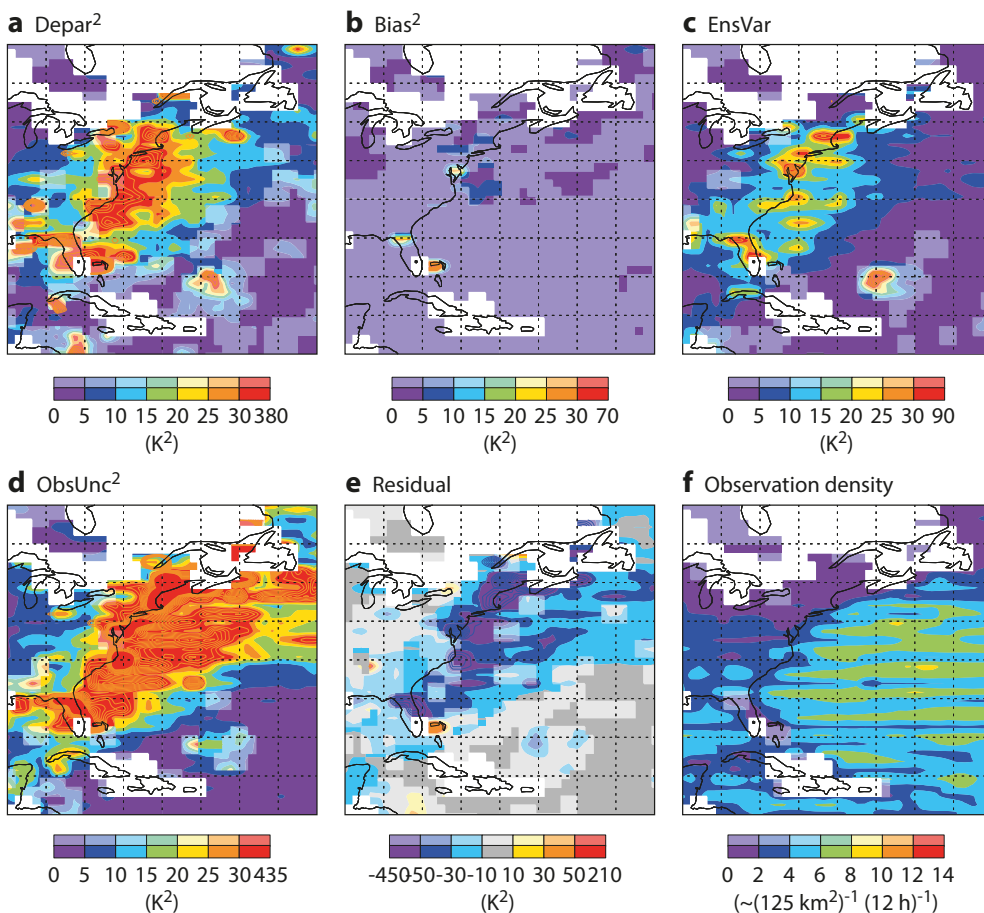
Figure 10 The EDA reliability budget applied to the strongest 50 WCB events off the east coast of North America in the period November 2015 to October 2016, showing (a) the mean-squared difference between the observations and the ensemble-mean (Depar^2), (b) the squared estimated bias (Bias^2), (c) the mean background variance (EnsVar), (d) the squared observation uncertainty (ObsUnc^2, the variance of modelled observation errors), (e) the residual (the variance required to close the budget Depar^2= Bias^2+ EnsVar+ ObsUnc^2+Residual), and (f) the observation density. Saturated colours indicate statistical significance at the 95% confidence level.

applied to the EDA for a composite of the 50 strongest WCB inflow cases off the east coast of North America between November 2015 and October 2016. Here the variance budget is applied to satellite Microwave Humidity Sounder observations of lower-tropospheric humidity and modelled values mapped to these observations. In a 'perfect' forecast system, and with no observation errors, the mean background (short-range forecast) variance (EnsVar, Figure 10c) would match the mean-squared difference between

the observations and the ensemble-mean (Depar^2, Figure 10a); an example of the so-called 'spread-error' or 'spread-skill' relationship. In reality, while both panels show larger values in the WCB region compared to adjacent regions, the mean ensemble variance (Figure 10c) is smaller than the mean squared departure (Figure 10a). The more accurate relationship, which takes observation uncertainty into account, can be written as

Depar^2 = Bias^2+EnsVar+ObsUnc^2+Residual, where Bias^2

and Residual indicate mean and variance deficiencies. What we find for this observational data in WCB situations is that the bias is not significant (Figure 10b) but that our modelled observation uncertainties (ObsUnc^2, Figure 10d) are very large, so a large and statistically significant negative residual (Figure 10e) is required to close the budget. The implication is that the observation errors, as modelled within the data assimilation system, are considerably larger than they could be. While the goal would be to reduce these observation error estimates, this may only be sensible after improvements to, e.g., cloud detection and modelled boundary-layer heights, due to the deep weighting function of this observation type. This budget can be applied to any observation type and gives useful insight into the initialisation of other model fields including wind, temperature and surface pressure.

Another approach to improved initialisation of humidity might be to focus on upstream surface humidity fluxes (*Pfahl et al.*, 2014) in less cloudy regions. In May 2017, a workshop on the Meteosat Third Generation Infrared Sounder was held at ECMWF. Such hyper-spectral infrared observations from geostationary satellites could provide better humidity profile information with excellent time sampling. Preliminary results show that, provided radiative transfer errors are kept low, the radiance associated with hypothetical elevated humidity in the lower troposphere, e.g. humidity associated with the start of a WCB or an atmospheric river, could potentially be detected.

Future directions

It is clear that WCBs have a major impact on medium-range predictability in the extratropics, in particular as a result of their role in developing downstream ridges, initiating downstream blocking and amplifying uncertainty. It is also clear that improvements could be made to the initialisation and representation of WCBs in current forecasting systems. Promising areas for research and development, already under way, include:

- Improved use of observations by the EDA during WCB events
- Improved representation of physics during WCB events
- Improved ensemble reliability in situations where WCBs exist (or are likely to exist at a future date)
- Continued research into extended-range predictability, including teleconnections between predictable drivers (such as in the tropics), WCB events, and extratropical regime transitions (such as the initiation of blocking)

Work in these areas will benefit from continued collaboration with members of the atmospheric dynamics group at ETH and other scientists with similar interests.

FURTHER READING

Binder, **H.**, 2017: Warm conveyor belts: cloud structure and role for cyclone dynamics and extreme events. PhD thesis, ETH Zurich, No 24016.

Crezee, **B.**, **H. Joos** & **H. Wernli**, 2017: The microphysical building blocks of low-level potential vorticity anomalies in an idealized extratropical cyclone. *J. Atmos. Sci.*, **74**, 1403–1416.

Ferranti, **L.**, **S. Corti** & **M. Janousek**, 2015: Flow-dependent verification of the ECMWF ensemble over the Euro-Atlantic sector. *Quart. J. Roy. Meteorol. Soc.*, **141**: 916–924. doi:10.1002/qj.2411.

Gray, **S.L.**, **C.M. Dunning**, **J. Methven**, **G. Masato** & **J.M. Chagnon**, 2014: Systematic model forecast error in Rossby wave structure. *Geophys. Res. Lett.*, **41**, 2979–2987, doi:1002/2014GL059282.

Hoskins, **B. J.**, **M. E. McIntyre** & **A. W. Robertson**, 1985: On the use and significance of isentropic potential vorticity maps. *Quart. J. Roy. Meteorol. Soc.*, **111**, 877–946.

Joos, **H.** & **H. Wernli**, 2012: Influence of microphysical processes on the potential vorticity development in a warm conveyor belt: A case-study with the limited-area model COSMO. *Quart. J. R. Meteorol. Soc.*, **138**, 407–418, doi: 10.1002/qj.934.

Joos, **H.** & **R. Forbes**, 2016: Impact of different IFS microphysics on a warm conveyor belt and the downstream flow evolution. *Quart. J. R. Meteorol. Soc.*, **142**, 2727–2739.

Lavers, **D.A.**, **R.P. Allan**, **E.F. Wood**, **G. Villarini**, **D.J. Brayshaw** & **A.J. Wade**, 2011: Winter floods in Britain are connected to atmospheric rivers, *Geophys. Res. Lett.*, **38**, L23803, doi:10.1029/2011GL049783.

Madonna, **E.**, **H. Wernli**, **H. Joos** & **O. Martius**, 2014: Warm conveyor belts in the ERA-Interim dataset (1979–2010). Part I: Climatology and potential vorticity evolution. *J. Climate*, **27**, 3–26, doi: 10.1175/JCLI-D-12-00720.1.

Magnusson, **L.,** 2017: Diagnostic methods for understanding the origin of forecast errors. *Quart. J. R. Meteorol. Soc.*, **143**, 2129–2142.

Methven, **J.**, 2015: Potential vorticity in warm conveyor belt outflow. *Quart. J. Roy. Meteor. Soc.*, **141**, 1065–1071, doi:10.1002/qj.2393.

Pfahl, **S.**, **E. Madonna**, **M. Boettcher**, **H. Joos**, & **H. Wernli**, 2014: Warm conveyor belts in the ERA-Interim data set (1979-2010). Part II: Moisture origin and relevance for precipitation. *J. Climate*, **27**, 27–40.

Pfahl, **S.**, **C. Schwierz**, **M. Croci-Maspoli**, **C. M. Grams** & **H. Wernli**, 2015: Importance of latent heat release in ascending air streams for atmospheric blocking. *Nature Geosci.*, **8**, 610–615.

Schäfler, **A.** & **F. Harnisch**, 2015: Impact of the inflow moisture on the evolution of a warm conveyor belt. *Quart. J. R. Meteorol. Soc.*, **141**, 299–310, doi: 10.1002/qj.2360.

Ocean coupling in tropical cyclone forecasts

KRISTIAN S. MOGENSEN, LINUS MAGNUSSON,
JEAN-RAYMOND BIDLOT, FERNANDO PRATES

Tropical cyclones (TCs) are one of the deadliest weather phenomena. Typhoon Haiyan, for example, caused more than 6,000 fatalities when it struck the Philippines in November 2013. TCs give rise to a devastating combination of extreme winds, storm surges, high waves and heavy rainfall. Correctly forecasting intense TCs several days in advance makes it possible to evacuate coastal regions and prepare society for the event. This happened, for example, with Hurricane Irma in September 2017, when hundreds of thousands of people in Florida had to leave areas deemed to be at risk. To decide whether such action needs to be taken, local authorities need high-quality forecasts of the cyclone path and intensity. One of the avenues being pursued at ECMWF to improve TC forecasts is to better take into account interactions between the ocean and the atmosphere during the forecast period. Experiments have shown that taking into account such interactions by coupling the ocean and the atmosphere leads to better predictions of TC intensity. Coupling is already operational for ECMWF's ensemble forecasts (ENS) and is due to be extended to high-resolution forecasts (HRES) in the next upgrade of ECMWF's Integrated Forecasting System (IFS).

In this article we present key points from ongoing research at ECMWF on the influence of ocean–atmosphere coupling on tropical cyclone intensity. We have selected two very different TCs for a case study. For TC Neoguri (2014), the operational forecast made at the time overpredicted the intensity significantly, and tests with the current 9 km (TCo1279) horizontal resolution in HRES lead to even more pronounced overpredictions. However, the forecast improves considerably with ocean–atmosphere coupling. For TC Haiyan (2013), the operational forecast severely underpredicted the intensity, and even with the current operational resolution we are unable to simulate the intensity accurately regardless of whether we use a coupled or an uncoupled model.

Significance of coupling

In the past ECMWF forecasts have tended to underpredict the intensity of TCs. This continues to be the case in ENS forecasts, whose horizontal resolution is currently 18 km. However, as the horizontal resolution of atmospheric forecasts has increased to currently 9 km in the HRES, we have seen a growing number of overpredictions of TC intensity. A possible reason for this is the fact that the main energy source for TCs is heat transport from the ocean. By not coupling the atmosphere and the ocean, the heat exchange at the surface is misrepresented and the ocean acts as an undiminished source of energy for the atmosphere during the forecast period. This allows the TC intensity to increase unrealistically. Previously errors resulting from the lack of coupling were partly compensated for by opposite-sign errors in predicted core pressure resulting from the low atmospheric resolution.

Using a coupled model introduces negative feedback between the TC and the sea-surface temperature (SST). As strong winds from the cyclone enhance the heat uptake from the ocean, the SST may decrease, which in turn reduces the energy available to the cyclone. Tropical cyclones interact with the SST in three ways: heat transport to the atmosphere, vertical mixing in the ocean, and upwelling by Ekman pumping. While the first process could be simulated by a slab ocean model, the second requires a model of the well-mixed layer at the top of the ocean, and to simulate all three processes a full three-dimensional model is required. This is especially important for slow-moving cyclones.

At ECMWF a coupled atmosphere–ocean model is currently used operationally for ENS, including the monthly extension, and seasonal forecasts (SEAS). It is due to be implemented for HRES in the next IFS upgrade, Cycle 45r1.

Coupled atmosphere–waves–ocean model

In the IFS, both the wave model (WAM) and the ocean and sea-ice model (NEMO with LIM2) are integrated into the time stepping in such a way that they can be called at every nth atmospheric time step to get updated ocean fields (surface roughness from WAM, SST, sea-ice concentration and surface currents from NEMO) based on updated atmospheric forcing inputs (such as winds for WAM and surface stress, heat and water fluxes for NEMO). On top of the two-way interaction between NEMO/WAM and the atmosphere, NEMO and WAM also exchange data: NEMO receives wave information to account for wave-induced mixing, Stokes-Coriolis drift and sea-state modified stress, and it passes back sea-ice concentration to WAM. The frequency of atmospheric time steps between WAM/NEMO calls determines the coupling frequency and is typically one time step (or 12 minutes) for WAM and 5 time steps (or one hour) for NEMO. While the LIM2 sea-ice model is active in all coupled integrations, it is not relevant to the issues discussed here.

In this article we will present results from simulations using the current operational HRES atmospheric resolution (9 km) and the oceanographic configuration used in NEMO (about 25 km horizontal resolution with a 1 m top layer) as implemented in IFS Cycle 43r1. For atmospheric initial conditions, operational analyses were used. For ocean initial conditions, we used the ocean reanalysis system 5 (ORAS5) for coupled integrations. The uncoupled simulations were carried out with persisted anomalies, with initial SST from the OSTIA product, as is currently done in operations for HRES.

The current ENS uses a partial coupling setup, which couples the SST tendencies rather than the actual SST field from the ocean model during the first four days of the model integration, with a gradual transition to full SST coupling over the next four days. The partial coupling

is intended to maintain the high spatial variability in the analysed SST used by the atmosphere in the early part of the forecast, and to ensure that errors in the position of boundary currents in the ocean analyses do not degrade the atmospheric forecast. Tests have shown that this scheme produces better results than full coupling of the SST predicted by the ocean model across the globe. However, it is planned to introduce full coupling from day 0 in IFS Cycle 45r1 in the tropics, since here full coupling has been found to be beneficial.

Simulating TC Haiyan and TC Neoguri

We have selected two extreme cases in terms of the impact of ocean coupling: Haiyan, for which coupling has only a small impact, and Neoguri, for which coupling has a very large impact.

Central pressure and heat fluxes

Figure 1 shows the position and central pressure for five-day HRES (squares) and 'best track' data (triangles) for each case. For both TCs, the predicted tracks agree well with the observed ones for the coupled and uncoupled setups. Regarding the intensity, the uncoupled and coupled forecasts for Haiyan both predict a cyclone which is too weak,

with only minor differences between the two. For Neoguri, the uncoupled forecast overpredicts the cyclone intensity for forecast days 3–5, while the coupled forecast is better at this range. The plots also show the net surface heat flux (sensible + latent) to the atmosphere averaged over five days. For Haiyan there is little trace in the heat flux in the wake of the cyclone, while for Neoguri we find an increased heat flux from the ocean in the uncoupled forecast.

Figure 2 shows a comparison between uncoupled and coupled forecasts of the evolution of the net (sensible + latent) surface heat flux averaged over 6 hours in a radius of 150 km around the centre of the cyclone, and of the evolution of central pressure, for Haiyan and Neoguri. The plots show three forecasts with different starting dates for the two TCs. Coupled and uncoupled forecasts produce similar heat fluxes for Haiyan, while for Neoguri the heat flux for the uncoupled forecast is almost twice as large as for the coupled forecast during the most intense stage of the cyclone. For Haiyan, there is little difference between coupled and uncoupled simulations for central pressure, which is too weak in either case. For Neoguri, there are large differences in central pressure: the uncoupled simulations are too intense and the coupled simulations are more realistic compared to the 'best track' estimates.
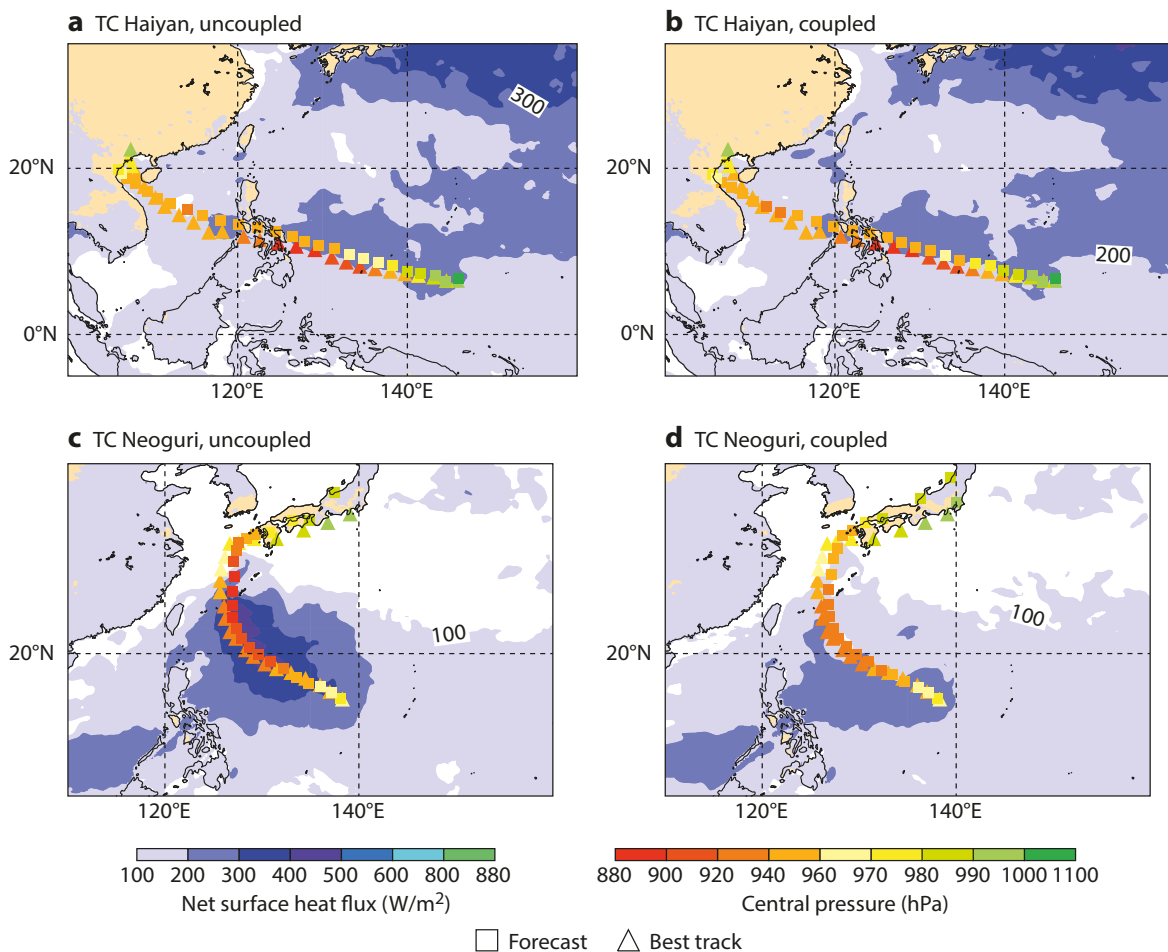
Figure 1 The plots show five-day HRES track and intensity forecasts (squares) together with 'best track' estimates (triangles) and the predicted net surface heat flux (shading) for (a) TC Haiyan (starting date 5 November 2013) using the uncoupled model, (b) TC Haiyan using the coupled model, (c) TC Neoguri (starting date 5 July 2014) using the uncoupled model, and (d) TC Neoguri using the coupled model.
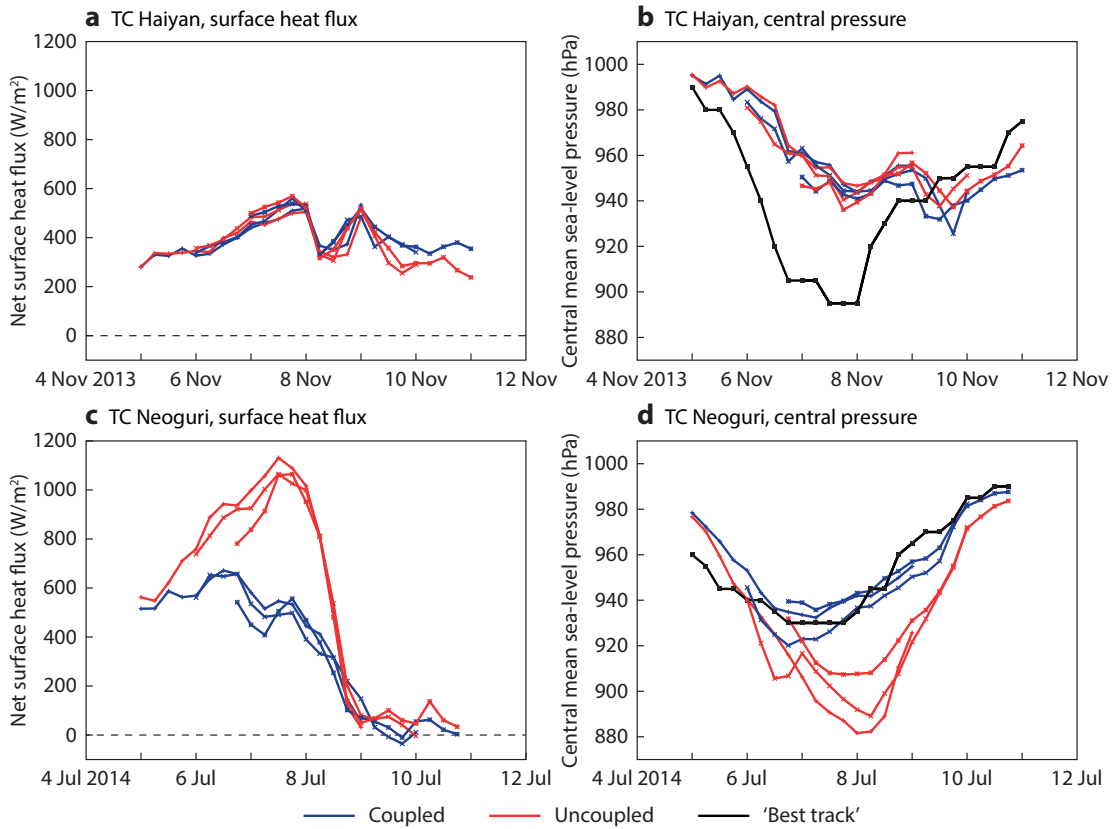
Figure 2 The plots show HRES forecasts of (a) net (sensible + latent) surface heat flux for TC Haiyan, (b) central pressure for TC Haiyan, (c) net surface heat flux for TC Neoguri, and (d) central pressure for TC Neoguri. 'Best track' estimates for central pressure are also shown.
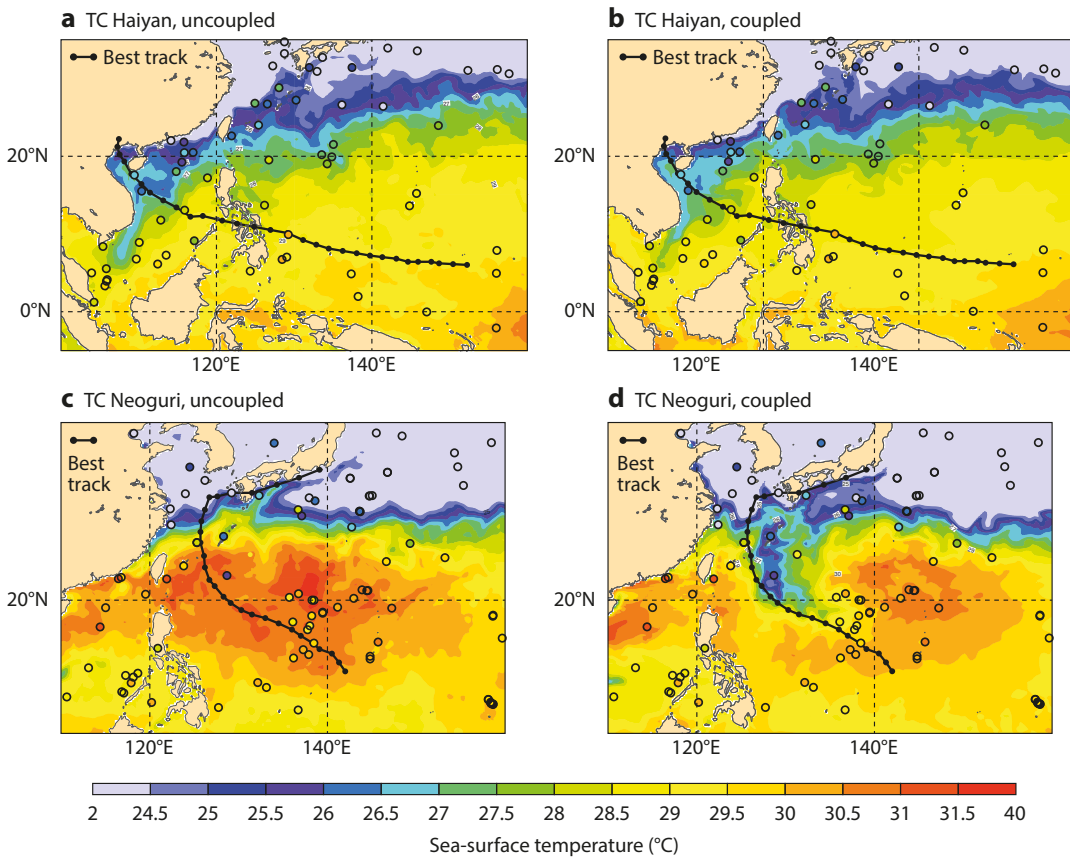
Figure 3 Five-day sea-surface temperature forecasts for (a) TC Haiyan (starting date 5 November 2013) using the uncoupled model, (b) TC Haiyan using the coupled model, (c) TC Neoguri (starting date 5 July 2014) using the uncoupled model, and (d) TC Neoguri using the coupled model, with SST observations (circles) valid at 00 UTC on 10 November 2013 and 00 UTC on 10 July 2014, respectively.

a DRIBU 52514

b DRIBU 21973

c DRIBU 52820

d DRIBU 52596

e Buoy tracks
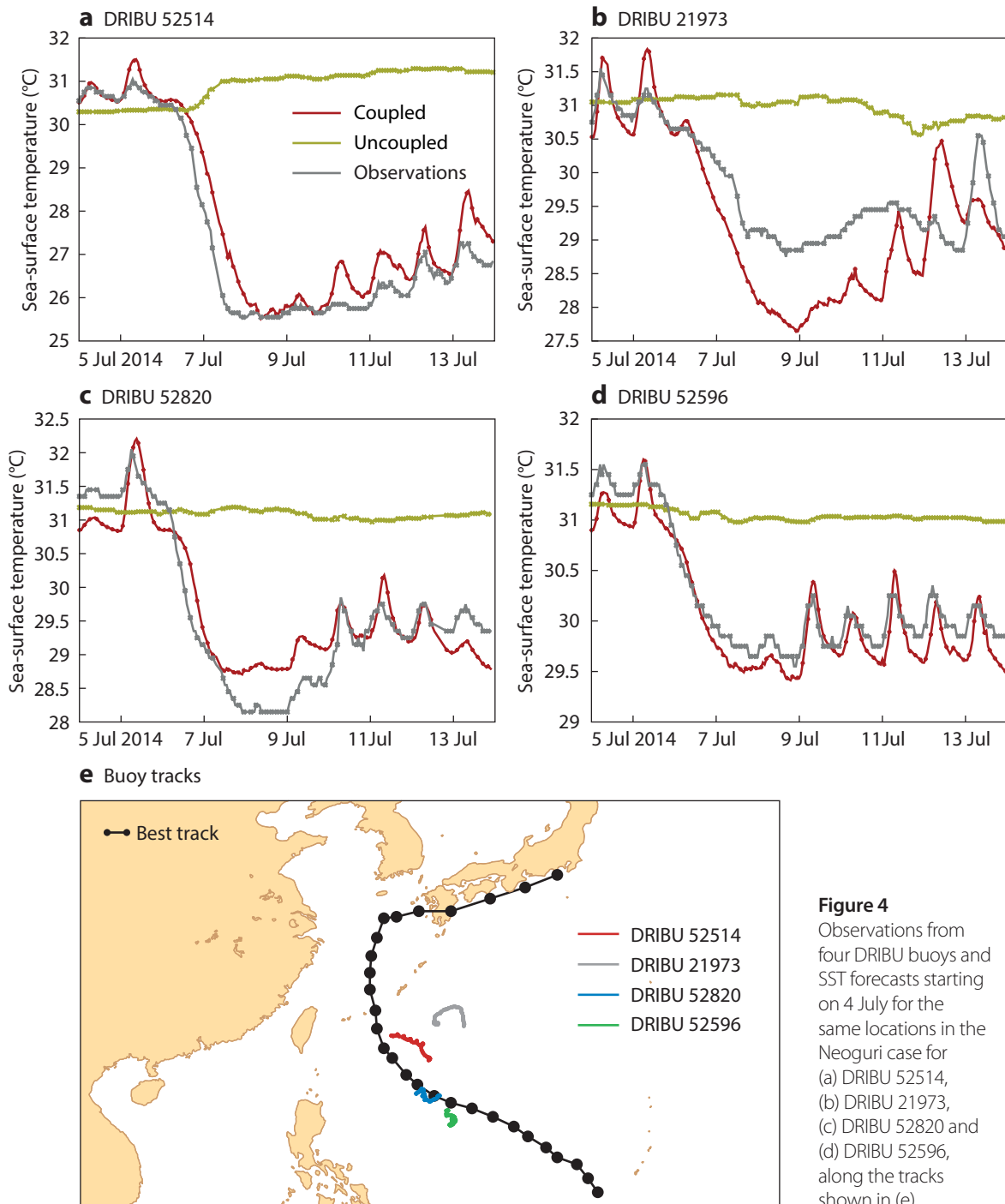
Figure 4 Observations from four DRIBU buoys and SST forecasts starting on 4 July for the same locations in the Neoguri case for (a) DRIBU 52514, (b) DRIBU 21973, (c) DRIBU 52820 and (d) DRIBU 52596, along the tracks shown in (e).

Sea-surface temperature

To verify whether the ocean response to the tropical cyclone forcing described above is realistic, we have compared the predicted SST to observations from drifting buoys and ships. Figure 3 shows the SST in 5-day coupled and uncoupled forecasts as well as observations of SST at the verification date. By construction, we do not find a cold wake in the uncoupled experiment as it uses SST from the analysis evolved daily with seasonal anomalies. There is no clear trace of a cold wake after Haiyan in the coupled forecast, either, nor is there such a trace in the

small number of available observations. The opposite holds true for Neoguri, where we find a strong cold wake east of the track in the coupled forecast, where the cooling reaches 5°C. The SST in the coupled forecast is in good agreement with the two observations inside the cold wake of the cyclone. To further quantify this agreement, Figure 4 shows time series of four drifting buoys (DRIBU) near the path of Neoguri. Especially in Figure 4a, the evolution of the SST in the coupled forecast agrees well with the buoy observations, which show a cooling of 5°C over 24 hours. Overall the conclusion is

that the cold wake predicted by the coupled IFS model is in reasonable agreement with observations for Neoguri, while for Haiyan the lack of a cold wake is also consistent between the model and observations.

Sub-surface oceanic response

The small effect of the coupling for Haiyan could be connected to the deep and well-developed ocean mixed layer present in this case, but it could also be due to the fact that the weak cyclone in the forecast is not able to increase the heat flux. In order to investigate this further, together with the strong effect of the coupling for Neoguri, we will now look at the sub-surface response in the ocean in the two cases. Figure 5 shows time series for predicted ocean fields of temperature and currents for
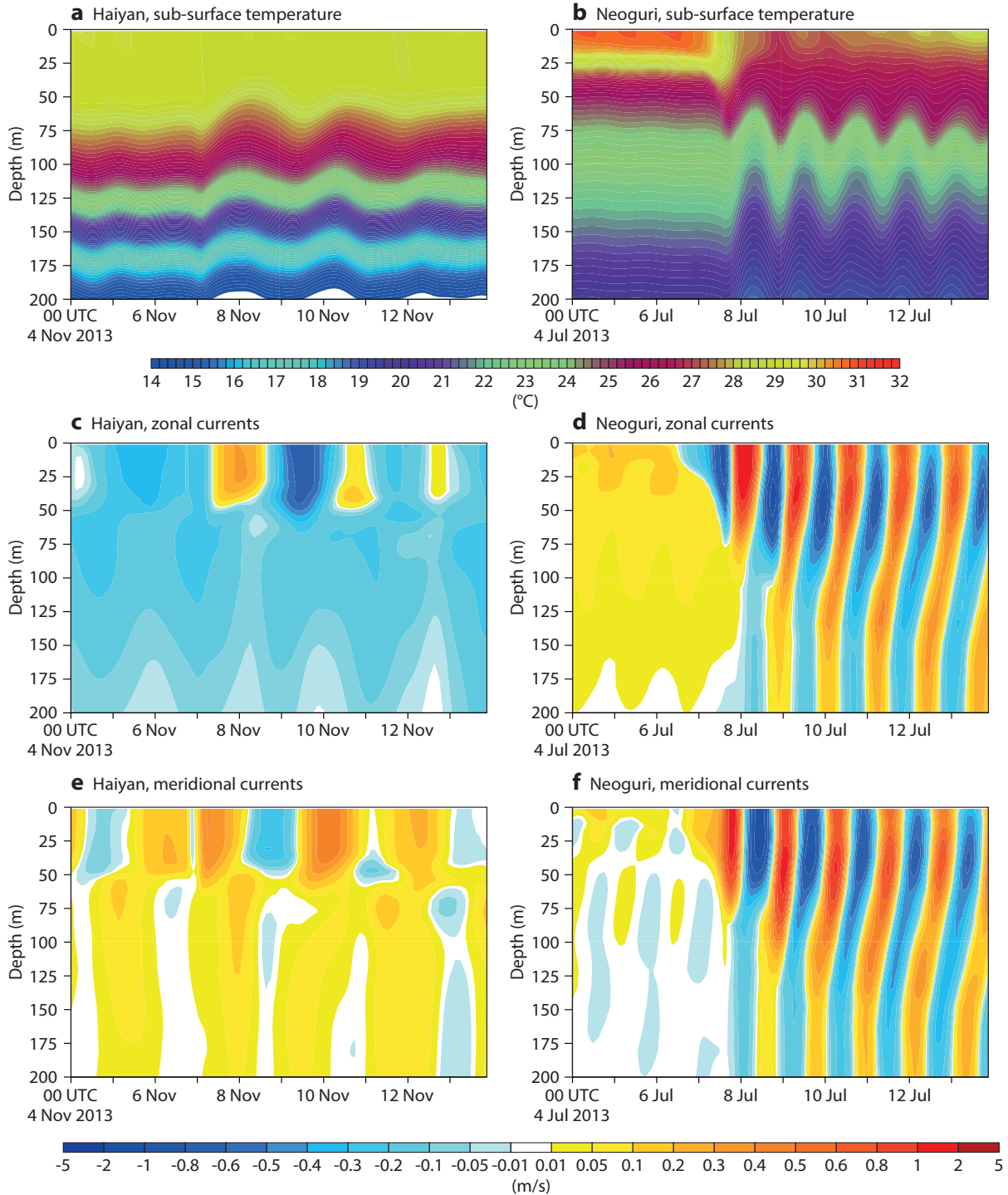
Figure 5 Plots of sub-surface temperature and currents for the two points on the model track closest to the estimated Haiyan 'best track' position at 00 UTC on 7 November 2013 and for Neoguri at 18 UTC on 7 July 2014, showing ocean forecasts of (a) sub-surface temperature for Haiyan, (b) sub-surface temperature for Neoguri, (c) zonal (east–west) currents for Haiyan, (d) zonal currents for Neoguri, (e) meridional (north–south) currents for Haiyan, and (f) meridional currents for Neoguri.
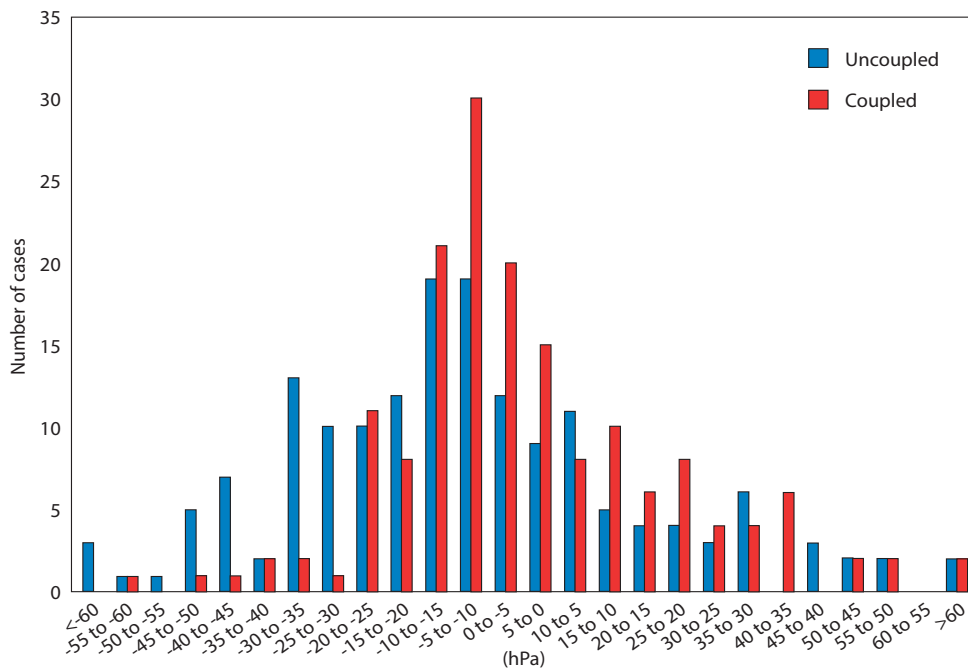
Figure 6 Distribution of 7-day TC intensity forecast errors for coupled and uncoupled high-resolution forecast experiments. The experiments cover the period of March 2015 to June 2017 and were carried out over all basins for a total of 163 TCs.

the point on the model track closest to the Haiyan 'best track' position at 00 UTC on 7 November 2013, and for Neoguri for 18 UTC on 7 July 2014. The points were chosen to reflect the response in the open ocean. Other nearby points and different starting dates for the two cases show very similar behaviour.

Looking at the temperature at initial time in the Haiyan case, it is clear that the ocean has a deep layer (about 80 metres) of warm water, whereas for Neoguri, the thermocline is steeper. This means that, even though the temperature at the surface is higher, for Neoguri the heat content in the surface region is lower. When the TCs reach the respective points (after 3 days for Haiyan and 3.75 days for Neoguri), the response is quite different. For Haiyan there is a small amount of cooling (not visible in the plot) of the whole of the thick warm layer, whereas for Neoguri the shallow warm layer is depleted of heat, causing a large amount of cooling in the upper ocean. It is worth noting that both TCs have a similar response in the currents, but of different magnitude, suggesting that the basic physics of the coupled response is the same even if the magnitude of the response is different.

Impact for many cases

To quantify the effect of ocean coupling on predicted TC intensity in general, rather than just for a few special cases, we have looked at a large set of coupled versus uncoupled forecasts at the HRES operational resolution. Two one-year periods were selected to test various aspects of HRES coupling: from 1 March 2015 to 1 March 2016, and from 1 June 2016 to 1 June 2017. An example of a comparison of coupled versus uncoupled forecasts is given in Figure 6, which shows a histogram of forecast errors for all identified TCs in the two periods for a lead time of 168 hours. There are a large number of uncoupled forecasts which are too intense, with negative errors of more than 25 hPa. Such errors are virtually absent from the coupled forecasts. There is a slight increase in the number of underpredicted TC intensities with

ocean coupling, but overall the distribution of errors looks much more reasonable with ocean coupling than without it. The issue that TC intensities are underpredicted in some cases cannot be addressed by coupling. Reducing such errors will require other improvements, such as higher resolution in the atmospheric model.

Conclusion

From the comparison of the behaviour of the upper ocean in the cases of Haiyan and Neoguri, we conclude that knowledge of the vertical stratification of the ocean is crucial in order to be able to predict the ocean–atmosphere interactions and thereby to predict more accurately the evolution of TCs. For Neoguri, we have shown that a shallow warm layer is the key to a strong coupled SST response, whereas for Haiyan the thick warm layer leads to a weak coupled SST response. The sea-surface temperature was actually warmer for Neoguri than for Haiyan, but we have shown that the ocean stratification is the main determining factor for the magnitude of the coupled response. This also means that good ocean initial conditions are vital for high-quality TC forecasts, since errors in the initial stratification in the coupled model will result in errors in the ocean response.

Ocean coupling will be even more important in the future, at higher atmospheric resolutions. At such resolutions the ability to generate stronger winds means that using a coupled model will be essential for cases with moderate to low upper ocean heat content.

FURTHER READING

Mogensen, **K.S.**, **L. Magnusson** & **J-R. Bidlot**, 2017: Tropical cyclone sensitivity to ocean coupling in the ECMWF coupled model. *J. Geophys. Res. Oceans*, **122**, 4392–4412.

Mogensen, **K.S.**, **L. Magnusson** & **J-R. Bidlot**, 2017: Tropical Cyclone Sensitivity to Ocean Coupling. *ECMWF Technical Memorandum*, **794**.

Using EC-Earth for climate prediction research

F.J. DOBLAS-REYES (ICREA and BSC-CNS – Spain)**,**
J.C. ACOSTA NAVARRO, M. ACOSTA, O. BELLPRAT,
R. BILBAO, M. CASTRILLO, N. FUČKAR, V. GUEMAS,
LL. LLEDÓ, M. MÉNÉGOZ, C. PRODHOMME,
K. SERRADELL, O. TINTÓ (all BSC-CNS)**,**
L. BATTÉ, D. VOLPI (both CNRM – France)**,**
A. CEGLAR (JRC – European Commission)**,**
R. HAARSMA (KNMI – the Netherlands)**, F. MASSONNET**
(Université Catholique de Louvain – Belgium)

Climate prediction at the subseasonal to interannual time range is now performed routinely and operationally by an increasing number of institutions. The feasibility of climate prediction largely depends on the existence of slow and predictable variations in the ocean surface temperature, sea ice, soil moisture and snow cover, and on our ability to model the atmosphere's interactions with those variables.

Climate prediction is typically performed with statistical-empirical or process-based models. The two methods are complementary. Although forecasting systems using global climate models (GCMs) have made substantial progress in the last few decades (*Doblas-Reyes et al.*, 2013), systematic errors and misrepresentations of key processes still limit the value of dynamical prediction in certain areas of the globe. At the same time, model initialisation, ensemble generation, understanding the processes at the origin of predictability, forecasting extremes, bias adjustment and model evaluation are all challenging aspects of the climate prediction problem. Addressing them requires both a large base of researchers with expertise in physics, mathematics, statistics, high-performance computing and data analysis interested in climate prediction issues and a tool for them to work with.

This article illustrates how one of these tools, the EC-Earth climate model (Box A), has been used to train scientists in climate prediction and to address scientific challenges in this field. The use of model components from ECMWF's Integrated Forecasting System (IFS) in EC-Earth means that some of the results obtained with EC-Earth can feed back into ECMWF's activities.

EC-Earth has been run extensively on ECMWF's high-performance computing facility (HPCF), among a range of HPCFs across Europe and North America. The availability of ECMWF's HPCF to EC-Earth partners, including the use of the successful ECMWF Special Project programme, means that a substantial amount of EC-Earth's collaborative work, both within the consortium and with ECMWF, takes place on this platform.

Why use EC-Earth?

There are several reasons that motivate the use of EC-Earth for climate prediction research. The following is a non-exhaustive list:

1) *Comparison across timescales and seamless modelling:* EC-Earth has been designed for climate research problems covering any timescale. For this reason, the model is tuned according to community standards, notably for conservation of both mass and energy. Long control experiments typical of climate change research are regularly produced with each new model version. They help to understand the characteristics of the model variability. Such a model also offers a unique opportunity to perform climate modelling experiments across timescales, from sub-seasonal climate prediction to long-term climate change or paleoclimate experiments. This means that EC-Earth is an ideal platform, albeit not the only one in the community, to investigate the physical reasons behind issues like the initial shock and drift by comparing initialised and long-term control simulations or the effects of the initialisation on the forced model response by analysing initialised and historical simulations.

2) *Inclusion of new components:* Although the EC-Earth model is based on the IFS and the NEMO ocean model, the consortium has introduced some modifications to ECMWF's coupled model and added new components. An example of a different component is the LIM3 sea-ice model, which has been introduced as part of the latest NEMO version, while a new component is the LPJG vegetation model. One reason why the latter has been added is to be able to take into account land-use changes and interactive vegetation in the simulations. Some of these components introduce

> ### The EC-Earth Earth system model **A**
>
> Earth system models (ESMs) such as EC-Earth are one of the most powerful tools to provide society with information on the future climate. EC-Earth is a non-operational ESM that generates predictions and projections of global climate change and variability, which are a prerequisite to supporting the development of national adaptation and mitigation strategies. As a climate model, EC-Earth is closely aligned with the ECMWF seasonal forecasting system, in which the IFS atmospheric model is coupled with the NEMO ocean model.
>
> EC-Earth is developed as part of a Europe-wide consortium, thus promoting international cooperation and access to both knowledge and data. It facilitates fruitful interaction between academic institutions and the European climate impact community. The EC-Earth model benefits greatly from IFS updates and in turn the consortium contributes to the development of the atmospheric model. EC-Earth makes significant contributions to a range of international climate modelling and service research projects, as well as to international initiatives, such as the Coupled Model Intercomparison Projects (CMIP).
>
> For more information, visit the EC-Earth website at:
> *http://www.ec-earth.org*

a EXP1   **b** EXP2   **c** EXP1 – EXP2

−1   −0.8   −0.6   −0.4   −0.2   0   0.2   0.4   0.6   0.8   1
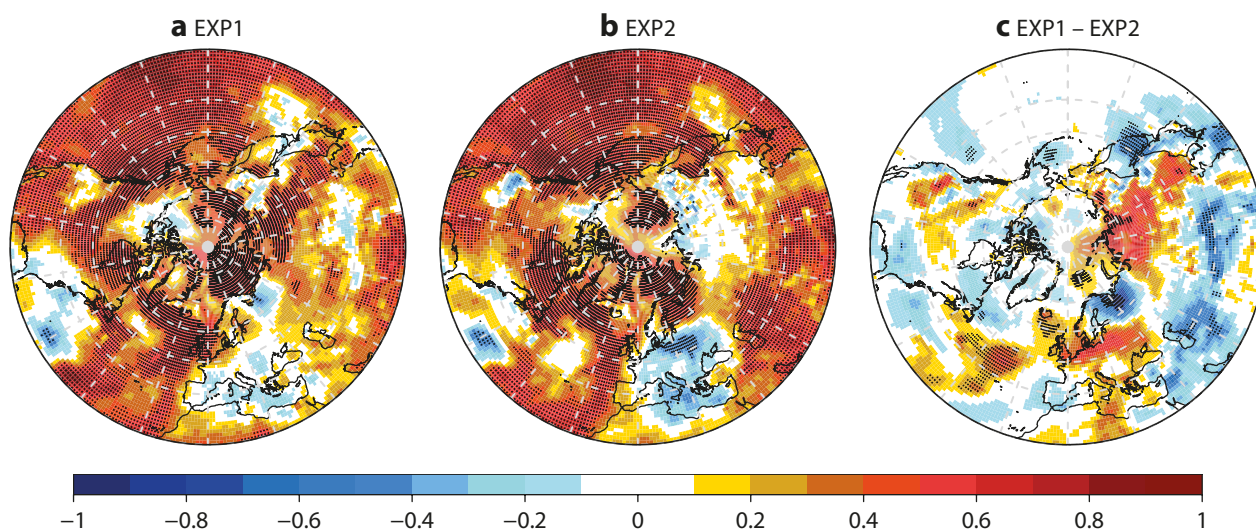
Figure 1 Correlation coefficients of the ensemble mean of 10-member ensemble seasonal predictions performed with EC-Earth3.2 over the period 1993 to 2008. The results shown are for boreal winter (December to February) near-surface temperature predictions with a starting date of 1 November. The panels show (a) the results for simulations initialised with the ERA-Interim reanalysis for the atmosphere, ORA-S4 for the ocean and a BSC (Barcelona Supercomputing Center) reanalysis using an ensemble Kalman filter approach for sea ice (EXP1), (b) the same but with sea ice initialised with data from a sea-ice reconstruction (no data assimilation) (EXP2), and (c) the difference in the correlation coefficient between the two experiments (EXP1 – EXP2). Stippling indicates statistical significance at the 95% confidence level.

more complexity into the system. Their use in a climate prediction context is opening up new avenues for exploring new sources of predictability and for further collaboration with ECMWF.

3) *Portability:* EC-Earth is a community model and, as such, it has been ported by the EC-Earth partners to their preferred computing platforms, including ECMWF's HPCF. Portability comes at a price, mainly in terms of computational performance, but it also enables the consortium to participate in very ambitious experiments. EC-Earth will, for example, make a significant contribution to the Sixth Phase of the Coupled Model Intercomparison Project (CMIP6), in particular by playing a key role in the Decadal Climate Prediction Project (DCPP; *Boer et al.*, 2016). Such endeavours would be beyond the reach of any individual partner in the consortium. To ensure that experiments performed on different computing platforms are comparable, an innovative reproducibility protocol has been designed following the example of other climate community models.

Climate prediction research with EC-Earth
EC-Earth has many uses as a climate prediction research tool. In what follows we give some examples. The details of the model characteristics and the experimental setup used in most of the simulations referred to in this section can be found in *Prodhomme et al.* (2016a) for EC-Earth2.3, also used in the CMIP5 exercise, and in *Prodhomme et al.* (2016b) for EC-Earth3, the version of the model that will be used in CMIP6.

Ensemble initialisation
Ensemble initialisation is a key aspect of all climate prediction experiments. While EC-Earth has benefited enormously from ECMWF reanalyses (both for the atmosphere and the ocean)

to initialise different re-forecast experiments, the consortium is exploring ways to improve its forecasting system by either assimilating new observations or by using different initialisation methodologies. Figure 1 shows the correlation coefficient of the ensemble mean of seasonal predictions of near-surface temperature performed with EC-Earth3.2 over the period 1993 to 2008 for the boreal winter. Figure 1a gives a first impression of the skill of the EC-Earth climate prediction system at seasonal timescales (EXP1). Note that the robustness of the skill is limited by the period considered. The skill can be compared with that obtained in a similar experiment (EXP2), in which the sea ice is initialised with data from a sea-ice reconstruction (no data assimilation). The difference between them suggests that the impact of the sea-ice data assimilation is small but mainly positive, with areas of positive impact over North America, the North Atlantic, Siberia and central Europe. The latter could be related to a similar difference in skill between EXP1 and EXP2 of predictions of the North Atlantic Oscillation (NAO) index, the variability of which has an important impact over central Europe. Experiments are under way to extend the re-forecast period to confirm the robustness of these results.

Impact of model resolution
The desire to better capture physical processes in the ocean and the atmosphere, alongside the growing efficiency of the HPCFs used to run GCMs, has led to an increasing number of studies using higher-resolution components of the climate system for climate prediction (*Prodhomme et al.*, 2016b). EC-Earth, with its range of configurations with different atmospheric and ocean resolutions, has proved to be an ideal tool for this type of study. The model has been used to assess the impact of atmospheric and ocean resolution on the quality of climate predictions. Figure 2 shows a comparison of the

a Different observations

b Different resolutions
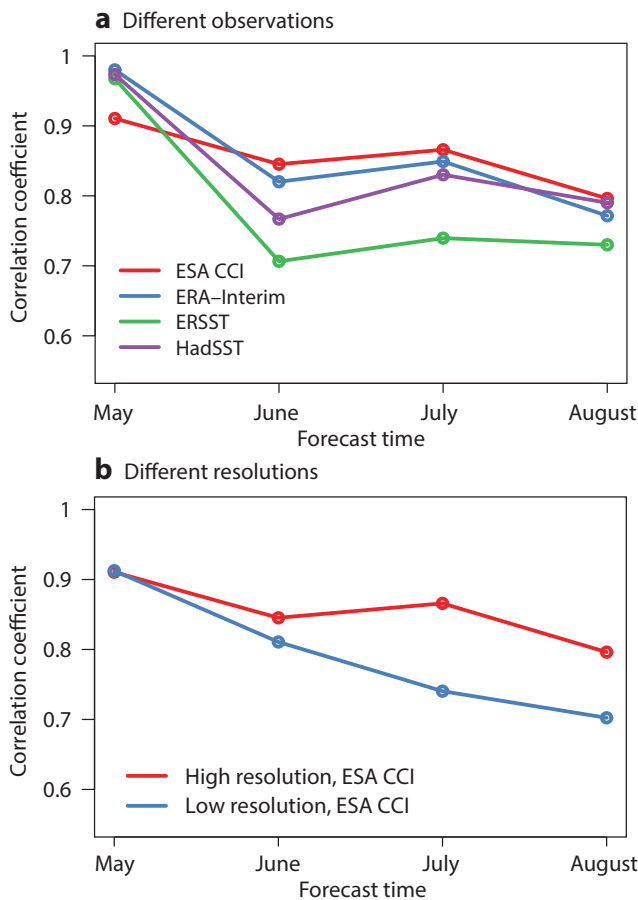
Figure 2 Correlation coefficient as a function of forecast time of ensemble-mean predictions of NINO3.4 sea-surface temperature performed with EC-Earth3.1 and initialised on 1 May using (a) the TL511-ORCA025 resolution configuration over the re-forecast period 1993 to 2009, for four different observational datasets, and (b) TL511-ORCA025 and TL255-ORCA1 re-forecasts verified against the ESA CCI dataset. All correlations are significant at the 5% confidence level and differences in the correlations in (b) are significant at the 1% confidence level.

quality of predictions (the correlation coefficient of the ensemble mean) of the sea-surface temperature (SST) index in the NINO3.4 region performed with EC-Earth3.1 in standard (TL255-ORCA1) and high-resolution (TL511-ORCA025) configurations. Although the high-resolution configuration shows sustained and statistically significant better skill with respect to the standard-resolution configuration, it is important to note that there are many sources of skill estimate uncertainty. Observational uncertainty is one of them, as Figure 2a shows in the range of correlations obtained when verifying a set of re-forecasts against different observational references.

Observational uncertainty
Observational uncertainty has traditionally been neglected in climate prediction quality assessments. In fact, when a comprehensive skill uncertainty analysis is performed (Figure 3), the observational uncertainty is found to be a substantial contributor to the total uncertainty.
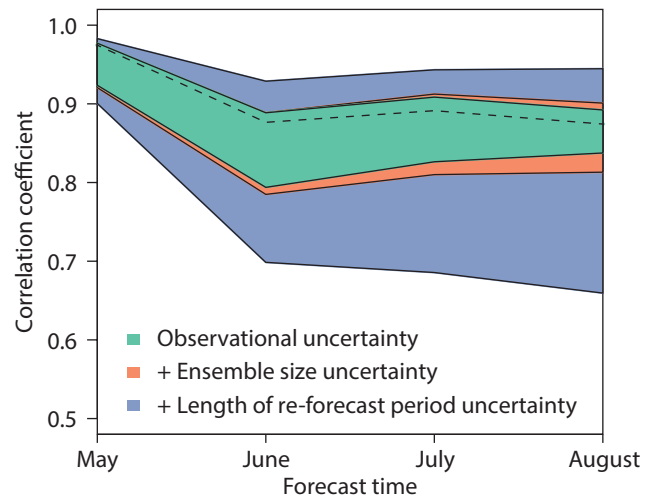
Figure 3 Correlation coefficient as a function of forecast time of ensemble-mean predictions of NINO3.4 SST performed with EC-Earth2.3 over the re-forecast period 1993 to 2009, initialised on 1 May. The shaded areas show the 5–95% range of the bootstrapped uncertainty around the correlation coefficient, broken down into the uncertainty in the observational reference using the CCI SST, and the uncertainties due to a limited ensemble size and limited re-forecast length. The entire shaded area corresponds to the total uncertainty obtained by resampling all sources (see text) at the same time.

In this analysis, three sources of uncertainty of a skill assessment are considered: 1) uncertainty due to the limited number of re-forecasts available resulting from the limited set of robust initial conditions, 2) uncertainty due to the limited ensemble size resulting from limited computational resources, and 3) observational uncertainty. The uncertainties are assessed by resampling the ensemble members of the re-forecast prior to computing the ensemble mean and resampling the years in the verification period, both with replacement.

Model inadequacy
Another aspect of uncertainty relevant in climate prediction is model inadequacy, which is one of the sources of the overconfidence of ensemble forecasts over some areas of the globe. The Stochastically Perturbed Parametrization Tendencies (SPPT) method developed at ECMWF was tested in EC-Earth3 to investigate this issue. Several sets of boreal summer and winter 10-member ensemble seasonal re-forecast experiments were run over the period 1993 to 2009. The summer re-forecasts were initialised on 1 May and the winter re-forecasts on 1 November. The experiments explored different options for the time and spatial scales of the perturbations. Figure 4 shows the impact of two combinations of SPPT patterns on the root-mean-square error (RMSE) and ensemble spread as a function of the forecast time for the May initialisations for SST averaged over the NINO3.4 area. While the SPPT3 option uses parameters similar to the ECMWF Seasonal Forecast System 4, SPPT2L favours longer and larger time and spatial scales to take into account the misrepresentation of a number of global-scale atmospheric patterns. These experiments are compared to a reference

(REF) ensemble with only initial perturbations. As expected, the SPPT perturbations increase the ensemble spread, and in the case of the NINO3.4 index, they improve the RMSE (as well as other forecast quality measures) of the re-forecast with respect to REF. However, the larger-scale SPPT2L perturbations lead to over-dispersion of the ensemble at longer forecast times, which reflects results found for most variables over the tropical Pacific basin.

Land-surface initialisation

Many EC-Earth experiments have been performed to
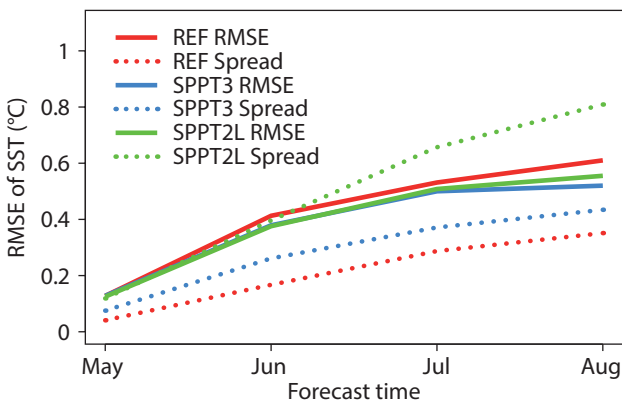
Figure 4 Root-mean-square error (RMSE) of SST predictions averaged over the NINO3.4 region and ensemble spread computed as the standard deviation around the ensemble mean for three 10-member ensemble EC-Earth 3.0.1 re-forecast experiments initialised on 1 May over the period 1993 to 2009 with initial perturbations only (REF) and with additional Stochastically Perturbed Parametrization Tendencies (SPPT) perturbations using different time and spatial correlation scales.

investigate sensitivity to the initialisation of model components. These include seasonal forecast experiments in which the land-surface scheme of the model is initialised with either climatological or realistic data (taken from a reanalysis). The objective is to estimate the role of the land-surface initialisation in seasonal forecast quality, recognising that the land surface is an untapped source of predictability for near-surface air temperature predictions over land in the mid-latitudes. The experiment showed that the model manages to capture a positive feedback between high temperature and low initial soil moisture content. Such feedback tends to dominate over other processes in re-forecasts of the warmest summers in Europe. This result has been confirmed using both versions of the model at both standard and high resolutions.

An innovative exercise that can be undertaken with this type of sensitivity experiment is to estimate to what extent the resulting differences in forecasts are relevant for climate prediction users. Such an exercise was carried out by formulating seasonal maize yield predictions for European countries based on empirical climate-yield relationships and using the re-forecasts of the two land-surface sensitivity experiments as climate input. Figure 5 shows re-forecasts of maize yield in 2003 and 2007 calculated using an empirical stress index that estimates the impact of heat and drought stress events on maize yield anomalies.

In 2003, the observed yield anomalies were in the lowest quartile for all countries except the former Yugoslav Republic of Macedonia and Romania. The predictions obtained with the experiment with realistic soil moisture initialisation suggest an anomalously low yield for re-forecasts starting as early as May. The forecast probability
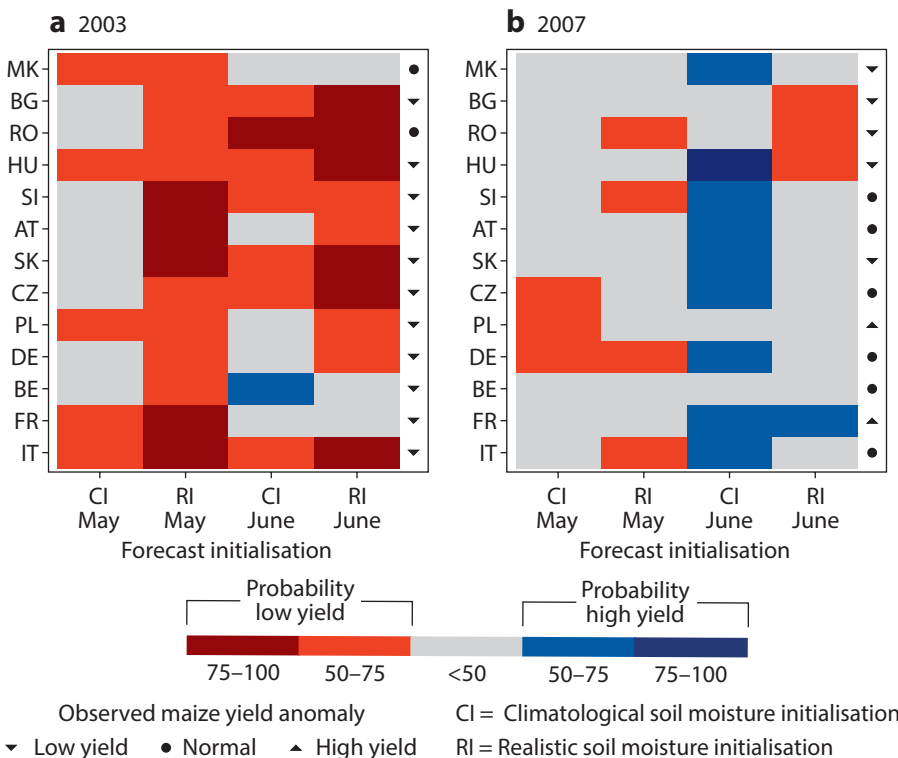
Figure 5 Forecast probabilities for low- or high-yield events (maize yield anomaly in the lower quartile or the upper quartile, respectively) in different countries in (a) 2003 and (b) 2007. The shading indicates the probability of such events from different seasonal re-forecast experiments performed with EC-Earth2.3 initialised with land-surface climatological (CI) and realistic (RI) conditions on 1 May and 1 June. The observed maize yield anomaly is indicated on the right-hand side of each panel. The countries listed from top to bottom are the former Yugoslav Republic of Macedonia, Bulgaria, Romania, Hungary, Slovenia, Austria, Slovakia, the Czech Republic, Poland, Germany, Belgium, France and Italy.

of a low yield event increases when using re-forecasts initialised in June, particularly over south-eastern Europe. Yield estimates that use re-forecasts initialised with climatological soil moisture show lower probabilities for the observed category.

In 2007, south-eastern Europe experienced a severe summer drought and a heat wave, resulting in substantially negative maize yield anomalies. Yield estimates that use re-forecasts initialised in June with climatological soil moisture fail to indicate high probabilities for low yield in the region, while those from the re-forecasts with realistic land-surface initial conditions show slightly higher probabilities for a low yield anomaly. At the time of the re-forecast initialisation in both May and June, soil moisture levels were depleted due to a persisting drought from the preceding winter in most of central and south-eastern Europe. A forecast quality assessment over the period 1981–2010 clearly demonstrates the overall benefit of land-surface initialisation of climate predictions for maize yield forecasting in Europe. It also illustrates the benefits that can be obtained when climate modellers work with users.

Decadal predictions

EC-Earth has been one of the pioneering models used in the development of decadal climate prediction, defined as climate simulations for forecast periods up to ten years into the future. Decadal prediction relies on the combined result of a forced component due to changes in atmospheric composition, such as greenhouse gases, aerosols and other species of anthropogenic and natural origin, and an internal variability component that is initialised with current conditions. Decadal forecast systems have shown skill in predicting global near-surface air temperatures compared to climate projections for the same forecast period. The skill of EC-Earth2.3 as a decadal forecast system is illustrated in Figure 6. Skill is particularly high over the North Atlantic and Europe, among other regions. A large

part of the predictable signal in temperature is due to the forced component of temperature variations associated with recent changes in atmospheric composition. This is also reflected in climate projections. However, decadal predictions offer a more credible estimate of the amplitude of the forced signal than climate projections. More regionally, the North Atlantic has been singled out as one of the main regions that can benefit from decadal prediction. This is due to the ability of current systems to correctly predict the phase and amplitude of the Atlantic Multidecadal Oscillation, which impacts on the multiannual climate variability of the neighbouring continents, for at least several years ahead.

Extreme event attribution

Climate prediction systems are increasingly considered in the context of the attribution of extreme events. Extreme event attribution deals with similar challenges as climate prediction (e.g. systematic errors, lack of reliability) albeit from an ex-post perspective instead of the ex-ante stand adopted by climate prediction. Both communities are quickly learning to work together on aspects such as the importance of the initialisation or the reliability of the simulations. Extreme event attribution uses a multi-method approach to make probabilistic statements about the physical mechanism that might explain events with scientific interest and social impact. EC-Earth regularly contributes to this kind of exercise, not only in coordinated studies such as the annual report on 'Explaining Extreme Events from a Climate Perspective' of the *Bulletin of the American Meteorological Society*, but also to address specific questions from users. Figure 7 shows an example of the latter where the probability distribution of the 10-metre wind speed over a region in south-western North America has been drawn from three different ensemble simulations with specified SSTs and sea ice covering the late winter of 2015. That year an important negative wind anomaly highly relevant to the wind energy industry occurred. In
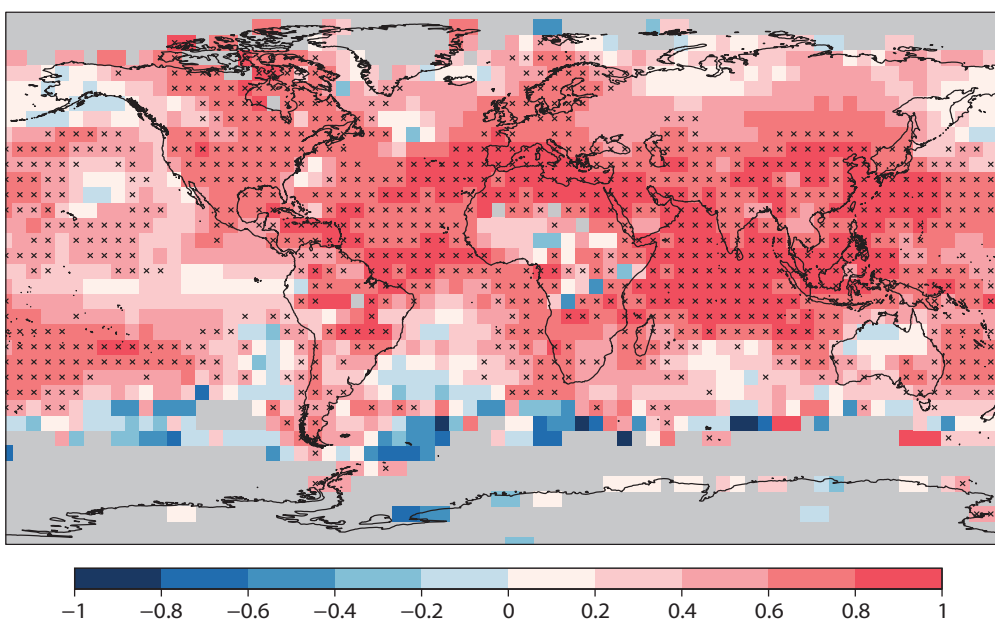
Figure 6
Correlation of five-member ensemble-mean predictions of near-surface temperature averaged over the forecast years 1 to 5 performed with the EC-Earth model over the period 1960–2016. One start date per year starting on 1 November was used. The observational reference is HadCRUT4. Areas with statistically significant correlation at the 95% level are marked by crosses.

−1   −0.8   −0.6   −0.4   −0.2   0   0.2   0.4   0.6   0.8   1
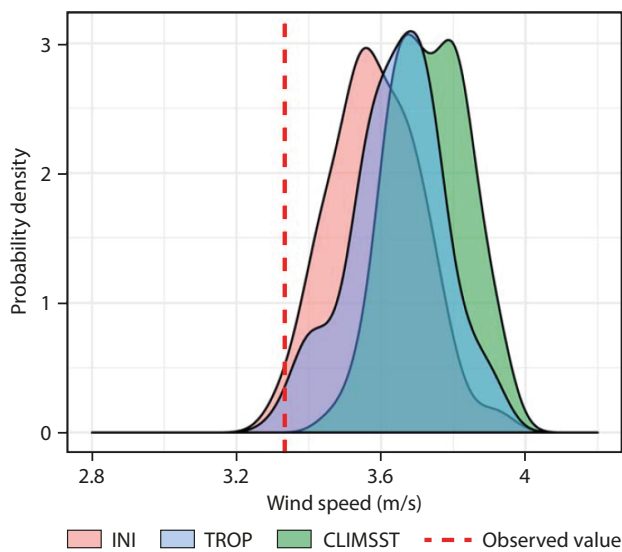
Figure 7 Probability distribution of mean wind speed in the south-western North America region (124ºW–95ºW, 26ºN–44ºN) for three different ensemble EC-Earth3.1 simulations with prescribed sea-surface temperature and sea ice covering the period January–February–March 2015. INI was forced with observed SSTs and sea ice, CLIMSST with climatological SSTs, and TROP with observed SSTs in the tropics only. The vertical dashed line indicates the ERA-Interim observed value.

one ensemble simulation the atmospheric component of EC-Earth was forced with observed SSTs and sea ice (INI). In a second experiment (TROP), the SSTs were as observed in the tropics and SSTs were climatological elsewhere, and in a third one (CLIMSST), climatological SSTs were used. The CLIMSST distribution shows that without the SST anomalies such a low wind speed episode would have been very unlikely, while the tropical SSTs play a central role in generating the anomaly. Singling out the role of the extra-tropical SSTs requires additional simulations where the observed SSTs are only specified in the North Pacific.

While working on these examples and many more, a number of young scientists have been trained in the formulation, validation and use of climate predictions. These scientists could at the same time engage in discussions and research projects involving users, offering them a wider perspective of what research in climate prediction might become in the near future.

Outlook

The possibilities that EC-Earth as a climate prediction research tool offers to the community are immense. As an ESM with state-of-the-art complexity, EC-Earth is now used to explore the predictability of the carbon cycle, one of the key aspects of the global stocktake process currently under discussion; the role of interactive aerosols; the complex relationship between sea ice and atmospheric circulation in lower latitudes to improve forecasts for the next few weeks; the sensitivity of forecasts to the specification of some forcings (e.g. volcanic aerosol load). These and many other issues were beyond the reach of most European climate scientists until recently.

While EC-Earth has been, and will continue to be, used as a research tool for climate prediction, there is a way in which EC-Earth is providing real-time information. One of the objectives of the World Climate Research Programme's Grand Challenge on Near-Term Climate Prediction is to set standards for the operationalisation of decadal prediction. One of the activities in this context is the exchange of decadal predictions issued once a year between institutions with this capability. The BSC (Barcelona Supercomputing Center) is contributing decadal predictions performed with EC-Earth to this exercise and plans to become a contributing centre to the future Lead Centre on Near-Term Climate Prediction.

The use of a frozen atmospheric model, largely outdated for ECMWF's purposes, has limited the feedback that EC-Earth could offer ECMWF. The use in the near future of OpenIFS for the atmospheric component in EC-Earth will strengthen the links between ECMWF and the consortium. OpenIFS is based on more recent IFS model cycles. Results obtained by EC-Earth using an ESM that incorporates OpenIFS cycles will thus be more relevant for IFS development work. The possible feedback that EC-Earth can offer with this new approach goes well beyond the development of physical aspects in the model. There is also intense collaboration already taking place on computational aspects. For instance, a substantial amount of work is already being carried out to improve the computational performance of both EC-Earth and OpenIFS. In particular, substantial efforts are being made to assess the impact of different coupling strategies to achieve an optimal load balance of the coupled model and to incorporate a portable I/O server into the IFS that could soon be inherited by OpenIFS.

This article should be read not as a comprehensive summary of the large amount of climate prediction research activities for which EC-Earth is used, but rather as an illustration of the advantages that developing a European community model can offer and of the opportunities brought by continuing and enhancing the close collaboration between EC-Earth and ECMWF.

FURTHER READING

Boer, **G.J.**, **D.M. Smith**, **C. Cassou**, **F.J. Doblas-Reyes**, **G. Danabasoglu**, **B. Kirtman**, **Y. Kushnir**, **M. Kimoto**, **G.A. Meehl**, **R. Msadek**, **W.A. Mueller**, **K. Taylor** & **F. Zwiers**, 2016: The Decadal Climate Prediction Project. *Geoscientific Model Development*, **9**, 3751–3777, doi:10.5194/gmd-2016-78.

Doblas-Reyes, **F.J.**, **J. García-Serrano**, **F. Lienert**, **A. Pintó Biescas** & **L.R.L. Rodrigues**, 2013: Seasonal climate predictability and forecasting: status and prospects. *WIREs Climate Change*, **4**, 245–268, doi:10.1002/WCC.217.

Prodhomme, **C.**, **F.J. Doblas-Reyes**, **O. Bellprat** & **E. Dutra**, 2016a: Impact of land-surface initialization on sub-seasonal to seasonal forecasts over Europe. *Climate Dynamics*, **47**, 919–935, doi:10.1007/s00382-015-2879-4.

Prodhomme, **C.**, **L. Batté**, **F. Massonnet**, **P. Davini**, **O. Bellprat**, **V. Guemas** & **F.J. Doblas-Reyes**, 2016b: Benefits of increasing the model resolution for the seasonal forecast quality in EC-Earth. *Journal of Climate*, **29**, 9141–9162, doi:10.1175/JCLI-D-16-0117.1.

ECMWF Council and its committees

The following provides some information about the responsibilities of the ECMWF Council and its committees. More details can be found at:

http://www.ecmwf.int/en/about/who-we-are/governance

Council

The Council adopts measures to implement the ECMWF Convention; the responsibilities include admission of new members, authorising the Director-General to negotiate and conclude co-operation agreements, and adopting the annual budget, the scale of financial contributions of the Member States, the Financial Regulations and the Staff Regulations, the long-term strategy and the programme of activities of the Centre.

President Prof. Miguel Miranda *(Portugal)*

Vice President Prof. Juhani Damski *(Finland)*

Policy Advisory Committee (PAC)

The PAC provides the Council with opinions and recommendations on any matters concerning ECMWF policy submitted to it by the Council, especially those arising out of the four-year programme of activities and the long-term strategy.

Chair Mr Rolf Brennerfelt *(Sweden)*

Vice Chair Mr Eoin Moran *(Ireland)*

Finance Committee (FC)

The FC provides the Council with opinions and recommendations on all administrative and financial matters submitted to the Council and exercises the financial powers delegated to it by the Council.

Chair Mr Mark Hodkinson *(United Kingdom)*

Vice Chair Dr Gisela Seuffert *(Germany)*

Scientific Advisory Committee (SAC)

The SAC provides the Council with opinions and recommendations on the draft programme of activities of the Centre drawn up by the Director-General and on any other matters submitted to it by the Council. The 12 members of the SAC are appointed in their personal capacity and are selected from among the scientists of the Member States.

Chair Prof. Alan O'Neill *(United Kingdom)*

Vice Chair Prof. Wilco Hazeleger *(The Netherlands)*

Technical Advisory Committee (TAC)

The TAC provides the Council with advice on the technical and operational aspects of the Centre including the communications network, computer system, operational activities directly affecting Member States, and technical aspects of the four-year programme of activities.

Chair Mr Jean-Marie Carrière *(France)*

Vice Chair Dr Philippe Steiner *(Switzerland)*

Advisory Committee for Data Policy (ACDP)

The ACDP provides the Council with opinions and recommendations on matters concerning ECMWF Data Policy and its implementation.

Chair Mr Søren Olufsen *(Denmark)*

Vice Chair Mr Francisco Pascual Perez *(Spain)*

Advisory Committee of Co-operating States (ACCS)

The ACCS provides the Council with opinions and recommendations on the programme of activities of the Centre, and on any matter submitted to it by the Council.

Chair Mr Taimar Ala *(Estonia)*

Vice Chair Mr Nir Stav *(Israel)*

ECMWF Calendar 2017/18

Jan 22–25	Workshop on observations and analysis of sea-surface temperature and sea ice for NWP and climate applications
Jan 22–26	Computer user course: ecFlow
Jan 26	Symposium to mark 20 years of 4D-Var
Jan 29 – Feb 2	Training course: Use and interpretation of ECMWF products
Feb 5–9	Training course: Use and interpretation of ECMWF products
Feb 19–22	Computer user course: ecCodes, BUFR
Feb 26 – Mar 1	Computer user course: ecCodes, GRIB
Mar 12–16	NWP training course: Data assimilation
Mar 19–23	EUMETSAT/ECMWF NWP-SAF training course: Satellite data assimilation
Apr 9–13	Advisory Committee for Data Policy and data policy meetings of EUMETSAT and ECOMET
Apr 16–20	NWP training course: Advanced numerical methods for Earth system modelling
Apr 23–27	NWP training course: Physical parametrization of sub-grid scale processes
Apr 24	Policy Advisory Committee
Apr 25–26	Finance Committee

Apr 30 – May 4	NWP training course: Predictability and ensemble forecast systems
May 15–16	Security Representatives' meeting
May 16–18	Computing Representatives' meeting
May 21–24	Workshop on radiation in the next generation of weather forecast models
Jun 5–8	Using ECMWF's Forecasts (UEF)
Jun 8–12	Hackathon 2018
Jun 13–14	Council
Jul 10–12	Workshop on physics–dynamics coupling (PDC18)
Sep 10–13	Annual Seminar
Sep 24–28	Workshop on high-performance computing in meteorology
Oct 1–3	Training course: Use and interpretation of ECMWF products
Oct 8–10	Scientific Advisory Committee
Oct 11–12	Technical Advisory Committee
Oct 22–23	Finance Committee
Oct 24	Policy Advisory Committee
Dec 4–5	Council

ECMWF publications

(see *http://www.ecmwf.int/en/research/publications*)

Technical Memoranda

819 **Diamantakis**, **M.** & **A. Agusti-Panareda**: A positive definite tracer mass fixer for high resolution weather and atmospheric composition forecasts. *December 2017*

817 **Haiden**, **T.**, **M. Janousek**, **J. Bidlot**, **L. Ferranti**, **F. Prates**, **F. Vitart**, **P. Bauer** & **D.S. Richardson**: Evaluation of ECMWF forecasts, including 2016–2017 upgrades. *December 2017*

816 **Hogan**, **R.J.**, **M. Ahlgrimm**, **G. Balsamo**, **A. Beljaars**, **P. Berrisford**, **A. Bozzo**, **F. Di Guiseppe**, **R.M. Forbes**, **T. Haiden**, **S. Lang**, **M. Mayer**, **I. Polichtchouk**, **I. Sandu**, **F. Vitart** & **N. Wedi**: Radiation in numerical weather prediction. *October 2017*

815 **Geer**, **A.**, **M. Ahlgrimm**, **P. Bechtold**, **M. Bonavita**, **N. Bormann**, **S. English**, **M. Fielding**, **R. Forbes**, **R. Hogan**, **E. Holm**, **M. Janiskova**, **K. Lonitz**, **P. Lopez**, **M. Matricardi**, **I. Sandu** & **P. Weston**: Assimilating observations sensitive to cloud and precipitation. *October 2017*

814 **Massart**, **S.**, **A. Agusti-Panareda** & **J. Flemming**: Evidence of a stratospheric methane bias in the IFS against MIPAS data. *October 2017*

812 **Matricardi**, **M.**, **L. Puertas** & **B. Funke**: Modeling of nonlocal thermodynamic equilibrium effects in the classical and principal component based version of the RTTOV fast radiative transfer model. *October 2017*

811 **Bergman**, **D.L.**, **L. Magnusson**, **J. Nilsson** & **F. Vitart**: Forecasting tropical cyclone landfall using ECMWF's seasonal forecasts from System 4. *October 2017*

810 **Bonavita**, **M.**, **M. Dahoui**, **P. Lopez**, **F. Prates**, **E. Holm**, **G. De Chiara**, **A. Geer**, **L. Isaksen** & **B. Ingleby**: On the initialization of Tropical Cyclones. *September 2017*

809 **Polichtchouk**, **I.**, **R.J. Hogan**, **T.G. Shepherd**, **P. Bechtold**, **T. Stockdale**, **S. Malardel**, **S.J. Lock** & **L. Magnusson**: What influences the middle atmosphere circulation in the IFS? *October 2017*

804 **Bormann**, **N.**, **C. Lupu**, **A. Geer**, **H. Lawrence**, **P. Weston** & **S. English**: Assessment of the forecast impact of surface-sensitive microwave radiances over land and sea-ice. *October 2017*

EUMETSAT/ECMWF Fellowship Programme Research Reports

45 **Weston**, **P.**, **N. Bormann**, **A. Geer** & **H. Lawrence**: Harmonisation of the usage of microwave sounder data over land, coasts, sea ice and snow: First year report. *October 2017*

Index of Newsletter articles

This is a selection of articles published in the *ECMWF Newsletter* series during recent years.
Articles are arranged in date order within each subject category.
Articles can be accessed on ECMWF's public website – http://www.ecmwf.int/en/research/publications

Contact information

ECMWF, Shinfield Park, Reading, Berkshire RG2 9AX, UK

Telephone National	0118 949 9000
Telephone International	+44 118 949 9000
Fax	+44 118 986 9450

ECMWF's public website   http://www.ecmwf.int/

E-mail: The e-mail address of an individual at the Centre is firstinitial.lastname@ecmwf.int. For double-barrelled names use a hyphen (e.g. j-n.name-name@ecmwf.int).

Problems, queries and advice	Contact
General problems, fault reporting, web access and service queries	servicedesk@ecmwf.int
Advice on the usage of computing and archiving services	advisory@ecmwf.int
Queries regarding access to data	data.services@ecmwf.int
Queries regarding the installation of ECMWF software packages	software.support@ecmwf.int
Queries or feedback regarding the forecast products	forecast_user@ecmwf.int

ECMWF

Newsletter | Number 154 – Winter 2017/18

European Centre for Medium-Range Weather Forecasts

www.ecmwf.int